Title
Ubiquitin in host defense against pathogenic Mycobacteria

Author
Collins, Cathleen Ann

Publication Date
2009

Peer reviewed|Thesis/dissertation

Ubiquitin in Host Defense Against Pathogenic Mycobacteria

by

Cathleen A. Collins

DISSERTATION

Submitted in partial satisfaction of the requirements for the degree of

DOCTOR OF PHILOSOPHY

in

Biomedical Sciences

in the

GRADUATE DIVISION

of the

Acknowledgements

I am grateful to my advisor Rick Brown for his years of support and encouragement. I have always appreciated his enthusiasm, the breadth of his knowledge and his creativity and insight. I was thrilled to be able to continue in his lab when he moved to Genentech and know that this opportunity would not have happened without his generosity and commitment.

I thank my committee members Jayanta Debnath and Cliff Lowell for their time and great guidance that helped me to focus my project. I am grateful to our collaborators Ann de Mazière and Judith Klumperman for sharing their hard work and expertise. I would also like to thank the many people in the Brown lab who have helped me. Elsa N'Diaye Dulac taught me how to do Western blots, PCR, immunostaining and confocal microscopy, but most importantly that every day in the lab is an opportunity to discover something new. The postdocs of our lab, Fredric Carlsson, Shilpa Joshi, Chen Wang, and Delu Zhou helped me with their great questions and generosity. Brigitte Watkins shared the experience of coming to Genentech as a graduate student and always had kind words and encouragement. Hiroshi Morisaki and Wouter Hazenbos shared their space, perspective and humor in the lab.

I am grateful to my family for their support and love. I have had extremely patient parents and grandparents, who have completely supported me since early experiments in moldy bread and bean plants. I thank also my husband Keegan, his family and our daughter Ava for their constant motivation and unbelievable senses of humor.

Finally I thank the teachers who inspired and encouraged me.

Contributions of Others to the Presented Work

Chapter 2 of this dissertation is based on a manuscript published in the journal Public Library of Science Pathogens: Collins CA, De Mazière A, van Dijk S, Carlsson F, Klumperman J, *et al.* 2009 Atg5-Independent Sequestration of Ubiquitinated Mycobacteria. PLoS Pathog 5(5): e1000430. doi:10.1371/journal.ppat.1000430. The following co-authors contributed to this work: Ann de Mazière (University Medical Center, Utrecht), Suzanne van Dijk (University Medical Center, Utrecht), and Judith Klumperman (University Medical Center, Utrecht) performed the electron microscopy processing and quantification presented in Chapters 2 and 3. Fredric Carlsson (Genentech, South San Francisco) helped to perform the flow cytometry analysis in Chapters 2 and 3. Eric J. Brown (Genentech, South San Francisco) supervised this work.

Ubiquitin in Host Defense Against Pathogenic Mycobacteria

by

Cathleen A. Collins

Advisor: Eric J. Brown

Abstract

M. tuberculosis is one of the world's most prevalent pathogens, infecting one third of humans and contributing to 2 million deaths each year. *M. marinum* (Mm) has been increasingly studied as a model of *M. tuberculosis* due to its relative safety and its shared mechanisms of pathogenesis; for example, previous studies have highlighted the importance of the secretion system ESX-1 in pathogenesis of both *M. tuberculosis* and Mm. In this thesis we show that the host's ubiquitin system, best known for tagging host proteins for degradation, also recognizes Mm that have escaped their original phagosomes via an ESX-1–dependent mechanism and entered into the cytosol. Ubiquitinated bacteria have two distinct fates; ubiquitin tagged Mm can be sequestered into lysosome-like compartments, but they also can shed cell wall, which may allow them to evade sequestration. Lysosomal sequestration is independent of autophagy, a response to starvation or infection that leads to degradation of organelles and certain other intracytosolic pathogens. These experiments reveal ubiquitination as a mechanism of host cell recognition of Mycobacteria and the existence of a new interface between the host and invading microbe that may be amenable to therapeutic intervention.

Table of Contents

List of Figures

Chapter 2

Chapter 3

Chapter 1

Introduction: Ubiquitin & Mycobacteria

Abstract

This thesis focuses on the role of ubiquitin in host defense against pathogenic Mycobacteria. *Mycobacterium tuberculosis* is one of the world's most prevalent pathogens, currently infecting as much as a third of the world's population. Insight into mechanisms of host defense against Mycobacteria is needed in order to develop better therapies. This thesis examines ubiquitination by host macrophages of *Mycobacterium marinum*, a close relative of *M. tuberculosis*. This first chapter reviews ubiquitination in general and in the context of immune signaling, and provides background about pathogenic mechanisms of and defense against *M. tuberculosis* and *M. marinum* related to the studies described in Chapters 2 and 3.

Ubiquitin

Ubiquitin is a 76 amino acid protein expressed and highly conserved in all eukaryotes (1). Initially described as a tag targeting proteins to the 26s proteasome for degradation, it has been shown to regulate a diverse range of cellular functions, including endocytic trafficking, transcriptional regulation and DNA repair (2). Ubiquitin attachment requires a three-step reaction. This begins with ATP-dependent charging of the E1 activating enzyme on its active site cysteine with ubiquitin's C-terminal glycine (1). Ubiquitin is then transferred from the E1 to an E2 conjugating enzyme's active site cysteine. Finally, an E3 ligase brings both the substrate and the E2 conjugating enzyme in close proximity to allow attachment of ubiquitin to the ε-amino group of a lysine on the substrate (3). In addition, polyubiquitin chains can form through one of the attached ubiquitin's seven lysines and the C-terminal glycine on another ubiquitin.

Though there are only two E1's, there are dozens of E2's and hundreds of E3's, allowing for specificity in selecting substrates for ubiquitination (4). E3's have been categorized into three groups. The HECT-Type E3 ligases contain an active site cysteine with which they directly bind ubiquitin in a high energy thioester bond (2). A larger group, the RING-Type E3 ligases, often contain multiple subunits and do not bind covalently to ubiquitin but rather bring the E2 close to its substrate (2). The U-box E3 ligases work with a HECT-type E3 to elongate polyubiquitin chains (2).

The effect of ubiquitination depends on the length of the chains and the particular lysines through which of ubiquitin's seven lysines chains form. Broadly, K48 chains target proteins to the proteasome, while K63 chains are involved in signaling cascades and in trafficking of ubiquitinated receptors to mature late endosomes, or multivesicular

bodies for degradation (1, 4). The different linkages encode information spatially, with K63 chains extended like "beads on a string" whereas K48 chains are more compact (5). Models for the significance of a particular chain linkage will continue to be revised, as evidence for chain editing and mixed chains emerges (6, 7, 8).

As described above, K48 chains primarily target proteins for proteasomal degradation. The 26S proteasome is composed of a 20S core particle, formed of 28 subunits arranged in four stacked rings, and a 19S regulatory particle, made of a lid and a base including six AAA ATPases (9). The 20s core consists of alpha and beta subunits which act as a threonine protease to cleave products between 3 and 25 amino acids in length, with an average product of 7 to 8 amino acids (9). The 19s regulatory particle, in turn, recognizes ubiquitinated substrates and regulates opening of the tightly closed chamber of the core particle in an ATP-dependent manner (9, 10). In addition to the 26S proteasome, there is an IFN-gamma inducible "immunoproteasome," in which beta subunits in the core particle are replaced with homologous proteins; this change affects protein processing and which epitopes are available for antigen presentation (11; see below: ubiquitin in antigen presentation).

In contrast to the role of K48 chains in targeting proteins to the proteasome, K63 chains have been described primarily as inducing internalization of surface receptors and shuttling them through the endosomal pathway (4). After entry into the endosomal pathway, receptors may be recycled or trafficked to mature late endosomes, or multivesicular bodies (MVBs), which contain multiple internal vesicles (12). MVBs eventually fuse with lysosomes, allowing degradation of their contents. This process involves a variety of adaptor proteins that contain ubiquitin-associated (UBA) and/or

ubiquitin-interacting (UIM) motifs, such as Eps15 and Hrs, that bind to and shuttle these receptors through the endocytic pathway (13). In addition to their role in endocytic trafficking, K63 chains also modify proteins in ways that affect several signaling pathways, as discussed below.

Ubiquitin in immune system signaling

Ubiquitination is critical to activation and regulation of innate and adaptive immune responses. For example, in innate immune cells NF-κB activation in response to bacterial lipopolyssacharide (LPS) and the inflammatory cytokines interleukin-1 (IL-1) and tumor necrosis factor α (TNF-α) requires ubiquitination and degradation of the inhibitor of κB (IκBα) (14). Upon release from IκBα, NF-κB translocates to the nucleus and activates many genes involved in the inflammation. Further, the upstream signaling networks resulting in NF-κB activation also depend on ubiquitination. In response to stimulation of Toll-like receptors, TRAF6 acts a RING finger E3 ubiquitin ligase to ubiquitinate itself and the IκB kinase (IKK) subunit NEMO; K63 autoubiquitination allows TRAF6 to form a stable complex with the kinase TAK1, leading to activation of the IKK, which phosphorylates and finally allows IκB ubiquitination (15). NOD1 and NOD2, cytosolic sensors of bacterial products, also induce K63 polyubiquitination of NEMO, which also stimulates IKK activity (16). Ubiquitination also plays an important role in regulating the adaptive immune response. For example, Cbl acts as a RING-type E3 ubiquitin ligase to dampen signaling through the T cell receptor by targeting Src and Syk/ZAP-70 protein kinases (2).

Ubiquitination in antigen presentation

Pathogen derived molecules must often be processed in order to be presented as peptide-MHC complexes on the surface of professional antigen presenting cells (APCs) to activate T cells. In general, MHC class I (MHC-I) presents peptides from within the cell cytosol, derived from viral peptides or those secreted by bacteria and transported via TAP proteins and complexed with MHC-I in the endoplasmic reticulum, and activates CD8+ T lymphocytes (17). In contrast, MHC class II (MHC-II) primarily presents exogenous antigens that are internalized via the phagosome-endosome-lysosome pathway, and activates CD4+ T lymhocytes. The size of proteins that may be presented is restricted by the binding pocket of the MHC, particularly in MHC class I which has maximal binding with peptides 8 to 10 amino acids, and the ubiquitin pathway is important in processing peptides to this length (18). A role for ubiquitin in MHC-I presentation was first exemplified using temperature sensitive mutants in the E1 ubiquitin activating enzyme, which have defective ubiquitin conjugation at a restrictive temperature, and exhibited less presentation of ovalbumin on MHC-I (19). Proteasomes have been found to influence antigen processing during infection with Influenza, Hepatitis B, Adenovirus, and CMV, among other viruses (17). In addition, exogenous antigens taken up through phagocytosis may be translocated to the cytoplasm where they undergo ubiquitin-dependent endoplasmic reticulum-associated degradation (ERAD). This process of "cross-presentation" allows presentation of exogenous antigens on MHC-I (20, 21).

Ubiquitin in infection with bacterial pathogens

The ubiquitin system is crucial in signaling inflammation and preparing microbial products for antigen presentation, and since these are important components of the immune response there is strong evolutionary pressure on pathogenic microbes to evade, inhibit or dampen these pathways (22). For example, several bacteria have been found to secrete deubiquitinases that interfere with NF-κB signaling. Yersinia secretes YopJ, which is homologous to the cysteine protease of human Adenovirus type 2 and the yeast DUB ubiquitin-like specific protease Ulp1, a SUMO-ubiquitin like protease (22). YopJ is a promiscuous deubiquitinating enzyme, capable of removing ubiquitin from TRAF6 and IκBα (23). *Salmonella enterica* serovar Typhimurium (*Salmonella typhimurium*) secretes SseL, which is structurally similar to deubiquitinating cysteine proteases and preferentially deubiquitinates K63 chains *in vitro* (24). Commensal *Salmonella* also block ubiquitination of phosphorylated IκBα, possibly through inhibition of the E3 ubiquitin ligase $SCF^{\beta TrcP}$; it is possible that this allows the bacteria to establish an infection within their host without activating the immune system (25).

Though ubiquitin does not exist in prokaryotes, bacteria have evolved enzymes that mimic the function of E3 ubiquitin ligases; these ligases have been shown to influence the outcome of infection in eukaryotic cells. *Salmonella typhimurium*'s SopA, a protein secreted by the Type III secretion system which is encoded by the *Salmonella* pathogenicity island 2 that promotes survival within the *Salmonella*-containing vacuole, uses its HECT-like ubiquitin ligase activity on an unknown substrate to facilitate transmigration of polymorphonuclear cells through epithelial barriers (26). Among the many proteins Legionella pneumophila secretes via its Dot/Icm type IV

secretion system during its remodeling of the phagosomal compartment, LubX has two U-box-like domains and acts as an E3 ubiquitin in cooperation with host UbcH5a or UbcH5c E2 enzymes to polyubiquitinate host Cdc2-like kinase (Clk1) (27). Though inhibition of Clk1 decreases Legionella growth, the mechanism of this effect is unknown. Mimicry of ubiquitin ligases to interfere with the immune response seems to be a common strategy, as the plant pathogen Pseudomonas syringae uses AvrPtoB, which contains a RING finger/U-box-like domain, to disrupt signaling by the tomato kinase Fen and the resulting immune response (28). The discovery of a new class of ubiquitin ligases in *Shigella flexneri* points to the diversity of protein structures evolved to act as ubiquitin ligases molecules in bacteria (29).

Finally, in addition to providing peptides for antigen presentation, host ubiquitination of bacterial virulence factors can affect the outcome of infection. During infection of host cells, *Listeria monocytogenes* secretes listeriolysin O, a cholesterol-dependent pore-forming toxin necessary for bacterial escape from the phagosome (30). Targeting of listeriolysin O by the host ubiquitin system may be advantageous to the bacteria, since dampening its activity allows host cells to avoid lysis by the toxin. *Salmonella*'s Type III secretion system SPI-I permits invasion of cells by inducing ruffling of intestinal cells through activation of Cdc42 and Rac1 by the secreted bacterial guanine nucleotide exchange factor SopE (31). SptP, another secreted protein, deactivates Cdc42 and Rac1. Both SopE and SptP are ubiquitinated, but SopE's faster proteasomal degradation allows host cells to recover from the initial activation (31). In addition, the surface of *Salmonella* associates with ubiquitin and proteasomes during infection of HeLa cells and proteasome inhibition leads to enhanced growth (32).

Listeria monocytogenes also associates with ubiquitin, but not with proteasomes (32). The significance of this association is unclear.

In conclusion, the variety of strategies used by diverse pathogens to disrupt the ubiquitin system, from deubiquitinating enzymes to ubiquitin ligases to exploitation of ubiquitination of their own substrates to influence infection, suggest that the ubiquitin system plays an important role in host-pathogen interactions.

Autophagy

While particular cytoplasmic proteins are targeted for ubiquitination and degraded by the proteasome, whole organelles, protein aggregates and "bulk" cytosolic proteins can be degraded through a process called autophagy, meaning "eating oneself" (33). This carefully regulated pathway involves nucleation and formation of characteristic double membrane vesicles called autophagosomes which enclose cellular material and deliver their contents to lysosomes (34). Although there is basal autophagy, starvation relieves repression of autophagy by the central regulator mTOR, or mammalian target of rapamycin, which inhibits autophagy under normal conditions by hyperphosphorylating Atg13 (34). Relief of mTOR hyperphosphorylation of Atg13 allows it and other Atg proteins to begin nucleation of the initial autophagosome vesicle. This process also depends on the Class III PI 3-kinase Vps34 in complex with beclin 1, or Atg6 (34). Elongation and stabilization of the membrane requires a two conjugation reactions using Atg proteins that are similar to the three step ubiquitin conjugation reactions. Atg12 is covalently attached to Atg5, which binds noncovalently to Atg16, which can multimerize. This complex is necessary for the stable conjugation of Atg8 (also known as MAP1LC3, or microtubule-associated protein 1 light chain 3) to phosphatidylethanolamine (PE) (34).

Atg7 acts as an ubiquitin-activating E1-like enzyme for both reactions, while Atg3 acts as an ubiquitin- conjugating E2-like enzyme for Atg8 conjugation to PE (34). After enclosure of the autophagosome, it fuses with degradative lysosomes.

Autophagy has broad biological importance, with implications in tumorigenesis and neurodegenerative disease (33). It is also involved in defense against bacterial and viral pathogens (35, 36). Bacterial pathogens which penetrate the phagosome may be quickly targeted by autophagosomes; these include *Rickettsia conorii*, Group A *Streptococcus*, *Listeria* and *Salmonella* (36). Though whether *M. tuberculosis* escapes the phagosome is controversial, induction of autophagy also decreases its survival in macrophages (37, 38, 39). Other bacteria appear to replicate within autophagosomes or vacuoles with autophagosome-like features which do not undergo the final step of lysosomal fusion. These include *Brucella abortus*, *Coxiella burnetti*, and *Legionella pneumophila* (36). *Listeria* and *Shigella* both evade degradation by autophagy (40, 41); *Listeria*'s actin polymerizing protein ActA as well as other effectors allow it to avoid autophagic entrapment, while *Shigella*'s IcsB directly inhibits interaction between Atg5 and VirG.

As described above, starvation is the best known signal for activation of autophagy. However, key inducers of the immune response to viral and bacterial pathogens, Type I and Type II interferons, have been shown to induce autophagy. The Type I IFNα/ß inducible kinase PKR upregulates autophagy during infection of mouse embryonic fibroblasts with herpes simplex virus (42). Treatment of cells with Type II IFN-γ also activates autophagy through the GTPase LRG47 (mouse) or IRGM (human), which enhances acidification of the BCG phagosome (39, 43).

Like ubiquitination and proteasome degradation, autophagy can process antigens for presentation on professional antigen presenting cells. Autophagosomes can deliver peptides directly from the cytosol to the late endosomes where MHC class II loading occurs (44). This correlates well with evidence that up to 20% of the peptides found on MHC class II are from endogenous sources, rather than from phagocytosis and degradation of exogenous material (45). Autophagy may thus act reciprocally to cross-presentation, which allows presentation of exogenous peptides on MHC class I as described above. Autophagy may also contribute to CD4+ T-cell selection in the thymus, as cortical thymic epithelial cells exhibit high levels of basal autophagy and low endocytic capacity (45).

The signals targeting proteins for entrapment by autophagosomes are still emerging. Because large ubiquitinated aggregates, or aggresomes, are degraded by autophagy, ubiquitin is hypothesized to flag proteins for autophagic degradation in addition to proteasomal degradation (46). Attachment of a single ubiquitin was enough to target cytosolic proteins to autophagosomes (47). This required p62, or sequestosome 1, which contains a ubiquitin associating domain (UBA) that binds to ubiquitin (47, 48). p62 is often found in protein aggregates of neurodegenerative diseases, and may act as an adaptor protein bridging ubiquitinated proteins and LC3 (48). *Salmonella* associated with GFP-LC3 frequently co-localized with ubiquitin, suggesting a similar connection between ubiquitination of bacteria and clearance by autophagy (49).

Mycobacterium tuberculosis

Mycobacterium tuberculosis (TB) a highly prevalent pathogen, infecting about a third of the world's population and causing about 1.5 million deaths per year (50). Multiple drug resistant (MDR) strains of tuberculosis are becoming more common, particularly in the developing world (51). Some people infected with TB develop productive infections, while in others the bacilli appears to live dormantly and reactivate after many years (50). TB is an obligate intracellular pathogen, taken up by cells of the innate immune system, particularly macrophages, through actin-dependent phagocytosis (52). Macrophages form distinct structures called granulomas, which constitute a ring of infected cells surrounding a central area of necrosis. T cells interact with macrophages at the periphery of the granuloma (53).

Normally, the fate of particles internalized by phagocytosis is to traffic through the lysosomal pathway, resulting in an acidic vacuole containing acid hydrolases and other degradative enzymes (52). Phagosome maturation is driven by a series of Rab GTPases, particularly Rab5 and Rab7, that are recruited to the phagosome and promote fusion between the phagosome and early and late endosomes, respectively (52). A major mechanism of TB pathogenesis is interruption of this process. TB halts phagosome-lysosome fusion before recruitment of early endosomal antigen 1 (EEA1). The mechanism of this block may be through TB's inhibition of sphingosine kinase's release of calcium from the endoplasmic reticulum; increase in cytosolic calcium is necessary to initiate the calmodulin- Cam Kinase II interaction with the PI3 kinase hVPS34, which produces PI3P that recruites EEA1 to the maturing phagosome (54, 55). Lack of EEA1 recruitment effectively blocks maturation at the Rab5 to Rab7 transition. The

inhibitory effect appears to be through glycosylated phosphitidylinositol lipoarabinomannan (LAM), a major lipid in the mycobacterial cell wall, as beads coated with LAM showed similar defect in phagosome maturation (55). This block may account for exclusion of the vesicular proton-ATPase from mycobacterial phagosomes, allowing the pH to remain above 6.3 (56).

A region of 9.5 kb in the TB genome, known as region of difference 1 (RD1) is intensely studied for its role in Mycobacterial pathogenesis (57). This is because the attenuation of the vaccine strain of TB, *Mycobacterium tuberculosis* var. bovis Calmette Guérin (BCG), was shown to be due primarily to loss of RD1 (58). RD1 encodes a putative alternative secretion system called ESX-1. ESX-1 substrates include ESAT-6 and CFP-10, which are immunodominant antigens during TB infection and which do not contain classic signals for secretion through the Sec or Tat secretion systems (57, 59). RD1 includes several proteins with predicted transmembrane domains, encoded by Rv3869, Rv3870 and Rv3877, and these are thought to form the pore of ESX-1. Rv3871 is cytosolic, and interacts with Rv3870 to form an ATPase that may power protein secretion (59). Genetic disruption of Rv3870, Rv3871 and Rv3877 resulted in disrupted ESAT-6 and CFP-10 secretion and attenuation for growth in macrophages (60). Though the function of ESX-1 has not been determined in TB, in the related *Mycobacterium marinum* secreted ESAT-6 may form pores in the phagosomal membrane and allow escape to the cytosol (61). It is interesting to note that TB deficient in RD1 fails to infiltrate lung tissue, suggesting a defect in cell to cell spread (62).

Mycobacterium marinum

Mycobacterium marinum (Mm) is a natural pathogen of fish and reptiles, with an optimal growth temperature between 25-35 degrees C (63). Mm is a close relative of TB, sharing 99.4% homology of 16S rRNA sequences. However, Mm's genome is predicted to be 6.5 Mbp versus TB's 4 Mbp; the increased size of the genome appears to be due to duplication events (64). Mm has been developed as a model for TB for practical reasons, since it does not require BSL-3 facilities and grows much more quickly. More importantly, Mm shares similar mechanisms of pathogenesis, such as the ability to elude lysosomal acidification and to promote survival using ESX-1, which is important for Mm's growth in macrophages (65, 66). Mm has been studied during infection of zebrafish embryos and Drosophila melanogaster as well as the Drosophila S2 cell line, but also during infection of murine macrophages (64). Importantly, during infection of its natural hosts, Mm causes a granulomatous response similar to that of TB, with central caseous necrosis in some granulomas (64).

Despite the similarities described above, one apparent difference between TB and Mm is the latter microbe's ability to polymerize actin. During infection of macrophages, Mm escapes from phagosomes into the cytosol and recruits actin, forming "actin tails" which allow it to spread from cell to cell (67). Actin tails have not been observed during TB infection, and the ability to polymerize actin may be a key difference between the species. Further, TB's ability to escape the phagosome is an area of controversy; one group found no evidence of phagosomal escape but another found TB in the cytosol of human macrophages and dendritic cells after two days of infection (37, 38).

Use of the host's actin polymerizing machinery has been described for other

pathogens, in order to form actin tails (examples include *Listeria*, *Rickettsia*, *Burkholderia*, *Shigella*) or to create pedestals that allow attachment to gut epithelia (Enterohemorrhagic and enteropathogenic *E. coli* or EHEC) (64). Mm is like *Shigella* and EHEC in that it does not mimic WASP or N-WASP to initiate Arp2/3 depedent actin polymerization; rather it requires N-WASP's lipid phosphatidylinositol 4,5-bisphosphate-binding basic motif (68).

Host defense against mycobacteria

Defense against pathogenic Mycobacteria depends on both the innate and adaptive arms of the immune system. Activated CD8+ and Th1 CD4+ T cells produce interferon gamma (IFN-γ), which among many effects, activates macrophages to increase production of reactive nitrogen intermediates (69). IFN-γ upregulates several enzymes at the transcriptional level, including the enzyme producing the substrate (argininosuccinate synthetase to produce L-arginine), cofactor (GTP-cyclohydroxylase I, which makes tetrahydrobiopterin cofactor) and catalyst (inducible nitric oxide synthase) required for reactive nitrogen (69). Reactive nitrogen intermediates were found to be important for killing of TB by IFN-γ stimulated macrophages (70).

In addition, as discussed above, IFN-γ activates autophagy, resulting in increased proteolysis of long-lived proteins and increased translocation of GFP-LC3 to autophagic vesicles (39). IFN-γ induces Lrg47 (or IRGM in humans), a GTPase that enhances acidification of the mycobacterial phagosome and decreases survival of TB (71, 72). Lack of Lrg47 enhances susceptibility of mice to infection with TB, and correlated with defects in phagosome maturation (73). IFN-γ also enhanced delivery of BCG

phagosomes containing ubiquitin-derived peptides; these peptides have direct toxic activity on mycobacteria, through an unidentified mechanism (74). In addition to killing mycobacteria, enhanced delivery of mycobacterial products to degradative compartments may facilitate loading of antigens on MHC and enhance the important CD4+ and CD8+ T cell memory immune responses through the mechanisms described above (75).

Future questions: The role of ubiquitin and autophagy in infection with pathogenic mycobacteria

The purpose of this thesis is to explore the role of ubiquitin and autophagy in control of Mm infection. As described above, ubiquitin plays an important role in defense against several intracellular pathogens, both at the level of signaling and in targeting specific molecules for degradation. Autophagy also affects survival of several microbes through effects on membrane trafficking and compartment acidification. We hope that study of Mm's interaction with the ubiquitin system and the autophagy pathway will yield insight into mechanisms relevant to TB, a widespread and re-emerging human pathogen.

Chapter 2

Atg5-Independent Sequestration of Ubiquitinated Mycobacteria

Abstract

Like several other intracellular pathogens, *Mycobacterium marinum* (Mm) escapes from phagosomes into the host cytosol where it can polymerize actin, leading to motility that promotes spread to neighboring cells. However, only ~25% of internalized Mm form actin tails, and the fate of the remaining bacteria has been unknown. Here we show that cytosolic access results in a new and intricate host pathogen interaction: host macrophages ubiquitinate Mm, while Mm shed their ubiquitinated cell walls. Phagosomal escape and ubiquitination of Mm occured rapidly, prior to 3.5 hours post infection; at the same time, ubiquitinated Mm cell wall material mixed with host-derived dense membrane networks appeared in close proximity to cytosolic bacteria, suggesting cell wall shedding and association with remnants of the lysed phagosome. At 24 hours post-infection, Mm that polymerized actin were not ubiquitinated, whereas ubiquitinated Mm were found within LAMP-1–positive vacuoles resembling lysosomes. Though double membranes were observed which sequestered Mm away from the cytosol, targeting of Mm to the LAMP-1–positive vacuoles was independent of classical autophagy, as demonstrated by absence of LC3 association and by Atg5-independence of their formation. Further, ubiquitination and LAMP-1 association did not occur with mutant avirulent Mm lacking ESX-1 (type VII) secretion, which fail to escape the primary phagosome; apart from its function in phagosome escape, ESX-1 was not directly required for Mm ubiquitination in macrophages or *in vitro*. These data suggest that virulent Mm follow two distinct paths in the cytosol of infected host cells: bacterial ubiquitination is followed by sequestration into lysosome-like organelles via an autophagy-independent pathway, while cell wall shedding may allow escape from this fate to permit continued residence in the cytosol and formation of actin tails.

Introduction

Mycobacterium marinum (Mm) is a close genetic relative of the important human pathogen M. tuberculosis, and shares with M. tuberculosis the ability to infect host macrophages, as well as to induce a similar pathologic response (1,2). As in mammalian models of infection with M. tuberculosis, loss of the ESX-1 secretion system greatly attenuates the virulence of Mm in its natural fish and amphibian hosts (3–5). While the reason that ESX-1 is required for M. tuberculosis virulence remains unknown, there is some understanding of its role in pathogenesis of Mm infections. After Mm infection of host cells, ESX-1 is required for bacterial escape from the phagosome, recruitment of uninfected macrophages, and subsequent cell-to-cell spread (6–8). Although whether or not M. tuberculosis ever escapes from phagosomes remains highly controversial (9,10), loss of ESX-1 activity in this organism also leads to failure of cell-to-cell spread (11).

Some Mm polymerize actin, forming actin tails after entering the host macrophage's cytosol (12). However, this represents only a fraction (~25%) of the intracellular bacilli; the fate of the remaining 75% of infecting bacteria has yet to be established. To explore the fate of intracellular Mm, we developed an assay that accurately distinguishes intraphagosomal from cytosolic bacteria. Surprisingly, bacteria escaped from phagosomes to the cytosol many hours before actin polymerization was evident. A proportion of these newly-escaped cytosolic bacteria were ubiquitinated, as was bacteria-derived material that appeared to be shed from the mycobacterial surface and incorporated into host membranous structures.

Distantly related pathogens which can escape the phagosome, *Salmonella typhimurium* and *Listeria monocytogenes*, also associate with ubiquitin, but whether this

represents direct ubiquitination of the bacterial surface or close apposition of ubiquitinated host proteins remains unproven, and the significance of the association is unclear (13). Similar to ubiquitin associated *Listeria*, ubiquitinated Mm did not form actin tails; rather, they became associated with LAMP-1 positive macrophage lysosomes, suggesting a reuptake process from the cytosol.

The process of autophagy, which engulfs organelles and proteins into characteristic double membrane vacuoles during cell stresses including starvation and formation of intracytosolic protein aggregates (14,15), is a mechanism for host defense against some intracellular pathogens escape primary phagosomes, including *Salmonella*, *Listeria*, *Streptococcus pyogenes*, and *Shigella flexneri* (16–19). For each of these organisms, autophagic host defense is dependent on Atg5, a central component in the formation of autophagic membranes. Autophagy may also be important in host defense against Mycobacteria. Enhancement of autophagy in macrophages by starvation or rapamycin treatment leads to association of autophagy markers with M. tuberculosis var. bovis bacilli Calmette Guérin (BCG) phagosomes and overcomes the block in phagosome-lysosome fusion characteristic of infection with BCG and M. tuberculosis (20). However, sequestration of ubiquitinated Mm in LAMP-1 positive compartments did not require induction of autophagy and was independent of Atg5, suggesting an alternative pathway for reuptake of these organisms from the cytosol. These studies demonstrate that Mm undergo a complex kinetic interaction within the macrophages that are their preferred replication niche. After escape from phagosomes, some bacteria polymerize actin to facilitate cell-to-cell spread, while others become ubiquitinated, leading to reuptake into a host vesicular compartment by a mechanism distinguishable

from classic autophagy. These alternative fates may contribute to the wide variety of effects of ESX-1 on host-pathogen interactions during mycobacterial infection (21–23).

Results

M. marinum escape from phagosomes hours before activation of actin polymerization

We found that digitonin could permeabilize macrophage plasma membranes, while leaving phagosome membranes intact, as previously described (24) (Figure 1A). We combined macrophage permeabilization with digitonin with an antibody to Mm cell walls to detect cytosolic mycobacteria. A proportion of wildtype (WT) Mm in infected macrophages could be stained after digitonin permeabilization, whereas Mm lacking region of difference 1 (ΔRD1), which have no functioning ESX-1 secretion system, failed to be stained by antibody to the bacterial cell wall under these conditions (Figure 2A, top two rows). This was not due to failure of the antibody to recognize the mutant bacteria, since all intracellular ΔRD1 Mm were stained after macrophage permeabilization with Triton X-100, which solubilized phagosome as well as plasma membranes (Figure 2A, third row). Thus, lack of staining after digitonin permeabilization was indicative of the presence of ΔRD1 Mm in phagosomes. All WT Mm were also stained with antibody under the same conditions of Triton X-100 permeabilization (Figure 2A, bottom row). Using this technique, we found that ~21% of WT Mm had escaped from phagosomes by 3.5 hours post infection (HPI), a time before significant bacterial actin polymerization occurred, as detected by phalloidin staining (Figure 2A and 2B). Bacterial escape from phagosomes also was demonstrated by electron microscopy, which showed about 43% of WT Mm in the cytosol at 3.5 HPI, while 100% of ΔRD1 Mm were clearly enclosed within a membrane (Figure 2C, Figure 1B, 1C). As previously described (12), actin

polymerization by WT Mm was not detected at 3.5 HPI and increased dramatically by 24 HPI (Figure 2B and 2D). Thus, WT Mm escape from macrophage phagosomes several hours prior to initiation of actin-based motility.

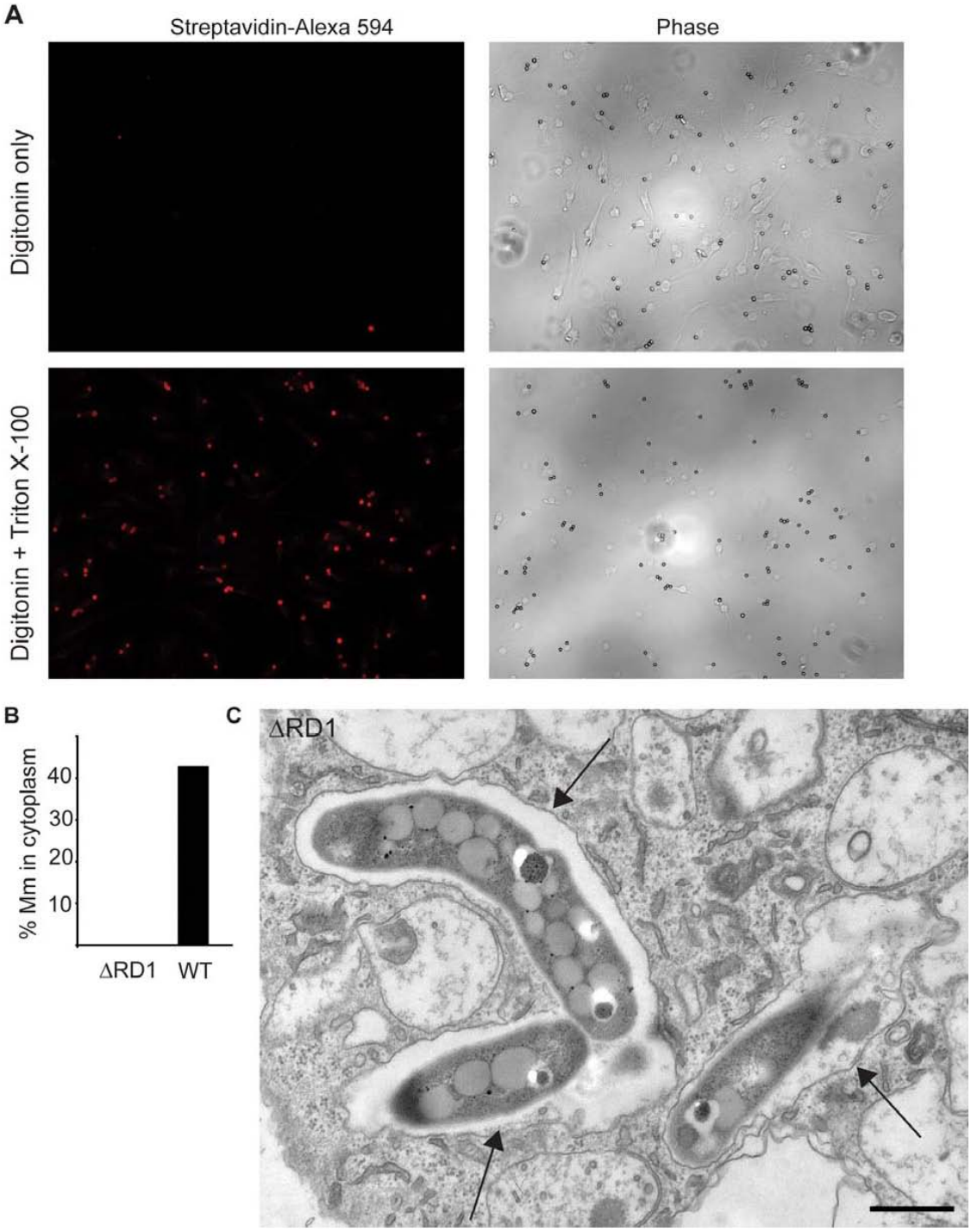

Figure 1. *Differential permeabilization of macrophage membranes by digitonin and electron microscopy quantitation of vacuolar association of phagocytosed Mm.*

(A) Macrophages were incubated with 4 μm latex beads carrying biotinylated BSA at 32

degrees for 2 hours to mimic conditions of Mm infection. Following permeabilization with digitonin (top row) or with digitonin and Triton X-100 (bottom row), macrophages were incubated with streptavidin-Alexa 594 as described in Materials and Methods. Fluorescence (left panels) and phase (right panels) images of microscopic fields were compared to determine the percentage of latex beads that stained with streptavidin after each permeabilization condition. Note that the one latex bead stained after digitonin alone (lower right) appears to be at the edge of a cell and the fluorescent particle in the upper left is not bead-associated.

(B) The percentage of ΔRD1 (n=85) and WT (n=177) Mm in the cytoplasm, outside of a phagosomal membrane, at 3.5 HPI was determined by transmission EM.

(C) Electron micrograph ΔRD1 Mm surrounded by phagosome membranes (arrows) at 3.5 HPI. Scale bar, 500 nm.

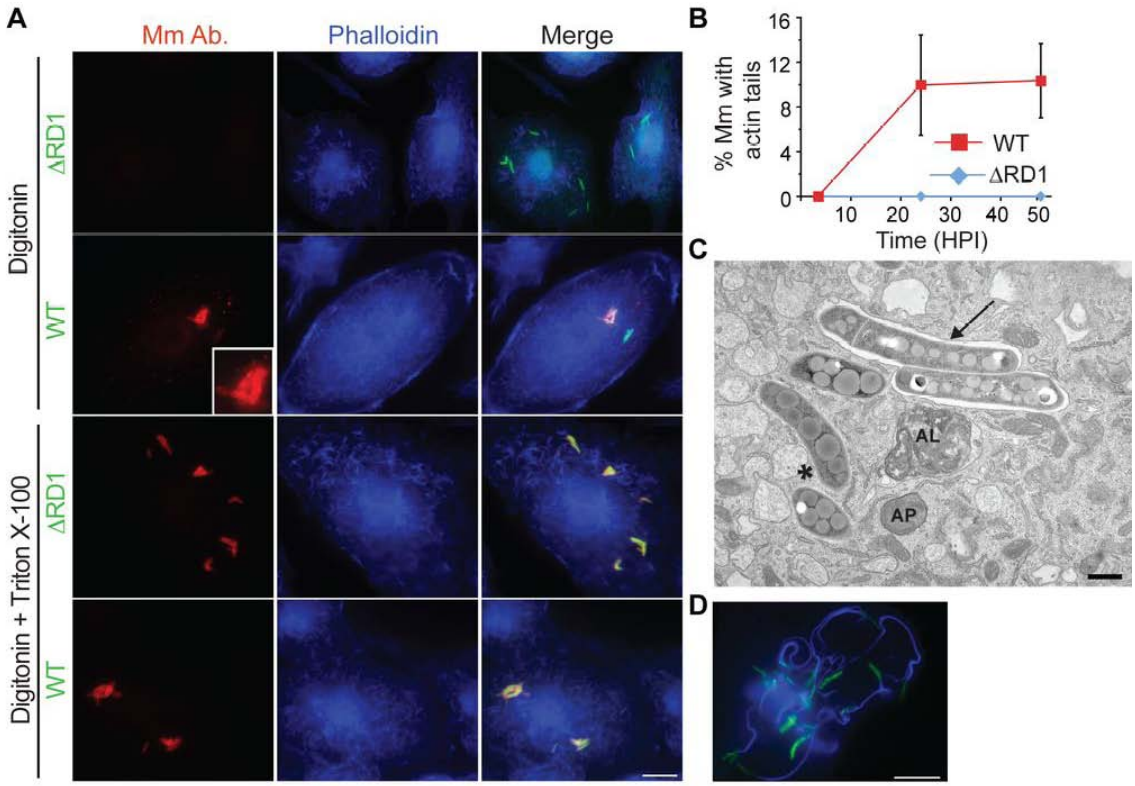

Figure 2. *Mm escapes from phagosome by 3.5 HPI.*

(A) 3.5 HPI with ΔRD1 (1st and 3rd rows) or WT (2nd and 4th rows) Mm expressing GFP, macrophages were permeabilized with digitonin alone (top two rows) or digitonin followed by TX-100 (3rd and 4th row) as described in Materials and Methods. Bacteria were stained with an anti-Mm antibody (1st column, red) and polymerized actin was visualized with phalloidin-Alexa 350 (2nd column, blue). Third column is a merge of the images in the first two columns. Inset in the first panel of the second row shows a 3.5 fold magnification of the cytosolic WT Mm in the larger panel, stained with the Mm antibody. (Scale bar, 10 μm).

(B) Actin tails, identified by phalloidin-Alexa 350 after digitonin and TX-100 staining, were quantified by counting all bacteria from at least 50 infected macrophages for WT

(squares, red line) and ΔRD1 (diamonds, blue line) at various times after infection in three independent experiments and graphed as mean ± SD.

(C) Epon section of a portion of a macrophage infected with WT Mm at 3.5 HPI. An asterisk denotes a Mm in the cytosol, an arrow points to Mm enclosed in phagosome membrane. AP, autophagosome; AL, autolysosome. Scale bar, 500 nm.

(D) A macrophage infected with WT Mm expressing GFP 24 HPI stained for phalloidin-Alexa 350 (blue) as in (A) (Scale bar, 10 μm). This image shows Mm exhibiting robust actin motility within a single cell, and is shown to illustrate several examples of actin polymerization at 24 HPI; it is not representative of the average 10% polymerizing actin in the entire population of infecting Mm as quantitated in (B).

Ubiquitination of cytosolic *M. marinum*

Because of the long delay between phagosome escape and initiation of actin-based motility, we hypothesized that cytosolic Mm might be recognized by ubiquitinating enzymes, similar to other bacterial species that escape the phagosome (13). Polyubiquitin was found associated with WT Mm, since bacteria were stained by an antibody recognizing only polyubiquitin (FK1), as well as an antibody that recognizes monoubiquitin-derivatized surfaces as well as polyubiquitin chains (FK2) (Figure 3A). Approximately 9% of WT Mm taken up by macrophages stained with FK2 at all times from 3.5 to 48 h (Figure 3A). Comparison of this percentage with the 21% escape observed at 3.5 HPI suggests that about 40% of all bacteria in the cytosol associate with polyubiquitin at this time.

Often, the cell biologic effects of polyubiquitin are determined by whether the ubiquitin chains are assembled through K48 or K63 linkages. While K48 polyubiquitin is most often a signal for proteasomal or lysosomal degradation, K63 linkages have been associated with assembly of signaling scaffolds (25). By using antibodies specific for K48 and K63 poyubiquitin linkages (26), we found that both chain types associated with WT Mm. Though K48-linked polyubiquitin association with Mm was more variable than K63, the proportions were not statistically distinct (Figure 3B). Specificity of the linkages was demonstrated by competition with K48 or K63 tetraubiquitin chains (Figure 4A).

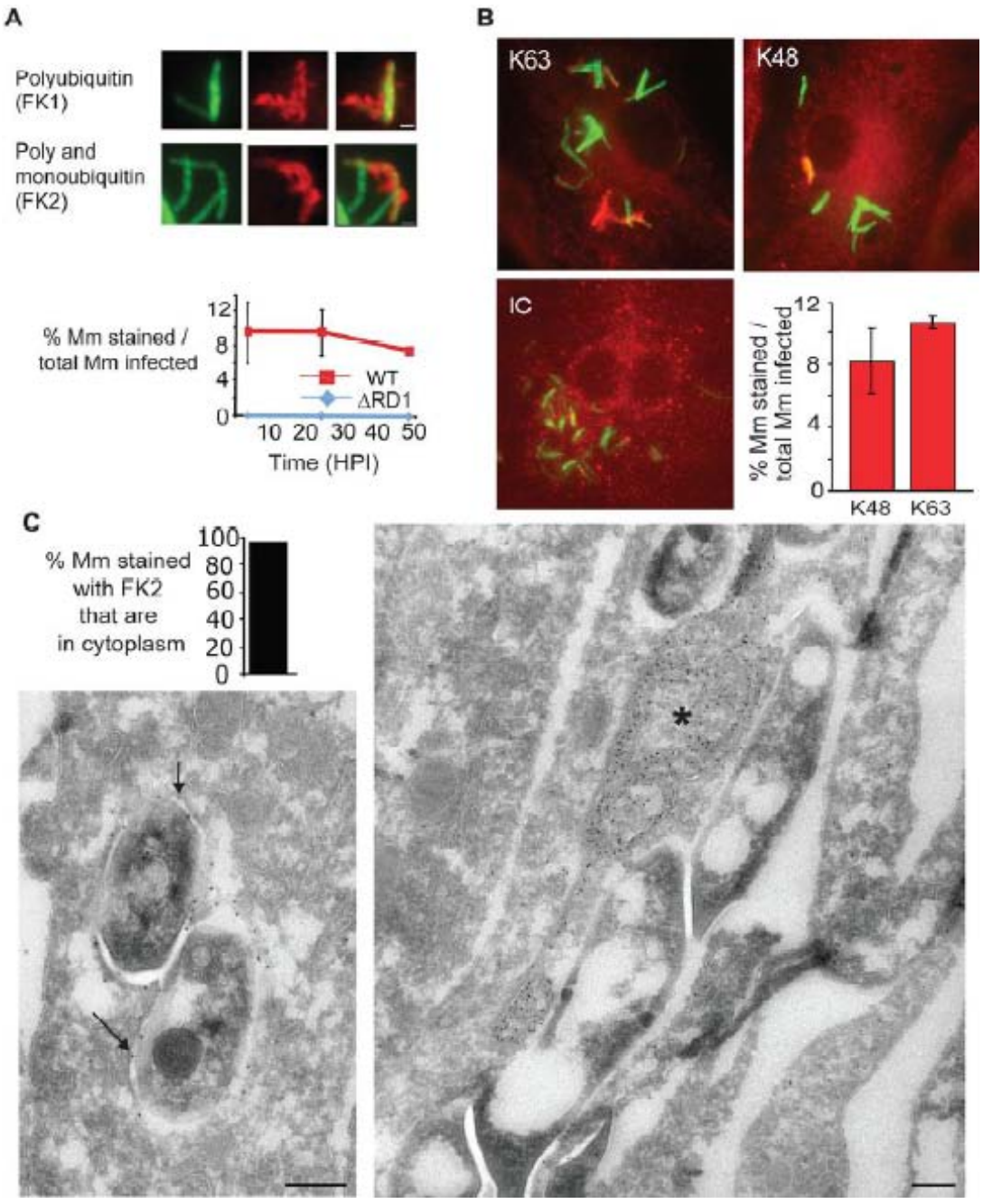

Figure 3. *Cytosolic Mm associates with polyubiquitin.*

(A) 48 HPI with WT Mm expressing GFP, macrophages were stained with antibodies for polyubiquitin (FK1) or poly- and monoubiquitin (FK2). Left panel, GFP fluorescence; middle panel, anti-ubiquitin fluorescence; right panel is a merge of the two other panels,

showing co-localization of both anti-ubiquitin antibodies with Mm. (Scale bars, 1 μm). Graph shows quantification of percent FK2 staining of WT (squares, red line) and ΔRD1 (diamonds, blue line), Mm from at least 50 infected macrophages at each time point in three independent experiments and graphed as mean ± SD.

(B) 24 HPI post infection, macrophages were stained with monoclonal antibodies recognizing K63-linked polyubiquitin (left panel), K48-linked polyubiquitin (middle panel), or anti-her2 as an isotype control (IC). Specificity of linkage detection was demonstrated by competition with K48 or K63 tetraubiquitin chains (Figure 4A). Graph shows quantification of percent of intracellular WT Mm stained with K63- and K48-polyubiquitin linkage-specific antibodies in macrophages infected for 24 hours. The difference in K63 and K48 association with Mm were not statistically significant (P= 0.0662), determined as described in Materials and Methods. Data are from at least 50 infected macrophages at each time point in each of three independent experiments and graphed as mean ± SD.

(C) Ultrathin cryosection of 3.5 HPI of macrophages with WT Mm, labeled with FK2 anti-ubiquitin, and 10 nm protein-A gold particles. Left panel shows Mm with ubiquitin on bacterial surface, indicated with arrows. Right panel shows ubiquitin on membranous structures associated with Mm, labeled with an asterisk. Graph shows quantification percent of ubiquitin associated Mm which were cytosolic or intra-vacuolar. 48 out of 50 such organisms were cytosolic. Scale bars, 200 nm.

To determine whether the ubiquitinated Mm were cytosolic or intraphagosomal, infected macrophages were permeabilized with digitonin and stained with both anti-ubiquitin and antibody to the Mm cell wall, which under these conditions recognizes cytosolic but not intraphagosomal bacteria (Figure 2A). This procedure revealed that virtually all ubiquitinated WT Mm were cytosolic at 3.5 HPI, as WT Mm that bound FK2 also were stained by the Mm cell wall antibody (Figure 4B). Quantitative immunoelectron (EM) microscopy confirmed the cytosolic localization of ubiquitinated WT Mm at 3.5 HPI, as 96% of ubiquitin associated WT Mm were in the cytosol (Figure 3C, left image and graph). In addition to direct association with intact bacteria, ubiquitin was frequently found associated with adjacent dense membrane structures (Figure 3C, right image), which appeared as networks with meshes and broadened parts, containing electron-dense material and occasionally small vesicles (and are designated further in the text as dense membrane networks).

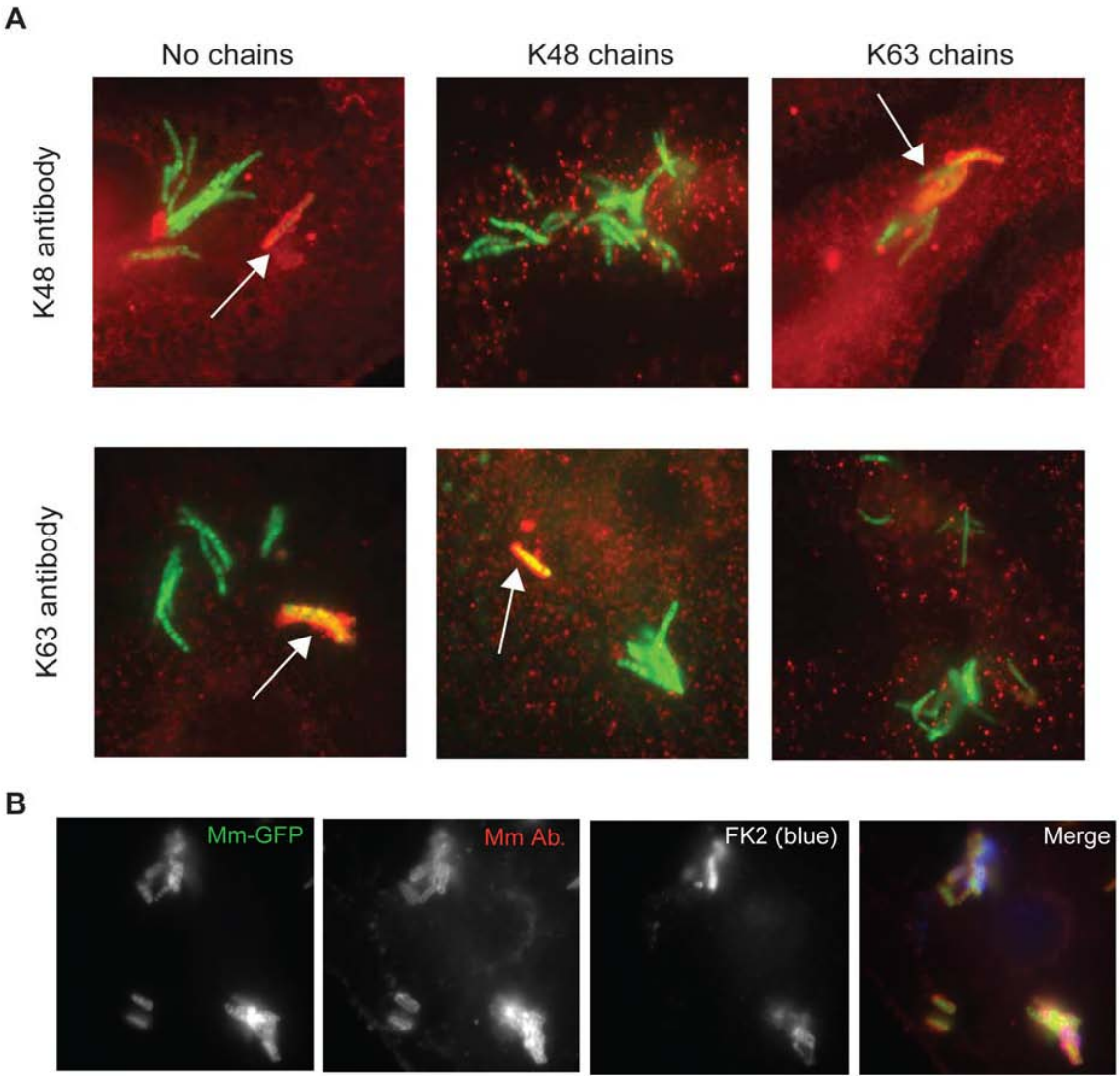

Figure 4. *Ubiquitin chain specificity of K48 and K63 antibodies and differential permeabilization showing cytoplasmic localization of ubiquitinated Mm at 3.5 HPI.*

(A) Macrophages were infected with GFP-expressing WT Mm, permeabilized, and stained with anti-K48 ubiquitin chains (top row) or anti-K63 ubiquitin chains (bottom row) in red. Specificity of K48 and K63 antibodies was tested by competition with K48 and K63 tetraubiquitin chains as described in Materials and Methods. Shown are representative images of staining with each antibody after addition of no competitor

(left), K48 (middle), or K63 chains (right). No ubiquitin chain-specific staining of bacteria was detected when the appropriate competitor was used.

(B) Macrophages infected with WT Mm expressing GFP were stained with anti-Mm antibody (red) and FK2 (blue) 3.5 HPI after permeabilization with digitonin to detect only cytoplasmic Mm. Merged image from the green, red, and blue panels is shown on the right. This image shows 100% phagosomal escape, which is not representative of the whole population of Mm at this time, but rather depicts several examples of detection of ubiquitinated Mm in the cytoplasm.

These results suggested that WT Mm ubiquitination occurred upon direct contact of the bacteria with macrophage cytosol, a hypothesis supported by the lack of ubiquitin association with ΔRD1 Mm, which never become cytosolic (Figure 2A, Figure 3A, data not shown). In contrast, the attenuated *iipA* mutant, which escapes phagosomes but grows poorly in macrophages (27), did become polyubiquitinated, suggesting that lack of ubiquitin association with ΔRD1 Mm did not reflect simple loss of virulence or decreased intracellular growth (Figure 5A).

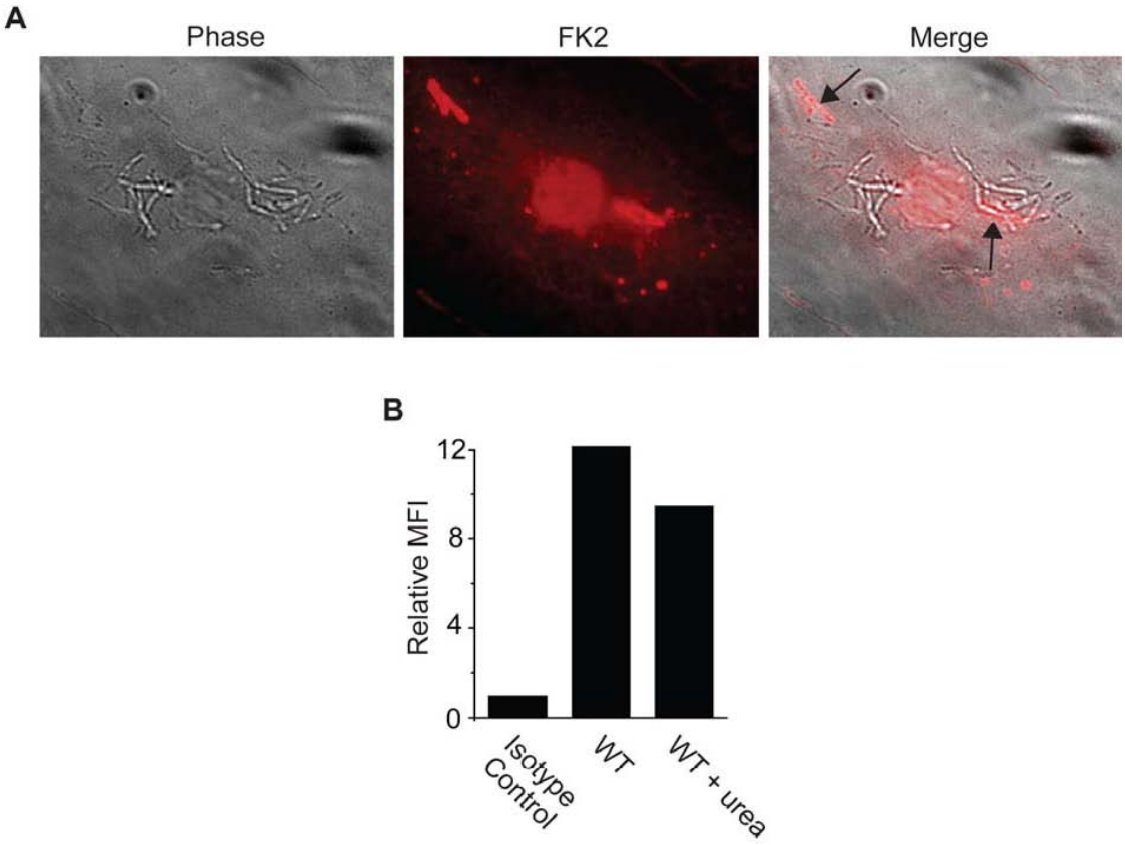

Figure 5. *Ubiquitin association of iipA mutant and urea washing to remove noncovalently attached ubiquitin from Mm.*

(A) Macrophages were infected with iipA mutant Mm (27) and ubiquitination of the bacteria was determined as described in Materials and Methods 48 HPI. Arrows point to several ubiquitinated Mm.

(B) Following ubiquitination *in vitro* as described in Materials and Methods, WT Mm were washed twice with PBS (for isotype control and WT) or with 8M urea (WT + urea), and bound ubiquitin quantitated using flow cytometry after staining with the isotype control anti-gp120 or FK2 for WT and WT + urea. Graph shows the mean fluorescence intensity divided by the mean fluorescence intensity of a ubiquitinated WT sample stained with isotype control in two independent experiments.

To determine whether defects in ΔRD1 Mm besides failure to escape phagosomes affected its ubiquitination, HeLa cell cytosol was incubated with WT and ΔRD1 Mm, as we found HeLa cells also ubiquitinated Mm during infection (data not shown). Deposited ubiquitin was detected with FK2. Immunofluorescence showed ubiquitin localization in bright patches on the surface of WT Mm, with little background staining from an isotype control antibody (Figure 6B). Quantification of ubiquitin deposition was done by flow cytometry (Figure 6C, top panel), which showed that bacterial ubiquitination was abrogated in the absence of HeLa cytosol, after chelation of divalent cations to remove Mg-ATP, which is required for activity of the E1 ubiquitin activating enzyme, and at 4^{o}C (Figure 6C, bottom). Binding of ubiquitin to WT Mm likely was covalent, as washing multiple times with 8M urea to disrupt noncovalent interactions did not inhibit staining with FK2 (Figure 5B). In this *in vitro* assay, ΔRD1 was ubiquitinated equivalently or at greater levels than WT, suggesting that the lack of ubiquitin association with ΔRD1 Mm during infection in macrophages was due to lack of phagosome escape rather than absence of the substrate for ubiquitination.

To test this hypothesis directly, we coinfected macrophages with ΔRD1 and WT Mm at a ratio of 1:1. Under conditions of coinfection, ΔRD1 Mm escaped from phagosomes, as shown by staining of ΔRD1-RFP with Mm cell wall antibody after permeabilization with digitonin alone (Figure 6D, top panel), presumably because of phagosome lysis by WT. Under conditions of coinfection, ΔRD1 also became polyubiquitinated (Figure 6D, bottom panel). These results demonstrate that both *in vitro* and in cells, ΔRD1 Mm can be ubiquitinated when exposed to host cytosol. Thus, the failure of ΔRD1 to be ubiquitinated in monoinfection (i.e., when used alone to infect

macrophages) results from its failure to escape from phagosomes.

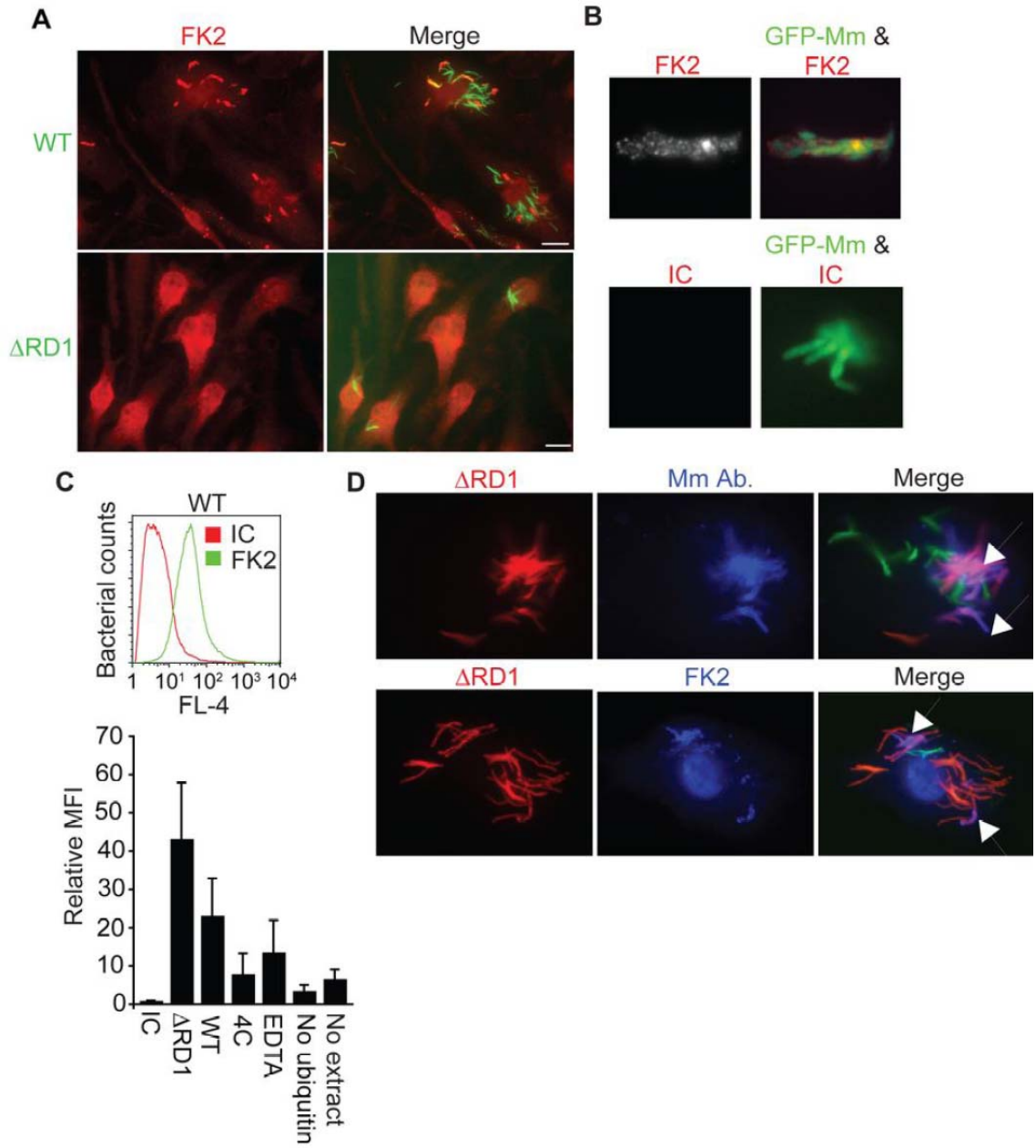

Figure 6. *ESX-1 is necessary for Mm ubiquitination in macrophages.*

(A) Macrophages were infected with WT (top panels) or ΔRD1 (bottom panels) Mm and stained with the FK2 antibody to poly- and monoubiquitin at 24 HPI (Scale bar, 10 μm). (B) Mm were ubiquitinated *in vitro* by incubating Mm with HeLa cell cytosolic extracts for 2 hours at 36°C as described in Materials and Methods. Polyubiquitination of bacteria was detected by immunofluorescence after staining with FK2; isotype control is an

antibody to HIV gp120.

(C) Flow cytometry was performed to quantify ubiquitination of Mm. Fluorescence of Mm incubated with HeLa cell extracts and stained as in (B) was measured using FACSCaliber. The histogram plot shows a representative log scale distribution of the number of bacteria (y axis) vs. fluorescence intensity for mAb staining of Mm (x axis) stained with antibody to poly- and monoubiquitin (FK2, green histogram) or with isotype control anti-gp120 antibody (IC, red histogram). The bar graph shows the ratio of mean fluorescent intensity of FK2 staining for each condition to ubiquitinated WT Mm stained with the isotype control antibody. Data expressed as mean ± SD from three independent experiments.

(D) Coinfection of macrophages with WT and ΔRD1 Mm. Macrophages were coinfected with WT Mm expressing GFP and ΔRD1 Mm expressing RFP at a ratio of 1:1. 24 HPI macrophages were permeabilized with digitonin and stained with anti-Mm (top row, middle panel) to detect cytosolic bacteria, or with FK2 after permeabilization with Triton X-100 to detect bacterial ubiquitination (bottom row, middle panel). Merged images in the right panels show WT-GFP (green), ΔRD1-RFP Mm (red) and anti-Mm (blue in top panel) or FK2 (blue in bottom panel). Arrows point to ΔRD1-RFP Mm stained by anti-Mm in cytosol (top right) or ubiquitinated (bottom right). In absence of coinfection, ΔRD1 Mm were never seen ubiquitinated or found in cytosol (data not shown).

Ubiquitin-associated Mm are incorporated into intracellular LAMP-1-positive compartments independent of autophagy

Despite the association of ubiquitin with cytosolic bacteria at 3.5 HPI, we did not observe any ubiquitin-associated WT Mm that formed actin tails at 24 HPI (Figure 7A). Instead, at this time the ubiquitinated bacteria appeared to be reinternalized into membrane bound compartments, because the frequency of detection of ubiquitinated bacteria stained after digitonin permeabilization decreased, even though the total number of ubiquitinated bacteria detected after Triton X-100 permeabilization did not change over time (Figure 7B). At 24 and 48 HPI, fewer than 20 to 25% of ubiquitinated WT Mm were detected after plasma membrane permeabilization with digitonin alone. In support of the hypothesis that lack of accessibility to FK2 represented resequestration into a membrane-bound compartment, ubiquitinated WT co-localized with the late endosomal/lysosomal marker LAMP-1 (Figure 8A). Some Mm appeared with LAMP-1 in discrete patches (top row of Figure 8A) while the entire contour of others appeared to be surrounded with LAMP-1 (bottom row of Figure 8A); these patterns suggested recruitment and fusion of lysosomes to surround ubiquitinated Mm. By 24 HPI, 64% of ubiquitinated bacteria were associated with LAMP-1, a frequency that did not change at later times (Figure 8B). At all time points, almost all bacteria associated with LAMP-1 were ubiquitinated (Figure 8C). In addition, in three independent experiments, at 3.5 and 24 HPI, respectively, 5.7% ± 6.15% (SD) and 0% of ΔRD1 Mm co-localized with LAMP-1 when macrophages were infected with these ESX-1–deficient bacteria alone, implying that WT Mm in LAMP-1 positive compartments were derived from those that had escaped into the macrophage cytosol. To further characterize the nature of the

LAMP-1 positive compartments, we next studied these at the ultrastructural level, using immunoEM. LAMP-1 positive membranes surrounded FK2 positive WT Mm and FK2 positive material close to the Mm (Figure 8D). The FK2 positive material was surrounded by two membranes enclosing a narrow, electron-lucent space, as in the case of an autophagosome, but containing LAMP-1, which is unusual for autophagosomal membranes (Figure 8D).

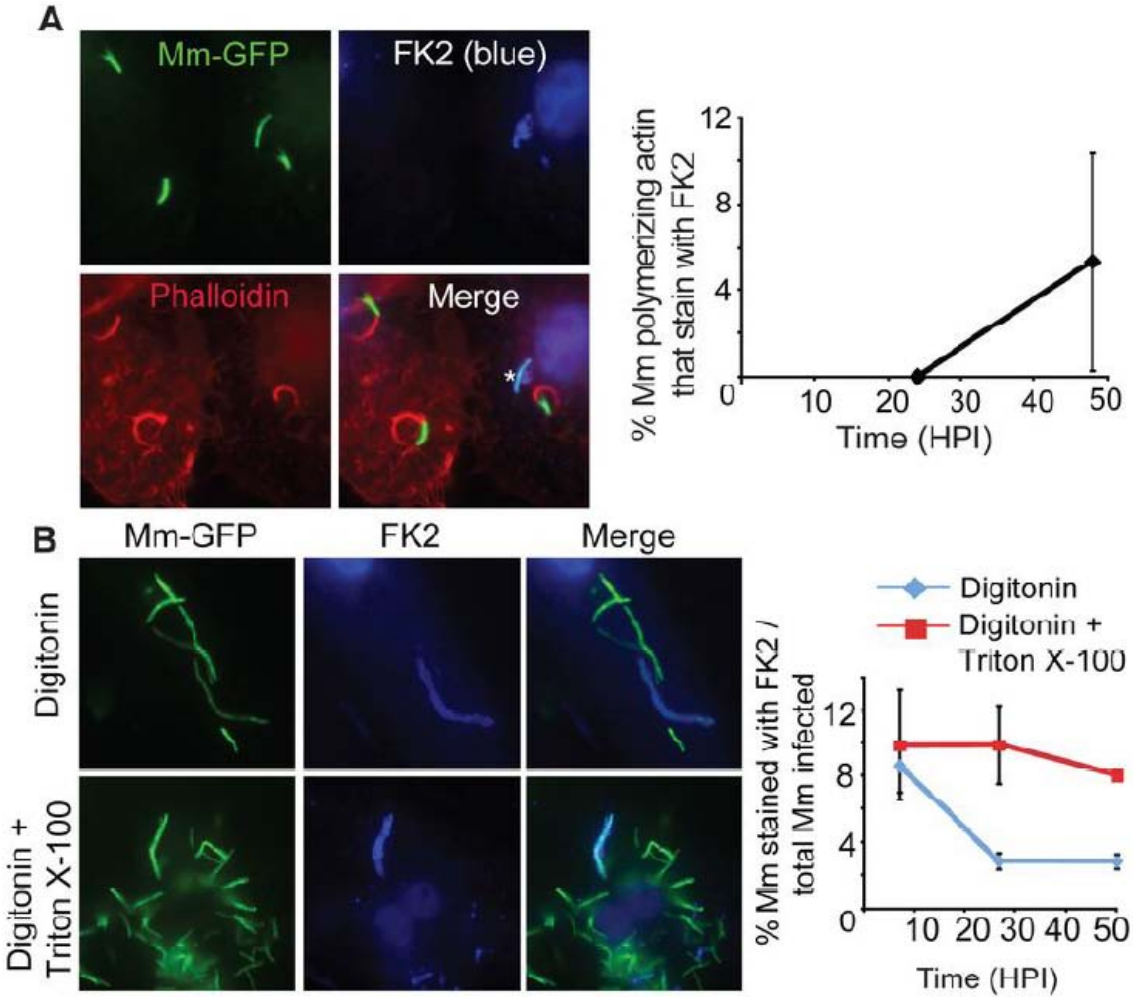

Figure 7. *Sequestration of ubiquitinated Mm.*

(A) 24 HPI with WT Mm expressing GFP, macrophages were permeabilized with Triton X-100 and stained with FK2 (blue, top right) and phalloidin-Alexa 594 (red, bottom left). In merged image (bottom right), ubiquitinated Mm (shown with asterisk) had no association with polymerized actin. The graph on the right shows the percentage of Mm with actin tails that also stain with FK2 quantified 24 and 48 HPI in fifty infected macrophages. Data shown as the mean ± SD of three independent experiments.

(B) 24 HPI with WT Mm, macrophages were permeabilized with digitonin (top row) or

digitonin followed by Triton X-100 (bottom row) and subsequently stained with FK2 (blue). Merged images of the two panels is shown in the right panels. Maintenance of phagosome integrity after digitonin permeabilization was confirmed by lack of staining of ΔRD1 with the Mm antibody (data not shown). The graph on the right shows the percentage of ubiquitinated Mm at various times after infection in macrophages permeabilized with digitonin alone (diamonds, blue line) or with digitonin followed by Triton X-100 (squares, red line). Data are mean ± SD of three independent experiments, each examining at least 50 infected macrophages at each time point.

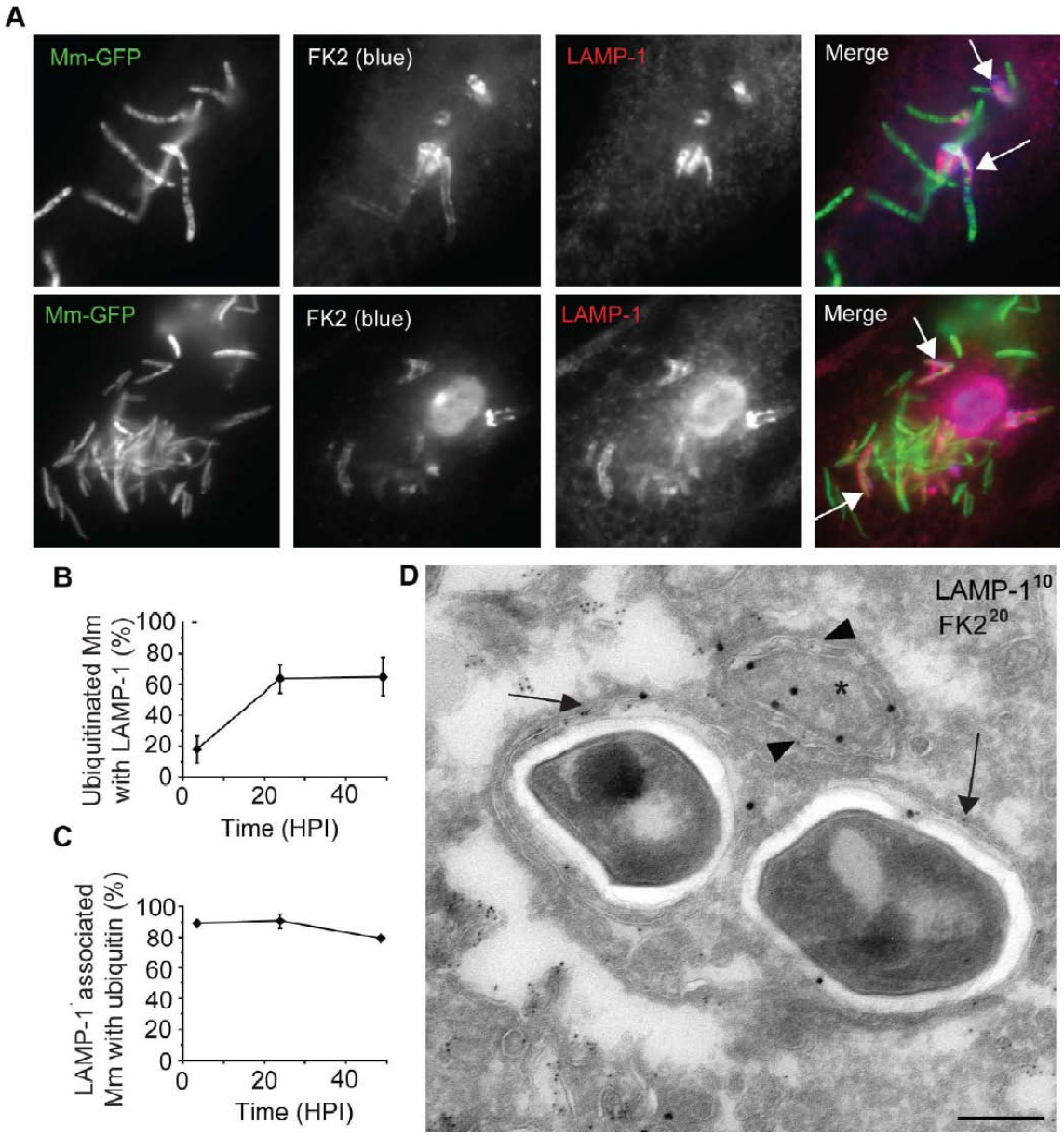

Figure 8. *Association of ubiquitinated Mm with LAMP-1.*

(A) 48 HPI macrophages infected with GFP-expressing WT Mm were fixed and permeabilized with Triton X-100 and subsequently stained with FK2 (2nd panel, blue) and antibody to LAMP-1 (3rd panel, red). Merged images of the green, red, and blue fluorescence is shown in the right panel. Arrows point to bacteria showing co-localization

of ubiquitin and LAMP-1, with top row showing LAMP-1 in discrete patches and bottom row showing ubiquitinated bacteria surrounded by LAMP-1.

(B) Quantification of percent of ubiquitinated Mm that co-localize with LAMP-1 at various times after macrophage infection. Data are depicted as mean ± SD of three independent experiments, with at least 50 macrophages counted per experiment.

(C) Quantification of percent LAMP-1 positive Mm that ubiquitinated at various times after macrophage infection. Data are depicted as mean ± SD of three independent experiments, with at least 50 macrophages counted per experiment.

(D) Ultrathin cryosections of macrophages 24 HPI with WT Mm were double-labeled with anti–LAMP-1 (10 nm gold particles) and FK2 anti-ubiquitin (20 nm gold particles). Arrows point to examples of LAMP-1 labeling on membranes surrounding ubiquitinated Mm. Immediately adjacent to the Mm, ubiquitinated material (asterisk) is enclosed within a double membrane positive for LAMP-1 (arrowheads). Scale bar, 200 nm.

The morphology of the LAMP-1 positive compartment containing ubiquitinated WT Mm was difficult to define by immunoEM, as it was compromised by the pre-embedding labeling procedure, including permeabilization, required for FK2 labeling (see Materials and Methods). Therefore, to examine in more detail the nature of the membrane compartments enclosing the Mm, electron microscopic analysis was performed on cells directly embedded (without permeabilization) in Epon resin at various times after macrophage infection. At 3.5 HPI, 43% WT Mm appeared to be in the cytosol and 53% in phagosomes. 2% appeared in double membrane vacuoles, consistent in morphology with autophagosomes (Figure 9A, top panel), and 2% were in lysosomes containing heterogeneous material including organelles and membranes (Figure 9A, bottom panel). By 24 HPI the number of WT Mm in vesicles with the morphologic characteristics of autophagosomes and lysosomes increased to 9% and 27%, respectively (Figure 9A and 6B). 100% of ΔRD1 appeared to be in phagosomes at 3.5 and 24 HPI (N=83 and 19 respectively for each time point, data not shown).

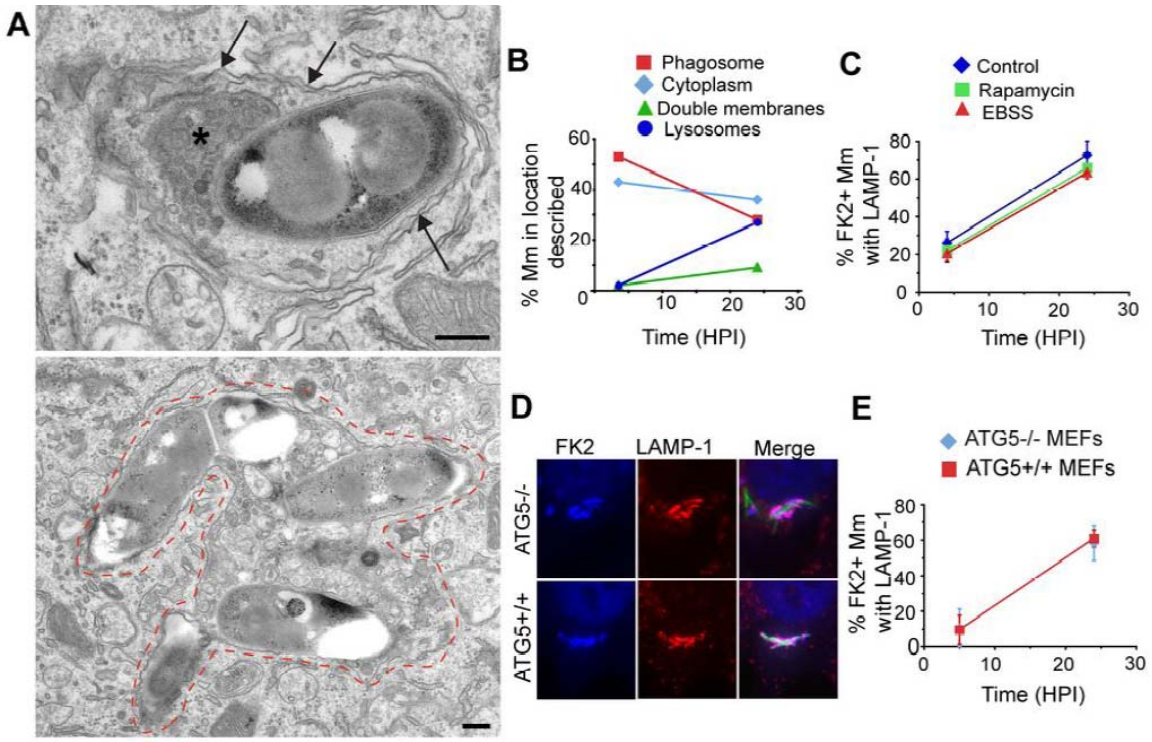

Figure 9. *Atg5-independence of Mm sequestration.*

(A) At 24 HPI, many Mm appear enclosed in membrane-lined compartments morphologically similar to autophagosomes and autolysosomes. The top image shows a bacterium in close association with a double membrane structure suggestive of an autophagosome (arrows). The double membranes also appear to extend around characteristic dense material (asterisk), similar to the ubiquitinated material shown adjacent to Mm in Figure 3C (right image). The bottom image shows Mm enclosed in an single membrane (auto)lysosomal vacuole containing a large amount of membranes and debris in addition to the bacteria, with dashes showing the outline of the vacuole. Scale bars, 200 nm.

(B) Quantification of number of Mm in single membrane phagosomes (squares, red line), the cytosol with no associated membranes (diamonds, light blue line), in double membrane structures (triangles, green line) or single membrane lysosomes (circles, dark

blue line) exemplified in Figure 9A. The 3.5 HPI data is from one experiment (N=177) and the 24 HPI data is the average of two independent experiments (N= 138 and 160).

(C) Autophagy was induced in macrophages by preincubating cells with rapamycin (squares, green line), or EBSS (triangles, red line) for 2 hours before infection. Control cells were incubated in standard macrophage growth media (diamonds, blue line). 4 or 24 HPI of these cells, the percentage of ubiquitinated bacteria co-localizing with LAMP-1 was determined as described in Figure 8. The graph shows the mean ± SD of 50 cells per condition at each time point for three separate experiments.

(D) ATG5-/- (top row) and ATG5+/+ (bottom row) MEFs were infected with GFP-expressing WT Mm for 24 hours and stained for ubiquitin (left panels, blue in merged image) and LAMP-1 (middle panels, red in merged image). As in macrophage infection, ubiquitinated Mm co-localizing with LAMP-1 are evident.

(E) The percentage of ubiquitinated Mm co-localizing with LAMP-1 was determined at 5 and 24 HPI. Graph represents mean ± SD of three independent experiments for ATG5+/+ MEFs (squares, red line) or ATG 5-/- MEFS (diamonds, blue line). At least 50 infected cells were counted at each time point in each experiment.

Because the double membrane structures into which ubiquitinated WT Mm were sequestered resemble autophagosomes, and M. tuberculosis has been reported to localize to autophagosomes and then to autolysosomes after induction of autophagy (20), we tested whether LC3, an early marker for autophagy (14), co-localized with ubiquitinated WT Mm at various times after infection. While LC3 occasionally appeared closely apposed to both FK2 stained and unstained WT Mm in both control and starved cells, (Figure 10A), fewer than 3% of ubiquitinated WT Mm co-localized with LC3 at 4 and 24 hours, and overall less than 1% of WT associated with LC3 (Figure 10C). As positive controls for LC3 staining, anti-LC3 detected LC3 aggregates in macrophages after induction of autophagy by starvation or after rapamycin treatment, associated with a conversion of LC3-I to the membrane bound form LC3-II, (Figure 10B, 10F). Thus, there was insignificant association of LC3 with ubiquitinated WT Mm at any point examined during macrophage infection.

To determine whether induction of autophagy could enhance association of ubiquitinated WT Mm with LAMP-1, macrophages were starved or treated with rapamycin 2 hours before infection, and co-localization of ubiquitinated bacteria with LAMP-1 positive vesicles was determined 4 and 24 HPI. Though LC3-I was converted to LC3-II under these conditions (Figure 10F), neither starvation nor rapamycin increased the rate of uptake of ubiquitinated WT into a LAMP-1 positive compartment (Figure 9C). Preincubation of macrophages with IFN-γ, which induces autophagy in the RAW264.7 macrophage cell line (20), also did not affect Mm targeting to LAMP-1 positive vacuoles (Figure 10D). In the absence of additional stimulation to autophagy, there was no increased conversion of LC3-I to LC3-II in infected macrophages between 6 and 24 HPI,

while resequestration of cytosolic WT Mm was occurring, over the minimal levels in uninfected controls (Figure 10E), suggesting that bacterial infection does not induce an autophagy response under these conditions. Thus, our experiments provide no evidence that the sequestration of WT Mm into LAMP-1 positive compartments depends on conversion of LC3 or its association with Mm-containing vesicles.

These results raised the possibility that an autophagy-independent pathway led to the sequestration of ubiquitinated WT Mm into LAMP-1 positive membrane-bound vesicles. To test definitively whether autophagy was necessary for the targeting of ubiquitin-associated WT Mm to LAMP-1 positive vacuoles, we assessed infection of $Atg5^{-/-}$ mouse embryo fibroblasts, since Atg5 is a required component of the pathway for autophagosome formation (28). As previously shown, $Atg5^{-/-}$ MEFs were unable to convert LC3-I to LC3-II after starvation and were thus incapable of activating the autophagy pathway (Figure 10G). During infection of MEFs, WT Mm escaped from phagosomes and polymerized actin (29), were ubiquitinated (Figure 9D), and ubiquitinated WT Mm were sequestered into LAMP-1 positive compartments (Figure 9E), thus recapitulating the major events in Mm infection of macrophages. Moreover, ubiquitinated mycobacteria associated with LAMP-1 in $Atg5^{+/+}$ and $Atg5^{-/-}$ MEFs with similar kinetics, increasing over time from about 10% at 5 hours to about 60% at 24 hours (Figure 9D and 9E). Thus, the incorporation of cytosolic ubiquitinated WT Mm into a LAMP-1 positive compartment occurred independently of the events of classical autophagy. In addition, lack of Atg5 had little effect on the survival and replication of Mm at 24 HPI, with infected $Atg5^{+/+}$ MEFs having 1.03 ± 0.32 fold the colony forming

units as Atg5$^{-/-}$ MEFs (average ± SEM of three independent experiments).

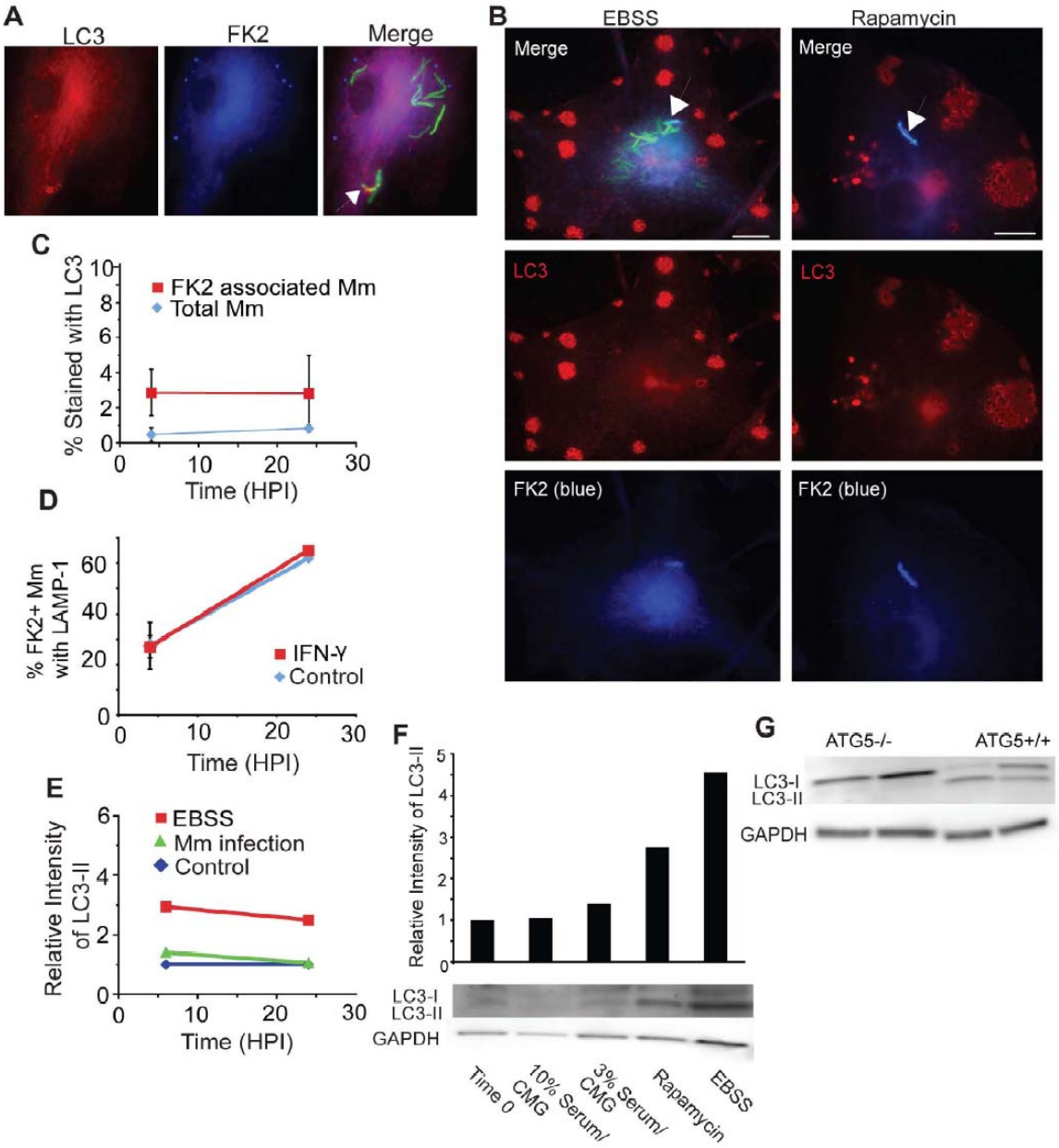

Figure 10. *LC3 staining and autophagy induction in macrophages.*

(A) Macrophages were infected with GFP-expressing WT Mm for 24 hours, permeabilized with saponin, and stained for LC3 (left panel) and FK2 (middle panel). Right panel shows a merge of LC3, FK2, and Mm-GFP; LC3 associates with a Mm that is not ubiquitinated (arrow).

(B) Macrophages were incubated for 2 hours with EBSS or rapamycin (50 μg/mL) and

then infected with GFP-expressing WT Mm in the same media. 24 HPI, infected macrophages were stained for LC3 (red) and FK2 (blue). Merged images of all fluorescence channels are shown for EBSS (left) and rapamycin (right). Although there is increased aggregation of LC3 in response to the autophagic stimuli (compare with LC3 staining in (A)), there is minimal association of LC3 with ubiquitinated bacteria (arrows) (Scale bars, 10 μm).

(C) LC3 association with Mm was quantitated for all intracellular Mm (diamonds, blue line) and for ubiquitinated Mm (squares, red line) 4 and 24 HPI. Data are graphed as mean ± SD for three independent experiments.

(D) Macrophages were incubated for 2 hours with media or 300 U/ml IFN-γ and infected with WT Mm for 4 or 24 HPI, fixed and stained for LAMP-1 and FK2. Graph shows the percent ubiquitinated Mm associated with LAMP-1 in at least fifty macrophages, ± SD for three independent experiments for 4 HPI and two independent experiments for 24 HPI.

(E) 2, 6, and 24h after infection with WT Mm, macrophages were lysed and LC3-II quantitated as described in Materials and Methods, as the relative level of LC3-II of infected macrophages (triangles, green line) or macrophages incubated with EBSS (squares, red line) compared to the uninfected control incubated in 3% FCS and 3% CMG (diamonds, blue line), normalized to the level of GAPDH intensity for each condition. Mm infection did not affect the low level of LC3-II present at any time point. Average of two experiments is shown.

(F) Macrophages were incubated in media containing 10% FCS and 10% CMG supernatant (2nd column); media containing 3% FCS and 3% CMG (third column);

rapamycin (4th column), or EBSS (5th column) for 2h. The 10% FCS/10% CMG condition was included to show that the 3% FCS/3% CMG media used during Mm infection does not induce autophagy. Cell lysate was separated by SDS-PAGE and LC3 detected by WB, and the levels of LC3-II normalized to GAPDH levels, quantitated as described in Materials and Methods. The graph depicts the average of the intensity of the normalized LC3-II band for each condition divided by the normalized LC3-II band from macrophages taken directly from culture at the start of the experiment (Time 0) for three independent experiments. The Western Blot is from a representative experiment.
(G) ATG5+/+ and ATG5-/- MEFs were starved in EBSS for 4h and LC3-II levels were compared by Western blot.

Mycobacterial cell wall alteration during infection

Our EM images suggested that, in addition to the ubiquitin attached directly to the mycobacterial cell wall, there was a large amount of ubiquitin associated with dense membrane networks in close proximity to the cytosolic bacteria (Figure 3C, right image). These typical membrane networks were only seen upon macrophage infection with WT Mm and not in uninfected cells or during infection by ΔRD1 Mm (data not shown). We found that these membranes were at least in part Mm-derived because when infected macrophages were permeabilized with digitonin and stained with anti-Mm cell wall antibodies, bacterial cell wall material was often localized in small dots or vesicles near cytosolic bacteria by immunofluorescence (Figure 11A). Moreover, when bacteria were fluoresceinated prior to macrophage infection, following methods developed previously (30), shed cell wall material could be seen at 3.5 HPI both by electron microscopy using an anti-fluorescein antibody and by direct fluorescence microscopy (Figure 11B and 11C). This shed cell wall material was often ubiquitinated, and appeared to be incorporated in the dense membrane networks adjacent to cytosolic bacteria (Figure 11B and 11D). Host membranes also contributed to this "peri-bacterial" ubiquitinated material: when cholera toxin B was used to label the macrophage lipid raft marker GM1 for 8 minutes before infection, it co-localized with these ubiquitinated membranes at 3.5 hours after infection (Figure 12). In addition, in immunoEM preparations, the fluorescein- and ubiquitin-positive membranes had the appearance of a bilayer and not of an Mm cell wall (Figure 3C, Figure 11C). These host- and Mm- derived dense membrane networks may represent residual phagosome membranes, with which mycobacterial cell wall molecules remain associated after Mm escape. Alternatively, released hydrophobic Mm cell wall molecules in the cytosol may mix nonspecifically with host membranes.

Thus, it appears that Mm shed ubiquitinated cell wall material in macrophages. Since we observed only ubiquitinated mycobacteria in LAMP-1 positive vacuoles, shedding of the cell wall may represent a strategy to evade this fate. This view is supported by the EM observation of the dense membrane networks enclosed in a double membrane lining (data not shown).

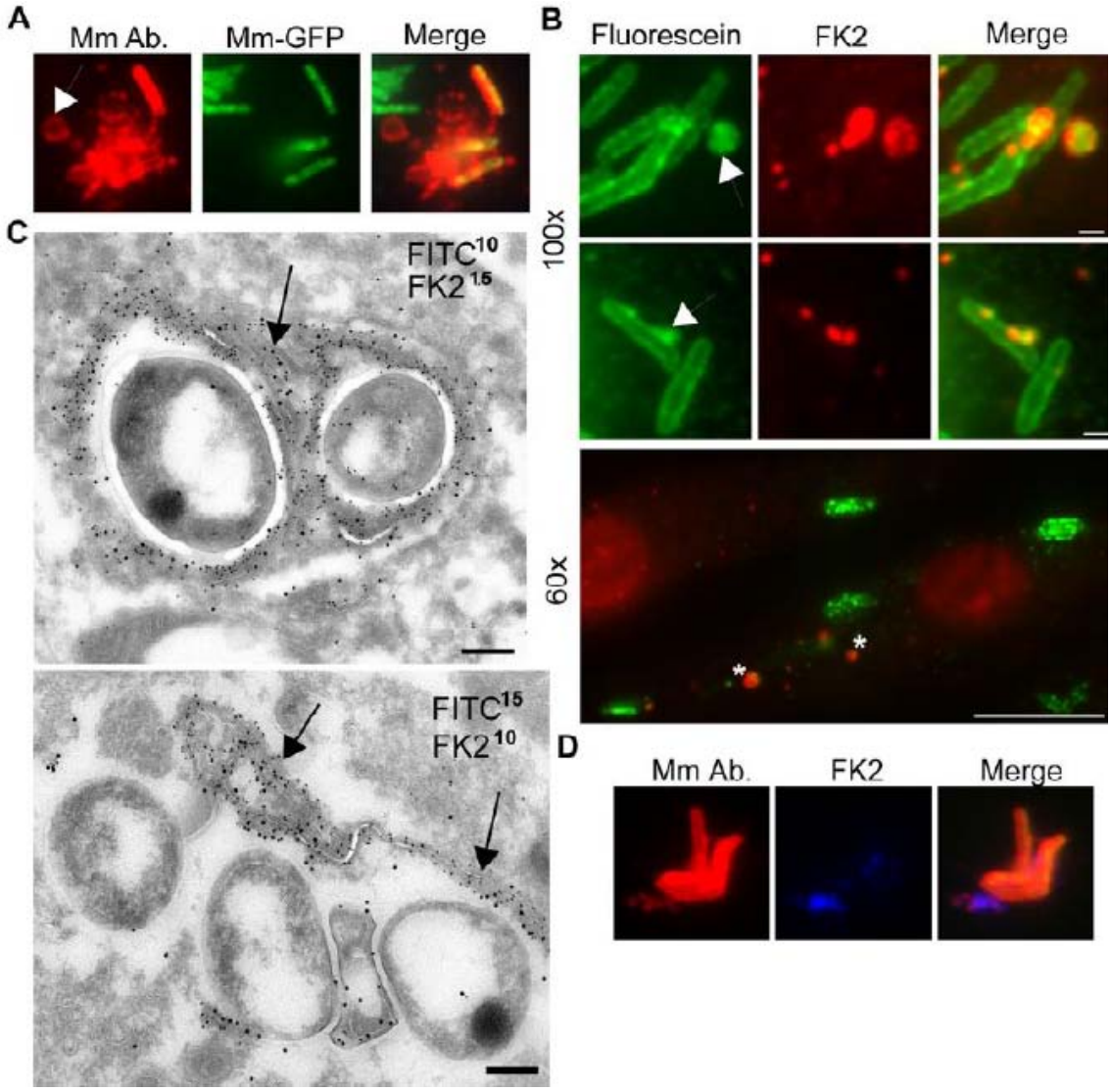

Figure 11. *Release of ubiquitinated Mm surface molecules in macrophage cytosol.*

(A) Macrophages infected for 3.5 hours with GFP-expressing Mm were permeabilized with digitonin and stained with anti-Mm antibody (left panel, red). Middle panel shows GFP fluorescence and right panel is a merged image of the green and red fluorescence. Arrow points to a region of Mm antibody staining distinct from intact bacteria.

(B) Mm were labeled with CFSE prior to infection of macrophages, which were subsequently stained with FK2 anti-ubiquitin. CFSE fluorescence is shown in the left panel (green), and FK2 staining in the middle panel (red). Top two rows show 100x

magnification of cells fixed at 6.5 HPI (Scale bar, 1 μm), demonstrating release of CFSE labeled, ubiquitinated material (arrows); bottom image shows a 60x magnification demonstrating multiple collections of released, ubiquitinated Mm material at 3.5 HPI (asterisks) (Scale bar, 10 μm).

(C) Mm were labeled with CFSE as above for immunoelectron microscopy. Ultrathin cryosections of macrophages at 3.5 HPI were double-labeled with FK2 and anti-fluorescein, each followed by protein-A gold particles of the indicated sizes in nm. Both images of co-localization at the bacterial surface (upper image) and co-localization on the characteristic membranes (arrows) associated with the bacteria (upper and lower image) were obtained. Note that in the lower image, there is little staining of the bacterial surface with either anti- fluorescein or anti- ubiquitin. Scale bars, 200 nm.

(D) Macrophages were infected with GFP-expressing Mm, stained with anti-Mm after digitonin permeabilization (left panel, red) and FK2 (middle panel, blue). Merge shows co-localization of anti-Mm with FK2 staining.

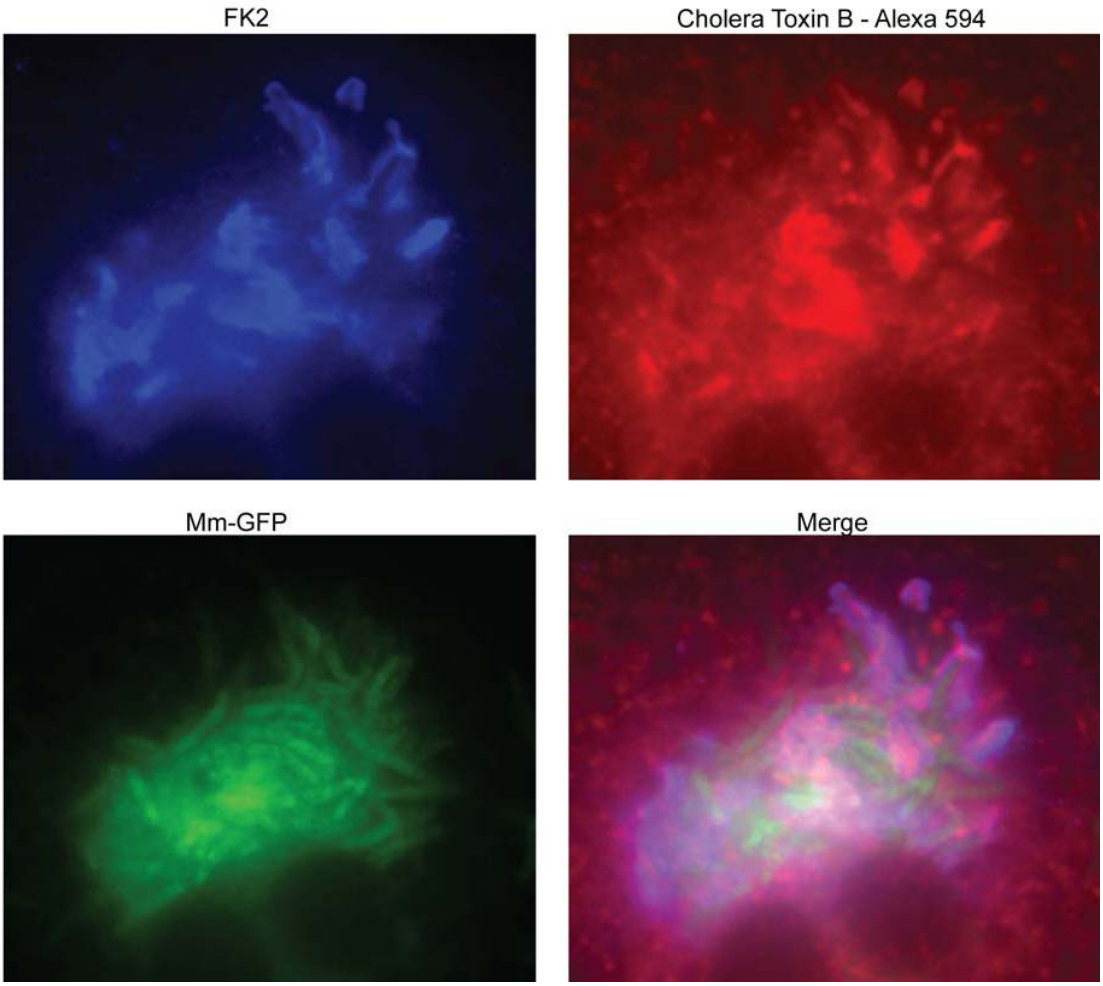

Figure 12. *Association of host-derived membranes with ubiquitinated shed Mm cell wall molecules.*

Macrophages were preincubated with Cholera Toxin B-Alexa 594 (red) for 8 minutes and infected with WT for 3.5 hours. Cells were then fixed and stained with FK2 (blue). Purple shown in the merge are areas of overlap between red and blue.

To test whether any alterations in Mm cell wall antigenicity might accompany the shedding of ubiquitinated cell wall antigens, Mm were stained with anti-cell wall antibody at various times after infection, using TX-100 permeabilization to allow the antibody access to all intracellular bacteria. 100% of both WT and ΔRD1 Mm stained with the antibody at 3.5 hours, and ΔRD1 continued to be recognized by the cell wall antibody throughout the 48h experiment (Figure 13, quantified in bottom right panel). In contrast, at 24 and 48 HPI, only about 60% of WT Mm stained with the antibody. The changes to the cell wall did not appear to be a direct mechanism of ubiquitin evasion, since at 24 and 48 hours only 71% and 28% of ubiquitinated WT Mm stained with the antibody, indicating that Mm which exhibited changes to their cell wall could still be ubiquitinated (data not shown). The ubiquitination of Mm exhibiting cell wall changes hints at a continuous process, since Mm exhibit these changes only at later time points of infection and thus must be ubiquitinated after many hours of residence within the macrophage, possibly after shedding their initial wall. In contrast to ubiquitin association, actin polymerization and staining with the anti-cell wall antibody were negatively correlated, since 20% of WT Mm with actin tails at 24 and 48 HPI stained with the Mm antibody (Figure 13, quantified in bottom right panel). This result suggests that cell wall alterations during residence in the cytosol may be required for WT Mm to gain the ability to polymerize actin.

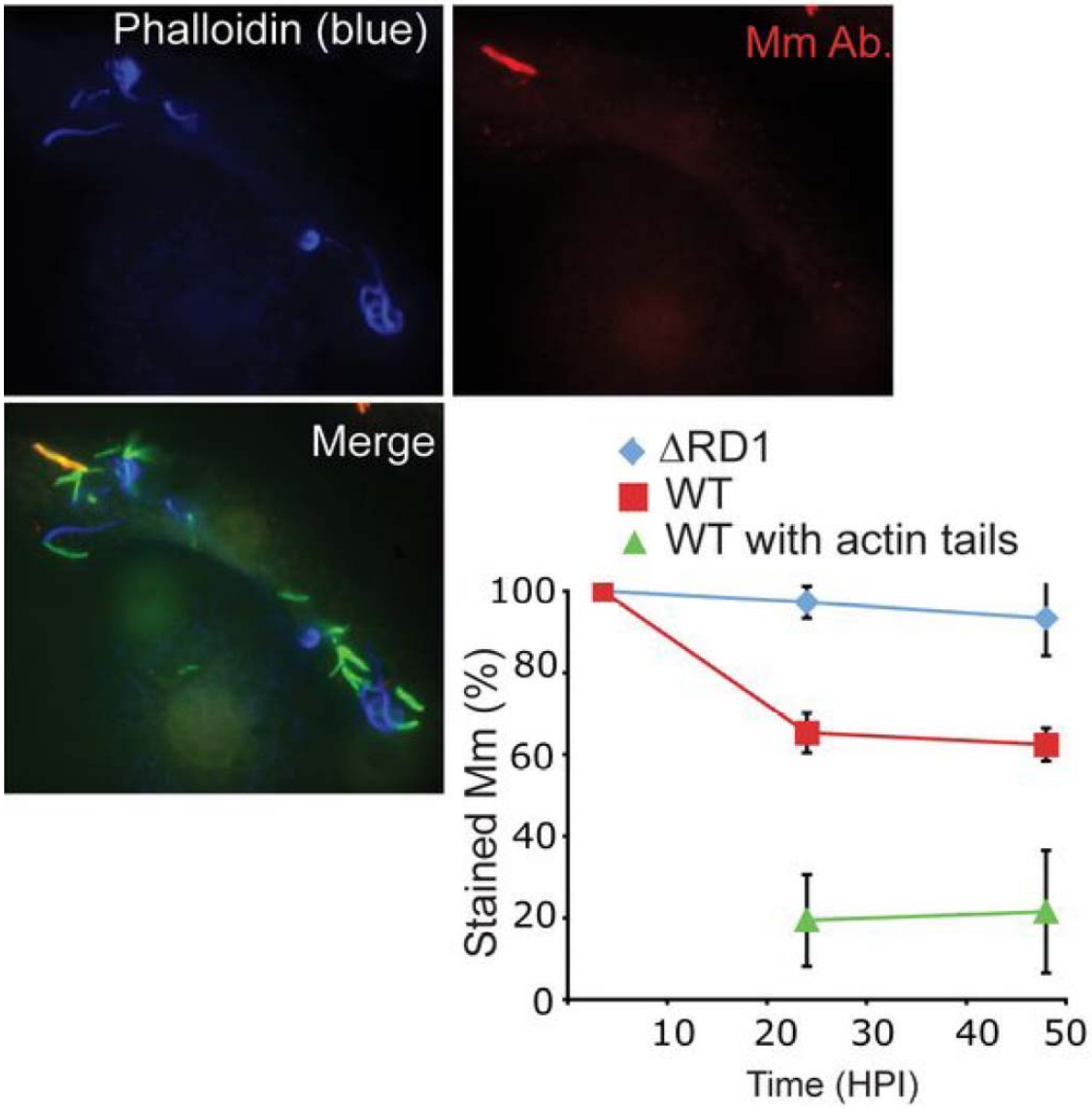

Figure 13. *Alteration in Mm antigenicity during macrophage infection.*

24 HPI with GFP-expressing WT Mm, macrophages were permeabilized with digitonin and Triton X-100 and stained with phalloidin-Alexa 350 (left panel, blue in bottom merged image) and anti-Mm (right panel, red in bottom merged image). Multiple cytosolic bacteria that polymerized actin failed to be recognized by anti-Mm. In bottom right panel, the percentage of infecting Mm that stained with the anti-Mm antibody was quantitated for ΔRD1 (diamonds, blue line) and WT Mm (squares, red line) during 48h of infection. The percentage of WT with actin tails that stained with the anti-Mm antibody

(triangles, green line) also was determined. Graph shows mean ± SD for three independent experiments.

Discussion

Escape from phagosomes underlies the mechanism by which Mm and distantly related bacteria such as *Shigella* and *Listeria* enhance cell-to-cell spread of infection (31). For Mm, phagosome escape requires a specialized secretion system, ESX-1 (6). Cytosolic bacteria polymerize actin to induce motility, the mechanism underlying the increased cell-to-cell spread. Cytosolic bacterial products also can activate innate immunity through sensors such as NODs (32). In this study we describe an entirely different fate for a subset of cytosolic bacteria. These bacteria become ubiquitinated and then are resegregated from the cytosol into a LAMP-1–positive compartment, which forms independently of Atg5, an essential component of classical autophagosome formation. Our data indicate that Mm may have evolved strategies to avoid sequestration, apparently involving cell wall shedding to deplete the ubiquitin signal and alterations in cell wall antigenicity that may promote actin polymerization, as illustrated in the model in Figure 14.

The observation that cytosolic bacteria were either ubiquitinated or motile (with actin tails), but not both, suggests that these are alternative fates. Since both actin polymerization and ubiquitination are self-reinforcing, there may be competition between the two reactions at the bacterial surface, with either outcome negatively feeding back on the other. If this is the case, the outcomes of actin polymerization or ubiquitination may be determined by specific characteristics of the bacteria's surface during residence in the cytosol.

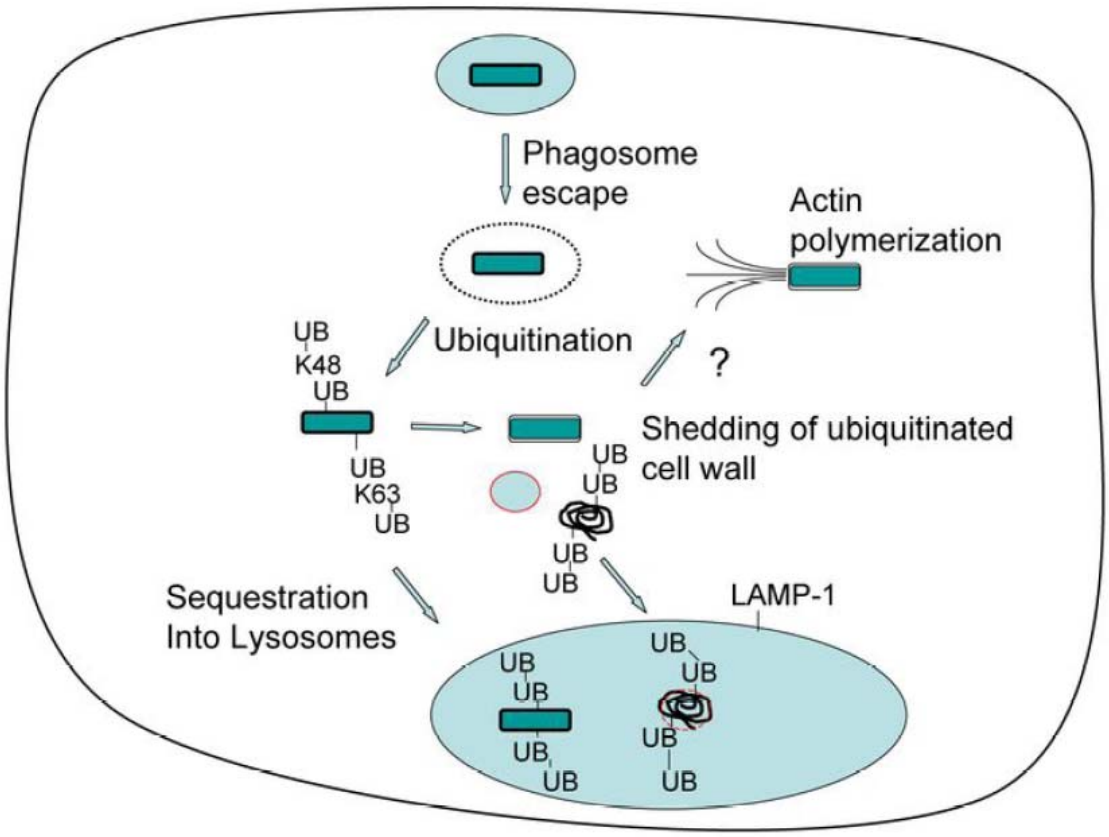

Figure 14. *Alternative fates for cytosolic Mm during macrophage infection.*

After uptake into a macrophage phagosome Mm (green bar) escapes quickly into the cytosol. Cytosolic Mm may be ubiquitinated, leading to resequestration of bacteria into a LAMP-1–positive vesicle. Alternatively, ubiquitinated bacteria may shed ubiquitin with components of the bacterial cell wall. Unubiquitinated bacteria polymerize actin.

Previous studies had determined that Mm do not gain the ability to polymerize actin until many hours after initial infection and had inferred from this fact that escape from phagosomes was likewise slow (12). In the current study, we have developed methods to examine phagosome escape independent of actin polymerization and show, both by differential solubilization techniques and by electron microscopy, that bacteria enter the cytosol much earlier than previously thought. By 3.5 HPI, 20-40% of internalized bacteria have escaped from phagosomes to the cytosol. Early escape allows access of the mycobacterial wall to ubiquitination machinery; because we observed that a large amount of ubiquitinated cell wall was lost from the bacteria, Mm may continuously shed ubiquitinated wall molecules into the cytosol, allowing time for the underlying deubiquitinated surface to express surface characteristics required for actin polymerization (Figure 14). The ubiquitination of Mm with significant cell wall alterations, as demonstrated by loss of reactivity with antibody to *in vitro* grown bacteria, hints at an ongoing process, since these Mm must be ubiquitinated after this antigenic shift, possibly after shedding their original wall.

Ubiquitinated Mm were sequestered in LAMP-1 positive vacuoles. We considered the possibility that the membranes recapturing cytosolic Mm were generated through autophagy, as this process has been identified as an important pathway in innate defense against several intracellular pathogens, including both Gram positive or (L. monocytogenes and S. pyogenes) and Gram negative (S. typhimurium and S. flexneri) bacteria as well as M. tuberculosis (17,18,16,19,20). However, our evidence suggests that resegregation of Mm from the cytosol by the LAMP-1–positive macrophage membranes is by a process distinct from classical autophagy, since the majority of bacteria-associated

host membranes do not express LC3, a marker of autophagosomal membranes, and their formation is independent of Atg5. This is quite distinct from the other bacterial pathogens known to be incorporated into cytosolic vesicles, which have clearly associated LC3-containing membranes dependent on Atg5 for their formation. These results also differ from studies highlighting the importance of autophagy in targeting M. tuberculosis var. bovis bacilli Calmette Guérin (BCG) to lysosomes, since autophagy induction enhances BCG co-localization with lysosomal markers LAMP-1, cathepsin D, LBPA and the V_oH^+-ATPase (20). Autophagy induction also decreased survival of BCG and M. tuberculosis H37Rv, while we observed no difference in Mm's survival in wild type or Atg5 deficient MEFs (20). It is possible that the differences we observe between Mm and BCG are due to the latter bacteria's propensity to remain in the primary phagosome, while Mm clearly has an intracellular phase when it is not enclosed in a membrane-bound vacuole. BCG appears not to activate autophagy as a direct consequence of infection, but to become entrapped in an autophagosome after induction by another signal or after IFN-γ activation of macrophages (20,33). In contrast, ubiquitinated Mm become resequestered in lysosome-like vacuoles without any additional extrinsic signal. Possibly, autophagy engulfs BCG because of a damaged phagosomal membrane, similar to the autophagic clearance of *Salmonella typhimurium* in response to perforation of the *Salmonella* containing vacuole (SCV) rather than full escape of the microbe (16). However, ubiquitination and non-autophagic sequestration may occur later during infection with M. tuberculosis, since there is evidence that after two days it escapes to the cytosol of human monocyte-derived dendritic cells and macrophages through an ESX-1 dependent mechanism (10).

We speculate that ubiquitination is required for Mm uptake into LAMP-1 positive compartments, since virtually all bacteria associated with LAMP-1 are ubiquitinated, but this hypothesis remains unproven. Our evidence suggests that the segregation of Mm that have escaped into the cytosol occurs by a process of membrane formation initiated by a biochemical pathway distinct from classical, Atg5 dependent autophagy. One possibility is that the reincorporation of ubiquitinated Mm into a membranous compartment intersects with the ESCRT pathway, which delivers ubiquitinated cargo to multivesicular bodies and finally to lysosomes (34). The double membranes could point to elongated or cup-shaped lysosomes as have been described in liver parenchymal cells (35). In addition, the function of these compartments needs to be further established. Clearly, the LAMP-1 positive membranes segregate Mm away from the cytosol, but whether they also act as degradative compartments remains to be established.

Ubiquitination is a signal for uptake of aggregated proteins into autophagosomes, a process that requires the ubiquitin binding protein p62 (36). At this time it is not clear why ubiquitinated Mm do not trigger this autophagy response. In this regard, it is interesting that both *Listeria* and *Shigella* actively inhibit entrapment by autophagy; *Listeria* uses actin polymerizing ActA as well as other proteins to evade autophagy, while *Shigella* secretes IcsB, resulting in disruption of the interaction between Atg5 and VirG, another actin polymerizing protein (17,19). Our results showing no effect of deficiency of Atg5 on Mm growth are similar to experiments with wild type *Listeria* (17). The low level of autophagy of Mm we observed, as well as its similar ability to polymerize actin, suggests the possibility of autophagy inhibition by Mm.

Ubiquitination of Mm may also have other functions, such as targeting of the

bacteria or ubiquitinated membranes to the proteasome. Ubiquitinated *Salmonella* seems to be degraded by the proteasome, while *Listeria* is not (13). While we observed little association of the 20s proteasome with ubiquitinated Mm at 24 and 48 HPI, attempts to study involvement of the proteasome were limited since inhibition of proteasome activity with MG-132 led to loss of ubiquitination of Mm, most likely through depletion of free ubiquitin (data not shown). Regardless of whether the proteasome can degrade whole bacteria, its degradation of ubiquitinated bacterial membranes may be important in presentation of bacterial antigens via the MHC Class I pathway, a prominent feature of Mycobacterial infection (37,38).

A growing list of bacterial effectors have been shown to interfere with the host's ubiquitination system, acting as ubiquitin ligases to target host proteins for degradation, dampening signaling through inflammatory pathways such as NF-κB (39). However, the reciprocal bacterial surface molecules recognized by the host ubiquitination machinery have yet to be identified. Our results expand the list of known bacteria that are targeted by ubiquitin, as both Gram-positive *Listeria monocytogenes* and the Gram-negative *Salmonella typhimurium* associate with polyubiquitin during infection as discussed above. The mycobacterial cell wall has many distinct features, including a thick mycolic acid layer which distinguishes it from those of conventional Gram-positive and Gram-negative bacteria (40). In addition, our *in vitro* ubiquitination experiments constitute the first evidence that bacterial association with ubiquitin is a true covalent association with the bacterial surface. A prior study demonstrated that ubiquitin can come into contact with *Mycobacterium tuberculosis* and BCG in the lysosome, where the ubiquitin peptides are toxic to the bacteria (41), but in the present study several lines of evidence

demonstrate that Mm ubiquitination occurs in the cytosol. Most significantly, at early times after infection the vast majority of ubiquitin-associated Mm are in the cytosol, as judged both by their exposure to antibodies after digitonin permeabilization and by electron microscopy. In addition, the ΔRD1 mutant is never ubiquitinated when infecting macrophages alone, but can be ubiquitinated when allowed to come in contact with cytosol by coinfection with WT Mm, or by mixing with host cell cytosol. This demonstrates that ESX-1 is not required for expression of the targets of ubiquitination, but is necessary for exposure of Mm to cytosolic ubiquitinating enzymes. Ubiquitination may be a response of the host to bacterial cell wall proteins or other molecules that it detects as abnormal in some way, similar to the response to unfolded or modified proteins. The large number of mycobacterial cell wall lipopeptides and proteins with high proline content or hydrophobic sequences (42) are likely candidates for recognition by the host ubiquitination machinery (43). However, the presence of K63-linked chains on the bacteria, usually associated with signal transduction pathways rather than protein degradation, suggests that marking bacterial proteins for destruction is not the only consequence of Mm ubiquitination (25).

In summary, Mm exhibits two apparently distinct fates upon prolonged residence in the cytosol of infected macrophages (Figure 14). On one path, ubiquitinated bacteria are sequestered into LAMP-1 positive compartments; this may limit spread of infection and lead to direct toxicity to the enclosed bacteria; on the other path, bacteria shed cell wall material and possibly escape ubiquitination and sequestration. This may permit further growth as well as dramatic changes to the mycobacterial cell wall, actin polymerization and spread of infection. We speculate that both fates may influence the

outcome of infection, since sequestration may enhance antigen presentation and activate or modulate pathways for cytokine production. At the same time, these data hint at a novel pathway for delivery of cytosolic material into lysosomes, independent of classical autophagy. It will be important and interesting to determine the mechanisms involved and whether these processes are shared by other pathogenic mycobacteria, as well as other microbes that share Mm's life style of phagosome escape and actin polymerization.

Materials and Methods

Antibodies and reagents

Antibodies to *M. marinum* (Mm) were generated by injecting rabbits with cell wall fractions from ΔRD1 Mm grown in Sauton's media. Phalloidin-Alexa 350 and phalloidin-Alexa 594 were from Invitrogen (Carlsbad, CA). Mouse monoclonal anti-conjugated ubiquitin antibodies FK1 and FK2 were from Biomol (Plymouth Meeting, PA). K48, K63, anti-her2, and anti-HIV gp120 antibodies were produced at Genentech (South San Francisco, CA). The ID4B rat monoclonal LAMP-1 antibody was from BD Biosciences (San Jose, CA) and the LC3 antibody was from Novus Biologicals (Littleton, CO). The fluorescein antibody was from Zymed Laboratories (South San Francisco, CA). The GAPDH antibody was from Millipore (Temecula, CA). Cholera toxin B-Alexa 594 was from Invitrogen (Carlsbad, CA). Secondary antibodies used for EM were rabbit anti-mouse IgG and anti-rat IgG (Dako, Glostrup, Denmark).

Bacteria and cell culture

WT Mm (strain M) and ΔRD1 Mm (44) were cultured in Middlebrook 7H9 (BD, Franklin Lakes, NJ) supplemented with 0.2% glycerol/0.05% Tween 80/10% ADC Enrichment (Fisher Scientific, Pittsburgh, PA). Bone marrow derived macrophages were harvested from 129/SvJ mice, cultured as previously described, and used between day 7 and 21 of growth (45). Wild type and Atg5-/- MEFs, a kind gift of Noboru Mizushima, were maintained in DMEM containing 10% FBS.

Infections

$2x10^5$ macrophages or $1x10^5$ MEFs were plated overnight in DMEM containing 10%FBS, 20 mM Hepes, 10% CMG14-12 supernatant (46) or DMEM with 10% FBS, respectively. 1 hour before infection, cells were washed with PBS and placed in DMEM containing 3% FBS and 3% CMG for macrophages or 3% FBS for MEFs. Mm were washed twice in PBS and passaged through a 26-gauge needle three times to disrupt aggregates. Mm were added to macrophages at MOI of 4 to 12 for 2 hours at 32°C, and macrophage monolayers then were incubated with 200 μg/ml amikacin for 2 hours, following PBS wash, to kill extracellular organisms. After a final PBS wash, macrophages were incubated in DMEM containing 3% FBS & 3% CMG14-12 supernatant at 32°C in a 5% CO_2 humidified incubator. Alternatively, MEFs were infected for 3 hours at an MOI of 40, washed and incubated with 200 μg/ml amikacin for 2 hours, washed to remove the drug and incubated for the indicated time. To count colony forming units, MEFs were infected for 5 hours, washed with PBS and lysed with 0.25% Triton X-100 in PBS after 24 hours.

Differential permeabilization with digitonin

Infected macrophages were washed 2x with KHM buffer (110 mM potassium acetate, 20 mM Hepes and 2 mM $MgCl_2$), incubated with KHM containing 25 ug/mL digitonin for 1 minute at room temperature and then washed 1x with detergent-free KHM buffer. Macrophages were then incubated with antibody (anti-Mm and/or FK2) in KHM containing 2% BSA or with buffer alone at 32°C for 12 minutes, washed with PBS and fixed with 4% PFA. Macrophages that had been incubated with buffer alone were then

permeabilized with 0.2% Triton X-100 for 4 minutes and then stained with the appropriate primary antibodies, or the appropriate secondary antibodies if they had already received the primary. Bound antibody was visualized with Alexa 350-conjugated goat anti- mouse $F(ab')_2$ (Invitrogen, Carlsbad, CA) for FK2 or Alexa 594-conjugated goat anti- rabbit $F(ab')_2$ (Invitrogen, Carlsbad, CA) by incubating in 2% BSA in PBS for 30 minutes. Controls omitting primary antibodies showed minimal fluorescence from the secondary antibodies alone, minimal crossreactivity of the anti-mouse $F(ab')_2$ or anti-rabbit $F(ab')_2$ with bound antibody of the other species, and insignificant bleedthrough of green fluorescence into the red channel and vice versa. Stained samples were viewed using an Axioplan 2 light microscope (Carl Zeiss MicroImaging) with a Semrock filter set and images were recorded with a $CoolSNAP_{HQ}$ CCD camera (Photometrics).

Immunoelectron microscopy

Macrophages were fixed with 2% PFA and 0.2% glutaraldehyde in 0.1 M phosphate buffer, pH 7.4 for 2 hours at room temperature. Alternatively, they were fixed for 12 minutes with 4% PFA, permeabilized with 0.1% saponin for 6 minutes, incubated with FK2 or isotype control anti-gp120 antibody for 45 minutes, washed with PBS and postfixed with 2% PFA and 0.2% GA for 2 hours. After rinsing with PBS, the blocks were embedded in 12% gelatin, cryoprotected with 2.3 M sucrose, and frozen in liquid nitrogen as previously described (47). Ultrathin cryosections were cut at -120 ºC, picked up with 1% methylcellulose, 1.2 M sucrose, thawed and collected on copper grids. After washing with PBS containing 0.02 M glycine, sections were incubated with rabbit anti mouse IgG followed by protein-A gold for the detection of FK2 in permeabilized cells, or

single- or double-labeled with primary (and secondary) antibodies followed by protein-A gold as described earlier (47). The sections were then contrasted with a 1.8% methylcellulose, 0.6% uranyl acetate mixture. Quantification of Mm ubiquitination was performed on minimally 200 randomly screened WT Mm from each time point (3.5 HPI, 24 HPI), from at least 2 experiments.

Electron microscopy

Cells were fixed either with 2% PFA and 0.2% glutaraldehyde in 0.1 M phosphate buffer, or with half-strength Karnovsky fixative (2% paraformaldehyde, 2.5% glutaraldehyde, and 0.1 M sodium cacodylate buffer) pH 7.4 for 2 hours at room temperature. After rinsing, the cells were in situ postfixed with 1% OsO_4 and 1.5% $K_3Fe(CN)_6$, in 0.07 M Na-cacodylate stained en bloc with 0.5% uranyl acetate, dehydrated in ethanol and embedded in Epon. Ultrathin sections were cut parallel to the culture flask bottom, and stained with uranyl acetate and lead citrate. Mm were quantified as present in a phagosome, and autophagosome, or an autolysosome, if they were enclosed by a single membrane lining an otherwise 'empty' vacuole, or were surrounded together with some cytosol for at least three quarters by a double membrane lining, or were contained together with irregular vesicles and membrane sheets by a single membrane, respectively.

***In vitro* ubiquitin reactions & FACS**

Cell free ubiquitination reactions were performed by adaptation of previously described methods (48). After preparation as described above for macrophage infection, approximately 10^9 Mm were added to 200 µg S-100 HeLa cell lysate, 5 mM MG-132, 4 µM ubiquitin aldehyde to inhibit deubiquitinases, 5 µL of energy regenerating system

including phosphocreatine and phosphocreatine kinase and 600 μM ubiquitin (Boston Biochem, Cambridge, MA). After 2 hours shaking at 500 rpm at 36° C, Mm were fixed with 4% PFA in PBS, and then stained with FK2 or anti-gp120 isotype control, followed by APC-conjugated goat anti mouse IgG (Jackson ImmunoResearch, West Grove, PA). To test whether urea could disrupt ubiquitin association, WT Mm were washed twice before PFA fixation with PBS or 8 M urea, fixed and stained as described above. Flow cytometry was performed on stained bacteria using a FACSCaliber (BD Biosciences, San Jose, CA), collecting between 10,000 and 100,000 events per sample. Data analysis was performed using FlowJo Flow Cytometry Analysis Software (Tree Star, Ashland, Oregon). The relative mean fluorescence intensity (MFI) for each sample was determined by dividing the MFI of the FK2- stained sample by the MFI of a ubiquitinated WT Mm sample stained with the anti-gp120 isotype control.

Fluorescein labeling of Mm

The surface of Mm was labeled with 6-(fluorescein-5-(and-6)-carboxyamido)hexanoic acid, succinimidyl ester 5 (Invitrogen, Carlsbad, CA) as previously described (30).

Staining with K48- and K63-linkage–specific polyubiquitin antibodies

Infected macrophages were stained with monoclonal antibodies recognizing K48-linked polyubiquitin or K63-linked polyubiquitin (26) after fixation and permeabilization with 0.1% saponin. In some samples, antibodies were incubated at room temperature for 1h with K48 or K63 tetraubiquitin chains in 10-fold excess (Boston Biochem, Cambridge, MA) prior to addition to the infected macrophages, as previously described (26). Four independent competitions were performed in parallel. Bound antibody was visualized

with goat anti-human IgG-Alexa 594 (Invitrogen, Carlsbad, CA). Comparison of the percent of Mm stained with K48 and K63 was made using a chi-square test for equality of proportions.

Induction of autophagy

Macrophages were washed with PBS and incubated for 2 hours at 32°C with either EBSS (Sigma Aldrich, St. Louis, MO) or macrophage growth media containing 3% FBS & 3% CMG14-12 supernatant with 50 μg/mL rapamycin (Calbiochem, San Diego, CA) added. As controls, macrophages were incubated in identically constituted growth media without rapamycin, or in full growth media containing 10% FBS & 10% CMG14-12. Cells were then infected and incubated as described for 4 and 24 hours. For immunofluorescence, cells were permabilized with 0.1% saponin for 6 minutes and stained with anti-LC3 followed by goat anti rabbit IgG- $F(ab')_2$ (Invitrogen, Carlsbad, CA). Murine IFN-γ was from Sigma Aldrich (St. Louis, MO).

Immunoblot analysis of LC3

Detection of LC3-I and LC3-II was performed essentially as previously described (49). Briefly, after cell lysis, protein separation by SDS-PAGE, and transfer, blots were incubated with anti-LC3 overnight at 4°C. Bound LC3 antibody was detected with goat anti-rabbit conjugated to horse radish peroxidase (Jackson ImmunoResearch, West Grove, PA). Blots were stripped and reprobed for GAPDH as a loading control. Chemiluminescence was quantitated with a ChemiDoc XRS from and quantified using Quantity One Analysis Software

(Bio-Rad Laboratories, Hercules, CA) by dividing the adjusted intensities for each sample to the adjusted intensity for GAPDH.

Acknowledgments

We are grateful to Laszlo Komuves, Meredith Sagolla, and Hiroshi Morisaki for help with microscopy, and to René Scriwanek and Marc van Peski for excellent photographical assistance. We thank Nicholas Lewin-Koh for help with statistics. We thank Jayanta Debnath, Cliff Lowell, Suzie Scales, and Matt Summers for helpful discussions.

Chapter 3

Further characterization of Mycobacterial Ubiquitination

Abstract

The previous chapter described the ubiquitination of Mm and its autophagy independent sequestration into LAMP-1 positive vacuoles. This chapter contains data that further characterizes Mm ubiquitination. We show that in addition to Atg5, LAMP-1 association with ubiquitinated Mm was independent of Atg3 and Atg7, suggesting that there may be a separate pathway of reuptake from the cytosol. We found that these compartments did not appear to be acidic, as Lysotracker Red did not colocalize with the ubiquitinated Mm at 24 hours post infection (HPI). Mm infection has been shown to activate the inflammasome, resulting in release of IL-1β and IL-18. However, absence of genes involved in inflammasome activation did not affect ubiquitination of Mm. Similar to ΔRD1 mutant deficient in ESX-1, the transposon mutant *espB*$_{M}$*::tn* had decreased ubiquitin association in comparison to WT and when it was complemented with EspB, while *Mh3866::tn* and *Mh3879c::tn* showed no decreased ubiquitin association. We observed previously that Mm in macrophages could be ubiquitinated with K48 or K63 chains and here show that ubiquitin containing only K48 or K63 can be used for ubiquitination *in vitro*. We also quantified the amount of cell wall material released from WT and ΔRD1, and found that WT released significantly more material. The final section is selection of electron microscopy images with descriptions.

Introduction

As described in the introductory chapter, autophagy is a process in which membranes enclose cytoplasmic material and target it for degradation by lysosomal enzymes (1). This multi-step process involves at least 18 Atg (autophagy-related) proteins (2). After induction of autophagy and nucleation of the initial vesicle, two ubiquitin-like conjugation reactions are necessary to expand and complete autophagosome formation. First, Atg12 is covalently attached to Atg5, which binds noncovalently to Atg16, which can multimerize (Figure 1). This complex is in turn necessary for the stable conjugation of Atg8 (also known as MAP1LC3, or microtubule-associated protein 1 light chain 3) to phosphatidylethanolamine (PE). Both Atg7 and Atg3 have been shown to be necessary for autophagosome formation (3,4). Atg7 acts as an ubiquitin-activating E1-like enzyme for both reactions. Atg3 acts as an ubiquitin-conjugating E2-like enzyme for Atg8 conjugation to PE. Though we had shown that ubiquitinated Mm associated with LAMP-1 in Atg5 deficient fibroblasts, it may be possible to stimulate autophagosome formation without Atg5 since Atg5 is not absolutely required for LC3 lipidation *in vitro* (5). To test whether LAMP-1 association was independent of Atg5 or of autophagy in general, we infected Atg7 and Atg3 deficient fibroblasts with Mm and looked for colocalization with LAMP-1.

We also tested the effect of lack of the Atg5 protein on growth of Mm during the initial 24 hours of infection. Lack of Atg5 has been shown to enhance growth of Group A *Streptococcus*, *Shigella flexneri*, *Listeria monocytogenes* and *Toxoplasma gondii*. In addition to its role in autophagy, Atg5 causes damage to the vacuole through the recruitment of IFN-γ inducible p47 to the phagosome membrane (6). Thus, it is possible

that Atg5 could effect growth of Mm through the autophagy pathway or independently of autophagy.

LAMP-1, or lysosomal associated membrane protein, is often used as a marker of lysosomes. Lysosomes are vesicles often characterized by low pH and as compartments sequestering degradative enzymes from the cytoplasm (7). Despite the association of Mm with LAMP-1 at later points during infection, we did not observe association with the lysosomal hydrolase cathepsin D (data not shown). To ask whether the ubiquitin associated Mm were in acidic compartments, we used Lysotracker Red, which diffuses into cells and accumulates in acidic vacuoles. Since we did not observe colocalization between ubiquitinated bacteria and Lysotracker Red, we attempted to quantify the metabolic state of the bacteria in different compartments by measuring the size of their lipid droplets. Mycobacteria in stationary phase generate large lipid droplets due to lack of a nitrogen source; instead of generating proteins, they use available carbons to make lipids (8). We examined the lipid droplets at 24 HPI for Mm in phagosomes, the cytosol, autophagosomes, and autolysosomes.

Unexpectedly, we found that Mm escapes from phagosomes during the first few hours after infection. Similarly, after 2 hours of infection, Mm also stimulates release of IL-1β and IL-18 in an ESX-1 dependent manner (9). IL-1β and IL-18 release requires activation of the inflammasome, a protein complex including nucleotide-binding and oligomerization domain (NOD)-like receptors (NLRs) that recognize molecules from pathogens, resulting in processing of the effector caspase-1 and processing and release of these cytokines (10). Cryopyrin, or NALP3, is the NLR responsible for recognizing mycobacterial material and inducing release of IL-1β and IL-18 (Figure 2). Due to the

similar timing of Mm's phagosomal escape (Chapter 2), inflammasome activation and this pathway's dependence on recognition of mycobacterial products, we hypothesized that inflammasome activation might be important to activation of mycobacterial ubiquitination. We infected macrophages from cryopyrin (NALP3) deficient mice, as well as macrophages deficient in ASC, which is necessary for assembly of the inflammasome, and examined ubiquitination at 24 hours.

Our initial observation was that the ΔRD1 mutant, completely deficient in ESX-1 secretion, was not polyubiquitinated due to lack of access to the cytoplasm (Chapter 2). However, several proteins encoded within ESX-1 have been shown through study of transposon mutants to have distinct roles in secretion. The gene Mh3881c has recently been renamed espB, for ESX-1 substrate protein B, because it is a substrate of the putative ESX-1 secretion system (11). A transposon mutant in espB, *espB*$_{M}$*::tn*, is attenuated for growth in macrophages (11), and we therefore hypothesized that it might exhibit defective phagosome escape and ubiquitination, similar to ΔRD1. We also studied ubiquitination of *Mh3866::tn,* which lacks secretion of CFP-10, and *Mh3879c::tn*, which does not secrete of EspB (11). We hypothesized that each mutant might have different defects in phagosome escape, which might be reflected through differences in the amount of ubiquitination.

Using monoclonal antibodies specific for K48 and K63 polyubiquitin chains, we found both types of linkages in polyubiquitin attached to Mm (Chapter 2). We found slightly more K63 linkages. To explore further whether there was a preference for K48 or K63 chains, we performed *in vitro* ubiquitination reactions using His tagged ubiquitin containing all 7 lysines or just K48 or K63.

As described in Chapter 2, Mm sheds cell wall material. We made an approximate comparison of the amount of shed material by counting pieces of fluoresceinated material larger than 1 μM that were separated from WT or ΔRD1 mutant. Finally, we quantified the number of ΔRD1 that escaped and that associated with ubiquitin when coinfected with WT.

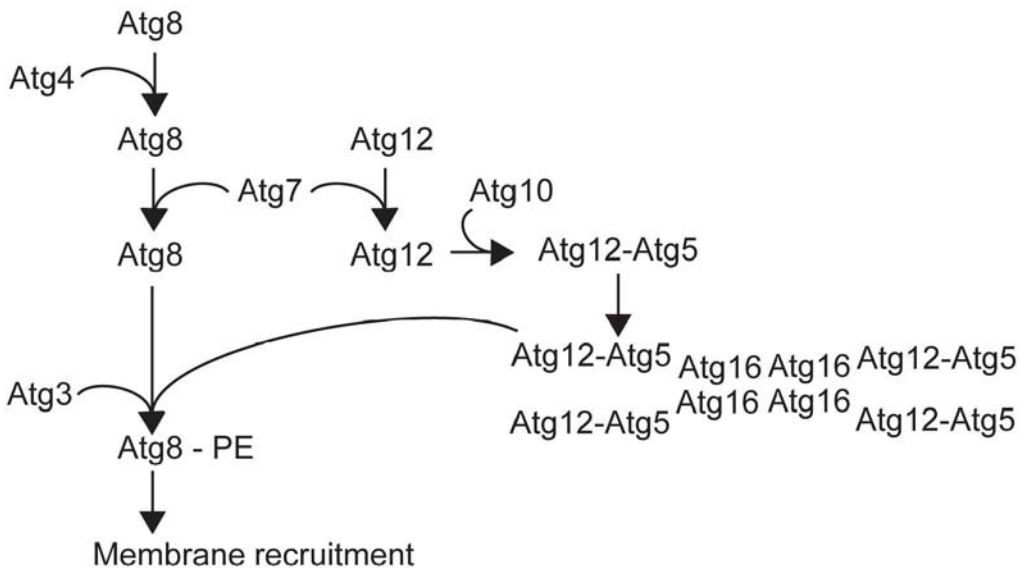

Figure 1. *The autophagy pathway* (modified from Klionsky (2005))

Extension and closure of the initial autophagosome membrane requires two conjugation reactions: one between Atg12 and Atg5 and the other between Atg8 and the lipid phosphatidylethanolamine (PE). After Atg4 clips the C-terminal arginine residue of Atg8 to expose a glycine, Atg7 and Atg3 act as ubiquitin-activating E1-like and ubiquitin-conjugating E2-like enzymes, respectively, to attach PE. Atg7 also acts as an E1-like enzyme to covalently link Atg12 to Atg5.

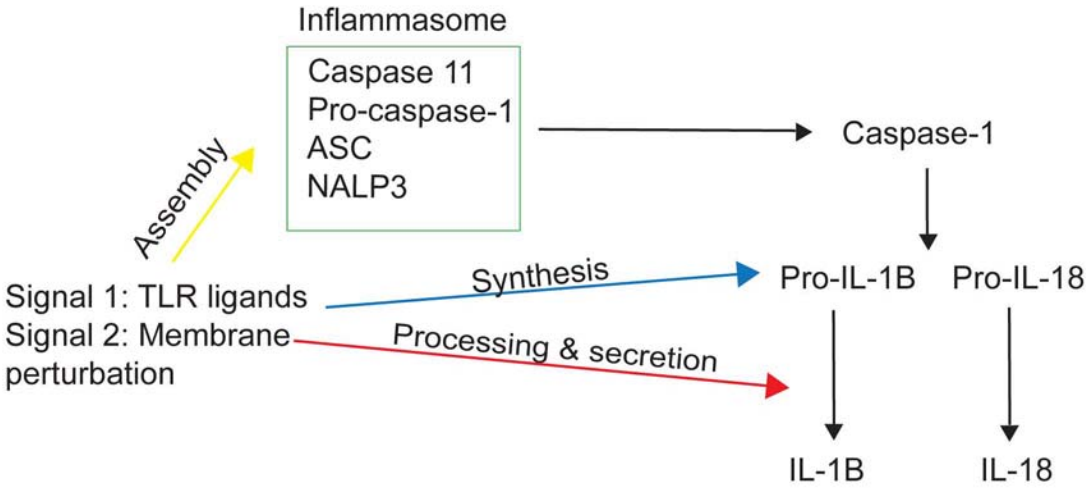

Figure 2. *Inflammasome activation by Mm results in secretion of IL-1β and IL-18.* (modified from Mariathasan and Monack (2007)).

Bacterial products, or Toll-like receptor (TLR) ligands, provide the first signal for inflammasome activation by inducing production of pro-IL-1β (red arrow) and by inducing assembly of the inflammasome (yellow arrow) through a conformational change in NALP3. This allows NALP3 to oligomerize and associate with the adaptor protein ASC, which binds to pro-caspase-1 through its caspase-recruitment domain. The second signal for inflammasome activation is membrane perturbation, which during mycobacterial infection depends on ESX-1 (8). Processing of pro-caspase-1 to caspase-1 results in cleavage of pro-IL-1β and pro-IL-18 to IL-1β and IL-18 and finally their secretion.

Results & Discussion

Ubiquitinated Mm associate with LAMP-1 in Atg3 and Atg7 deficient fibroblasts

We found that ubiquitinated Mm in the Atg3 and Atg7 deficient mouse embryonic fibroblasts (MEFs) associated with LAMP-1 (Figure 3A). About 60 to 70% of ubiquitinated Mm associated with LAMP-1 in cells deficient for or expressing Atg3 and Atg7 (Figure 3B). As expected, we confirmed that cells lacking Atg3 and Atg7 did not conjugate Atg8 to phosphatidylethanolamine during starvation in EBSS (Figure 3C). These results show that sequestration of Mm is independent of the autophagy pathway as defined by conversion of LC3-I to LC3-II and its association with autophagosomes, rather than solely being independent of Atg5.

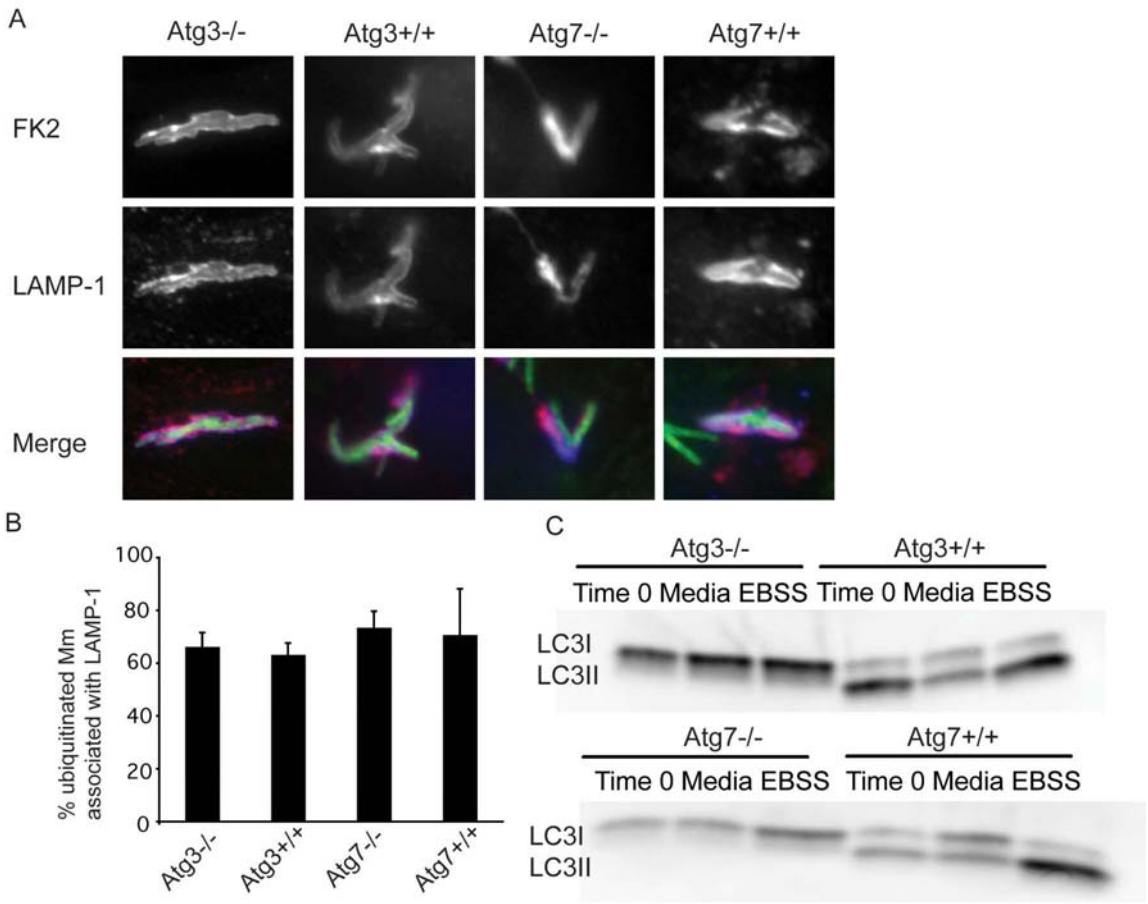

Figure 3. *Ubiquitinated Mm associate with LAMP-1 in Atg3 and Atg7 deficient MEFs.*

(A) Atg3-/-, Atg3+/+, Atg7-/- and Atg7+/+ MEFs were infected with Mm for 24 hours, fixed and stained with antibody to polyubiquitin (FK2, blue in merge) and anti-LAMP-1 antibodies (red in merge).

(B) Quantification of % ubiquitinated Mm that were associated with LAMP-1 in at least 50 infected cells in three separate experiments. Percentages are shown with standard deviations.

(C) MEFs were washed and incubated with media (DME-H21 + 10% FBS) or EBSS for 4 hours. Lysates were collected and LC3-I conversion to LC3-II was examined by Western blotting as described in materials and methods. Atg3-/- and Atg7-/- did not

convert LC3-I to LC3-II.

Infection of Atg5 deficient macrophages

To ask whether lack of the autophagy protein Atg5 might affect growth of Mm, we compared survival of Mm in Atg5 +/+ and Atg5-/- MEFs. We found no differences between the number of CFUs collected from these different cells at 5 and 24 HPI (Figure 4). This suggests, as mentioned in Chapter 2, that Mm may have mechanisms to evade killing by autophagy.

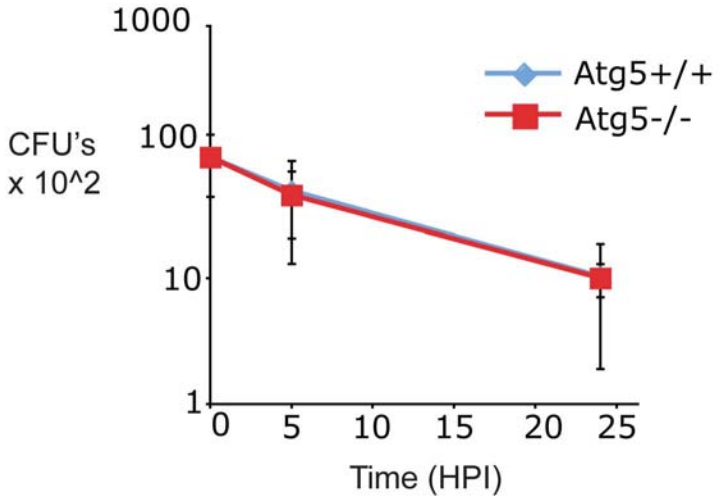

Figure 4. *Deficiency in Atg5 does not affect Mm survival during first 24 hours of infection.*

Atg5+/+ and Atg5-/- MEFs were infected with Mm for 24 hours, lysed and plated on 7H10 agar. CFU's were counted after several days of incubation at 32 degrees C. In three independent experiments, there was no difference in the growth or survival of Mm in the two cell types.

LAMP-1 positive compartments associated with Mm are not acidic

We asked whether the LAMP-1 positive compartment with ubiquitinated Mm were acidic, indicating a degradative environment. We looked for colocalization of ubiquitinated Mm with Lysotracker Red, which accumulates preferentially in acidic compartments. There was little association with ubiquitinated bacteria, though the majority at 24 HPI are contained in LAMP-1 positive compartments (Chapter 2).

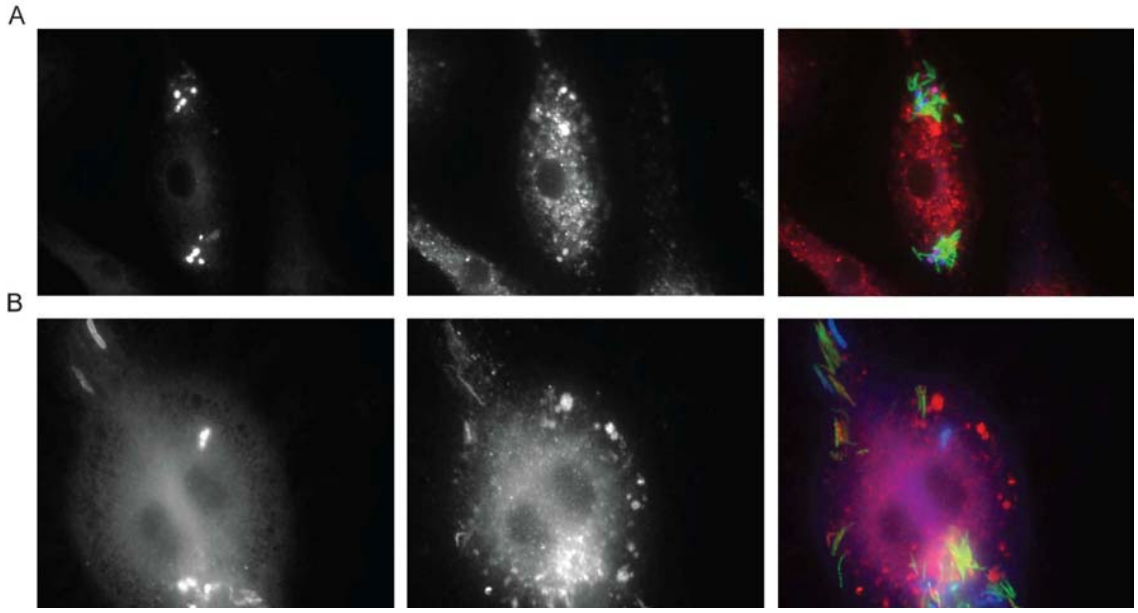

Figure 5. *Ubiquitinated Mm are not in acidic compartments.*

(A) Mm infected for 3.5 HPI. The ubiquitin associated Mm is not associated with Lysotracker Red (arrow). However, ubiquitin positive membrane-like structures appear to colocalize with Lysotracker Red (asterisk).

(B) Mm infected for 24 HPI. Several bacteria associated with Lysotracker Red are not ubiquitinated (arrow), while ubiquitinated bacteria are not associated with Lysotracker Red (asterisk).

Quantification of lipid droplets in Mm in different compartments

The experiments with Lysotracker Red did not show that ubiquitinated Mm were exposed to an acidic environment, though they colocalized with LAMP-1. In order to study their metabolic state, we measured the size of the lipid droplets in Mm in phagosomes surrounded by one membrane, in the cytosol, surrounded by double membrane autophagosomes, and in autolysosomes with membranes and vesicles. Examples of quantified lipid droplets are shown in Figure 6A, as well as Figure 2 from Chapter 2 (page 27), which also exemplies the difference in lipid size in phagosomal versus cytoplasmic bacteria. We found that Mm in phagosomes had smaller lipid vacuoles than under all the other conditions (Figure 6B). This suggests that mycobacteria may grow while in the initial phagosome and may enter stationary phase while within the cytosol, autophagosome and autolysosome. This supports the hypothesis that reuptake from the cytosol into autolysosomes may restrict mycobacterial growth.

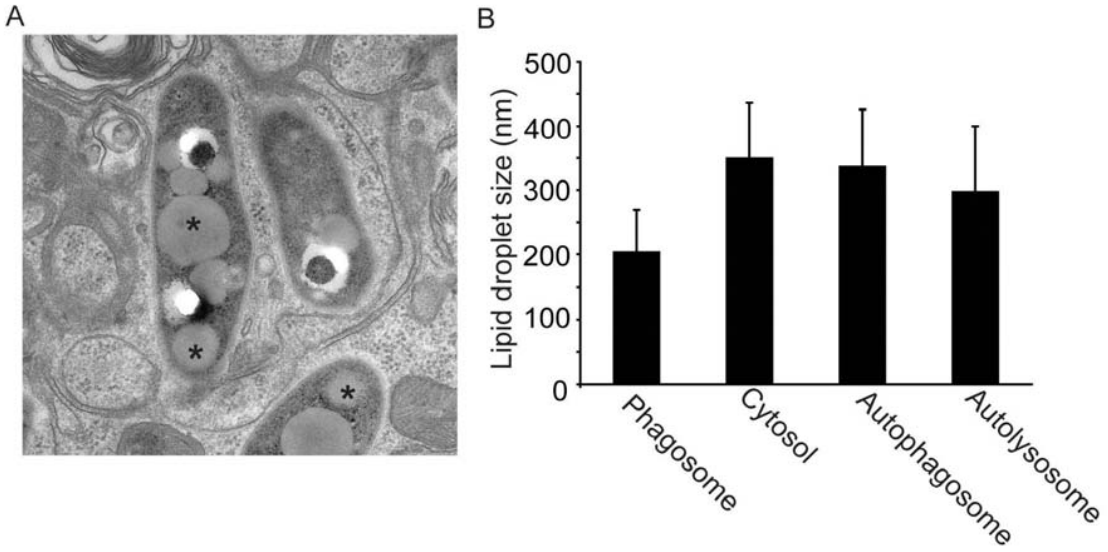

Figure 6. *Quantification of lipid droplets in Mm in different compartments.*

(A) Image showing example lipid droplets (asterisks) in infected macrophage directly embedded in Epon without permeabilization.

(B) Quantification of lipid droplets for bacteria similar to those in (A), in phagosomes, surrounded by one membrane containing no other content (n=24), in the cytosol (n=33), in autophagosomes with double membranes (n=61), and in autolysosomes with membranes and vesicles surrounded by 1 membrane (n=22).

Inflammasome does not affect ubiquitination of Mm

We infected bone marrow derived macrophages from mice lacking Nalp3/Cryopyrin and ASC, which are necessary for release of IL-1β and IL-18 during Mm infection. We also infected macrophages lacking IPAF-/-, another NLR which previously was found to not be important for release of these cytokines (9). We found that Mm in all types of macrophages had equivalent levels of ubiquitination, suggesting that the inflammasome is not important in activating ubiquitination (Figure 7).

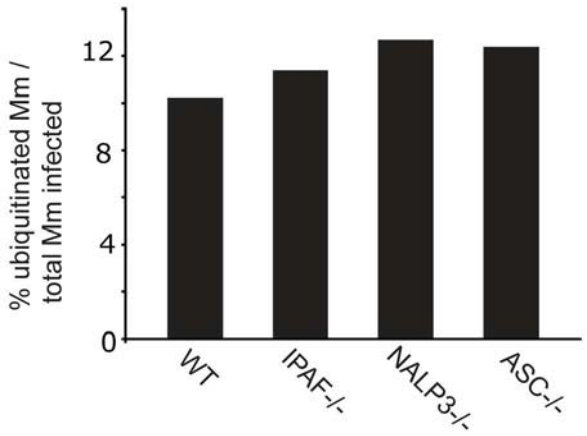

Figure 7. *Inflammasome does not affect ubiquitination of Mm.*

Bone marrow derived macrophages from WT, IPAF-/-, NALP3-/- and ASC-/- mice were infected with Mm, fixed and stained with FK2 antibody. Shown is the percent of ubiquitinated Mm out of the total number infected in at least twenty cells, as the average of two independent experiments. The normal level of ubiquitination in NALP3-/- and ASC-/-mice suggests that the inflammasome does not play a role in ubiquitination of Mm.

espBM::tn has decreased ubiquitin association

Neither *Mh3866::tn* or *Mh3879c::tn* had significantly decreased ubiquitin association from WT or from their complemented counterparts 48 HPI of bone marrow derived macrophages (Figure 8). *espBM::tn* had significantly less ubiquitin association which was complemented by expression from a plasmid or from an integrated copy (Figure 8). These results suggest that neither presence of Mh3866 and Mh3879c or secretion of CFP-10 and EspB are necessary for ubiquitin association, since Mh3866 is required for CFP-10 secretion and Mh3879c is required for EspB secretion. Rather, EspB may be required for additional functions independent of its secretion.

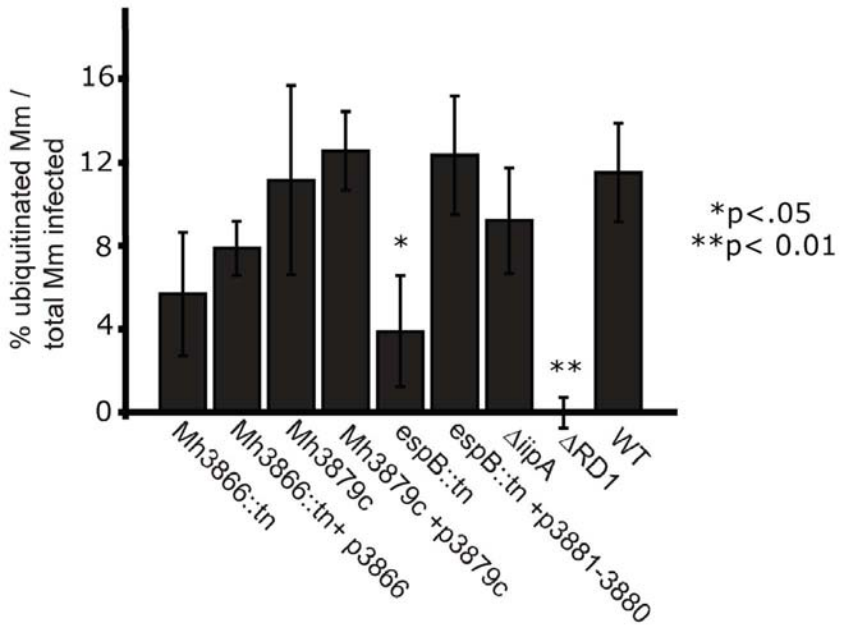

Figure 8. *espB::tn has decreased ubiquitination during infection.*

Bone marrow derived macrophages were infected for 48 hours, fixed and stained for polyubiquitin using the FK2 antibody. Shown is the percent ubiquitinated Mm out of total Mm infected in at least 20 macrophages in three independent experiments. P-values were determined using a Student's t-test.

Mm is ubiquitinated with K48 and K63 chains *in vitro*

We performed ubiquitination reactions (as described in Materials and Methods for Chapter 2) with His-tagged ubiquitin, or His-tagged ubiquitin containing only K48 or K63 chains (Figure 9). The results, particularly in with the K48 only chains, varied widely from experiment to experiment. In one experiment, there was a five-fold increase in mean fluorescence intensity (MFI) in Mm reactions containing His-tagged ubiquitin with all lysines and a four-fold increase in MFI for K63 only ubiquitin versus reactions performed without ubiquitin. In contrast K48 ubiquitin had a sixteen-fold increase in MFI in one experiment and a 258 fold increase in another experiment, for an average of 138 fold increase. The apparently low level of ubiquitination with WT ubiquitin compared with our previous results may be due to weaker binding of the His antibody to Mm compared to FK2. In addition, the high level of K48 ubiquitination may be due to ubiquitin aldehyde's possible specificity for K48 chain targeting deubiquitinases, allowing K48 ubiquitin specifically to remain bound and appear enriched (Ray Deshaies, personal communication). In addition, solubility of the ubiquitin seemed to be affected differently for each of the chains and this may account for the low signal for WT and K63 chains and the wide variability in the K48 MFIs.

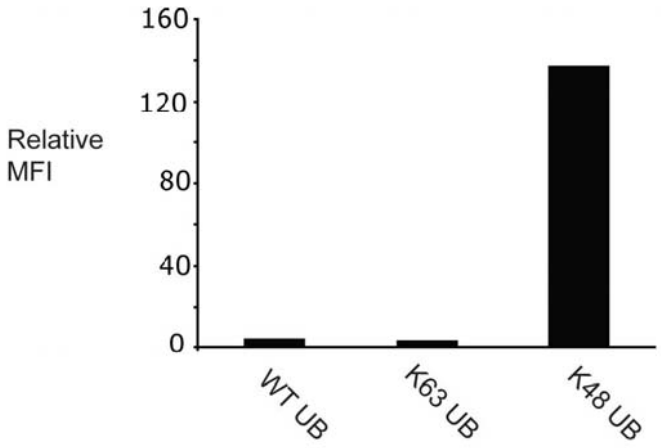

Figure 9. *K63 and K48 ubiquitination in vitro.*

In vitro ubiquitination reactions with Mm were performed using His tagged wild type ubiquitin (WT UB), containing all 7 lysines, or with ubiquitin containing K63 only or K48 only. After two hours of incubation with HeLa lysates as described in Materials and Methods of Chapter 2, Mm were fixed and stained with anti-His antibody. The results are shown as the relative mean fluorescence intensity (MFI) relative to a reaction performed with no ubiquitin but stained with the His antibody, and represent the average of two independent experiments.

Quantification of released Mm cell wall material during infection

Mm release cell wall material during infection of macrophages, as shown by staining with anti-Mm cell wall antibodies and presence of fluoresceinated material separate from Mm that were fluoresceinated before infection (Chapter 2). We counted blebs larger than 1 μm because this size of particle was rarely observed in uninfected cells, eliminating the chance of counting background fluorescence. We found that both the number of macrophages containing blebs greater than 1 μm and the number of blebs per bacteria were increased in WT versus ΔRD1. A little more than half of all blebs in WT infected cells were associated with ubiquitin (Figure 10). These results suggest that WT sheds more cell wall material than ΔRD1. This difference may be due to exposure of WT to the cytoplasm, where the change in environment may trigger increased shedding.

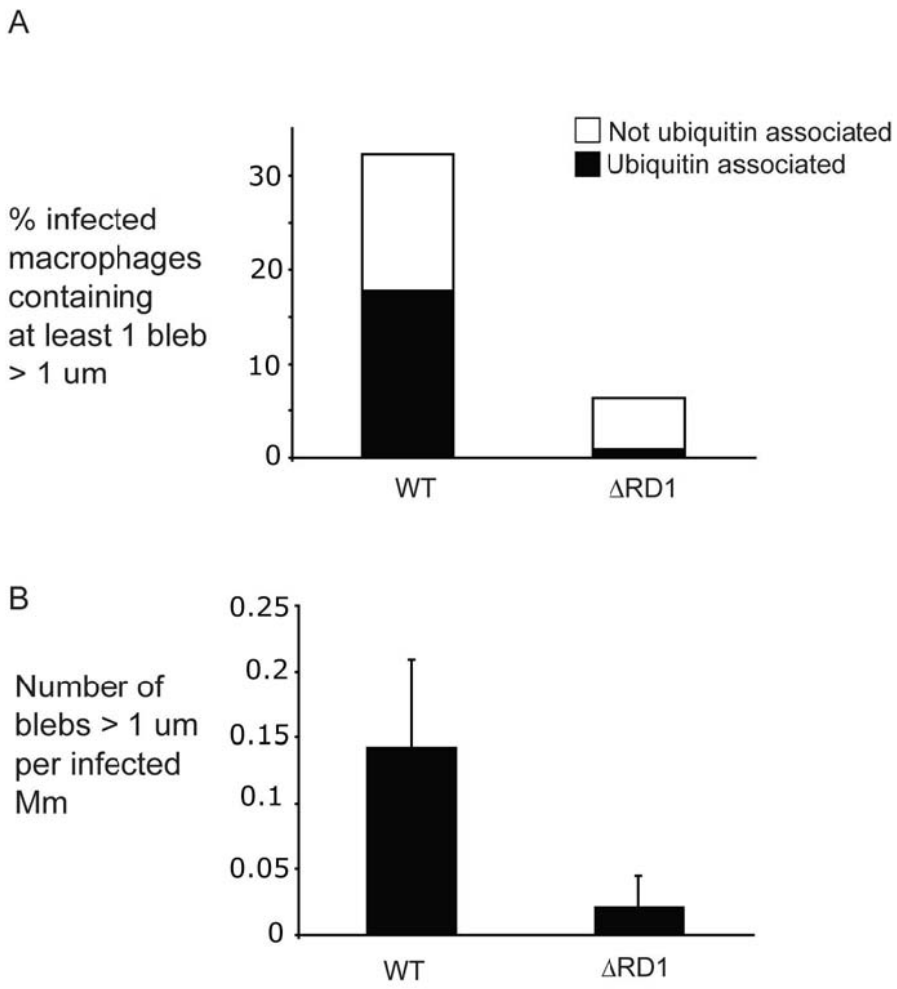

Figure 10. *Quantification of released Mm cell wall material during infection*

(A) Bone marrow derived macrophages were infected with CFSE labeled Mm for 6.5 hours, fixed and stained with anti-ubiquitin (FK2) and the fluorescein antibody. The number of fluoresceinated particles or blebs released from Mm larger than 1 μm were counted using Slidebook. Shown are the averages for fifty infected cells in three independent experiments.

(B) The number of fluoresceinated blebs per Mm in fifty infected cells in three independent experiments were counted as in (A).

Electron microscopy images

These images show more examples of infection at 1.5, 3.5 and 24 HPI. Cells directly imbedded in Epon resin have the best membrane morphology, and show Mm's interaction with the phagosomal membrane at early time points and inclusion in autolysosomes at 24 HPI. There are also examples of characteristic dense membranes which appear to correlate with ubiquitin labeled structures in saponin permeabilized cells. There are also examples using fluoresceinated Mm and LAMP-1 labeled lysosomes at 3.5 HPI.

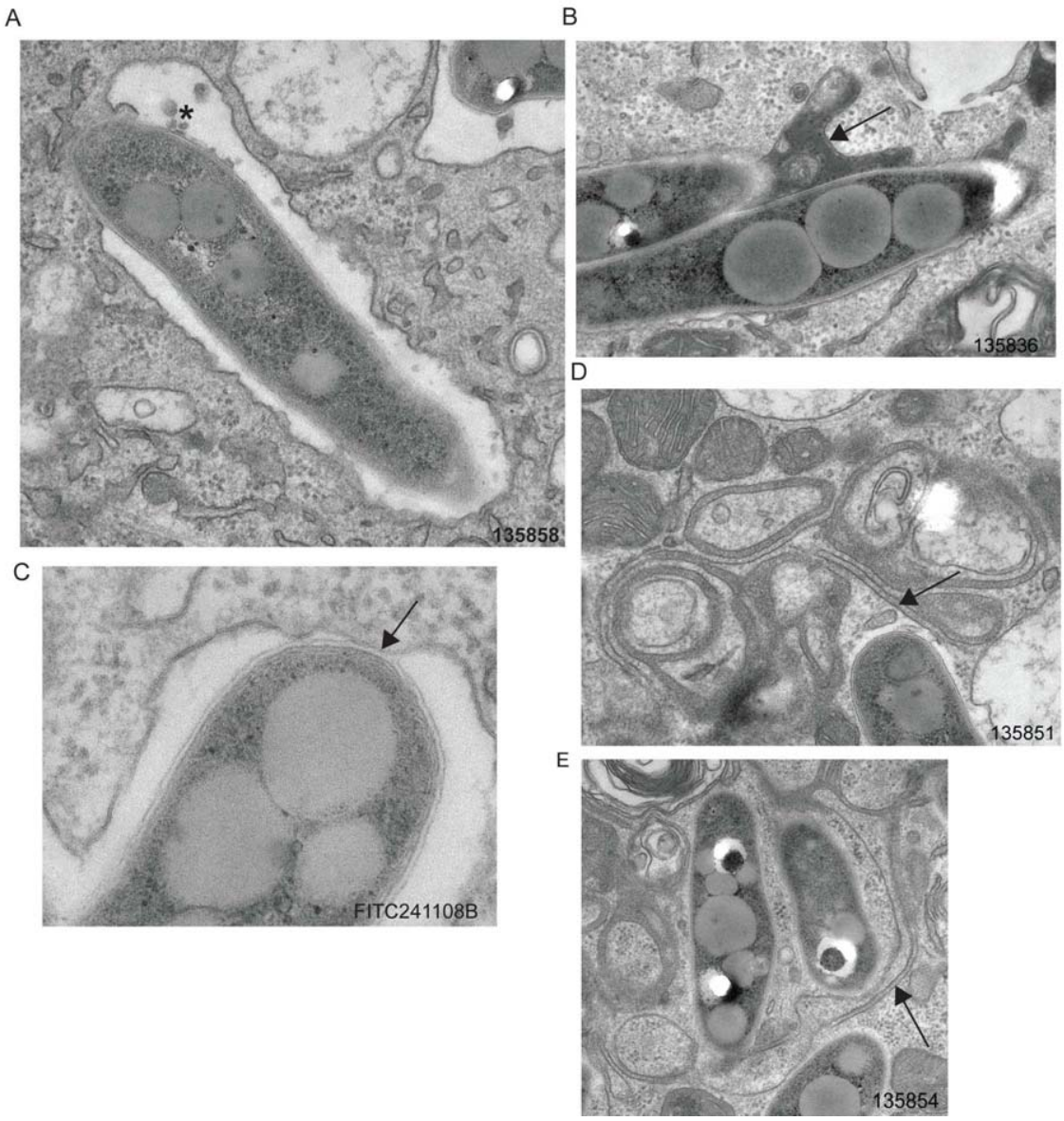

Figure 11: *Epon embedded cells 3.5 HPI without permeabilization.*

(A) Mm possibly perforating the phagosome, with dense material possibly being shed from the mycobacterial cell wall into the phagosome (asterisk).

(B) Mm with membrane-like structures adhering to their cell wall, possibly phagosome remnants (arrow).

(C) Mm closely apposed to phagosomal membrane, with some density between the bacterial cell wall and phagosome membrane (arrow).

(D) Double membrane with loose ends (arrow) near a Mm.

(E) Double membrane with loose ends (arrow) possibly surrounding a Mm.

Figure 12: *Double membranes surrounding Mm and dense network*

This image is of an epon embedded macrophage without permeabilization 3.5 HPI. On the left is Mm within a phagosome membrane, with two areas of density indicated with arrows. On the right is a Mm and a dense network surrounded by double membranes.

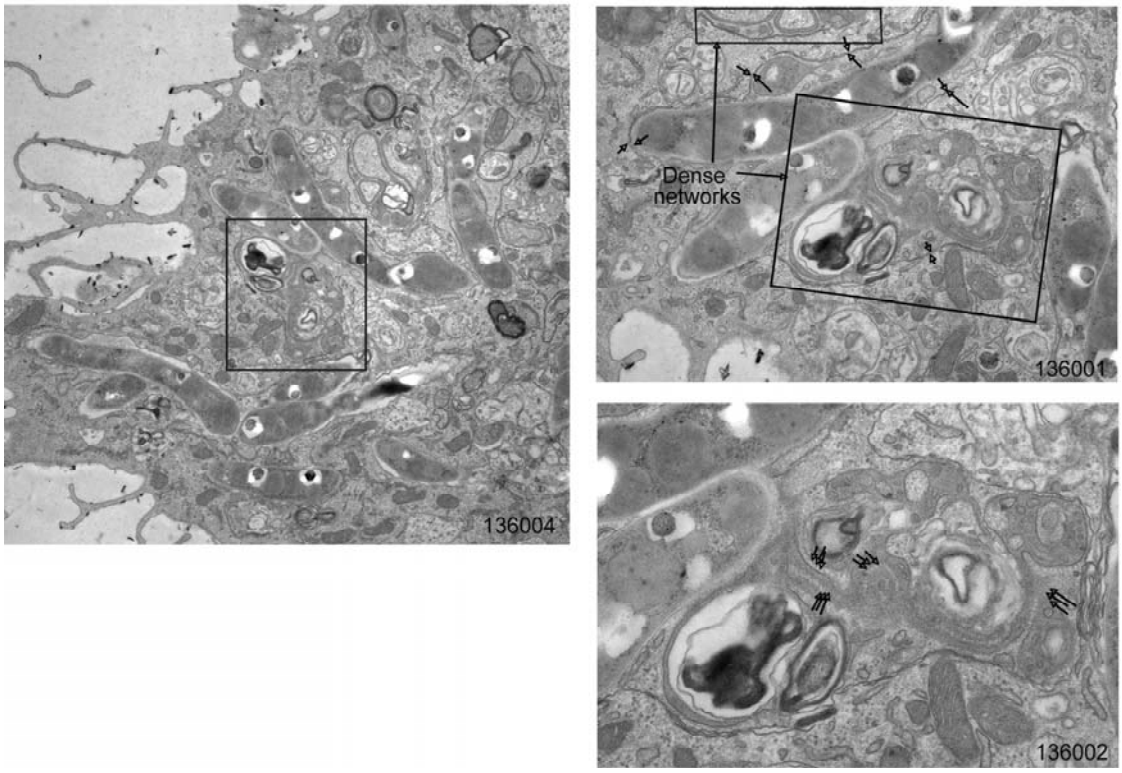

Figure 13: *24 HPI Epon embedded cell showing Mm in autolysosome.*

Right images show magnification of the square area of the image on the left, with Mm and dense membrane networks enclosed in a single membrane. Top right image has dense networks surrounded by boxes and arrows to indicate the single membrane. Arrows in bottom right image point to dense membranes in a further magnification of the boxed area in the left image.

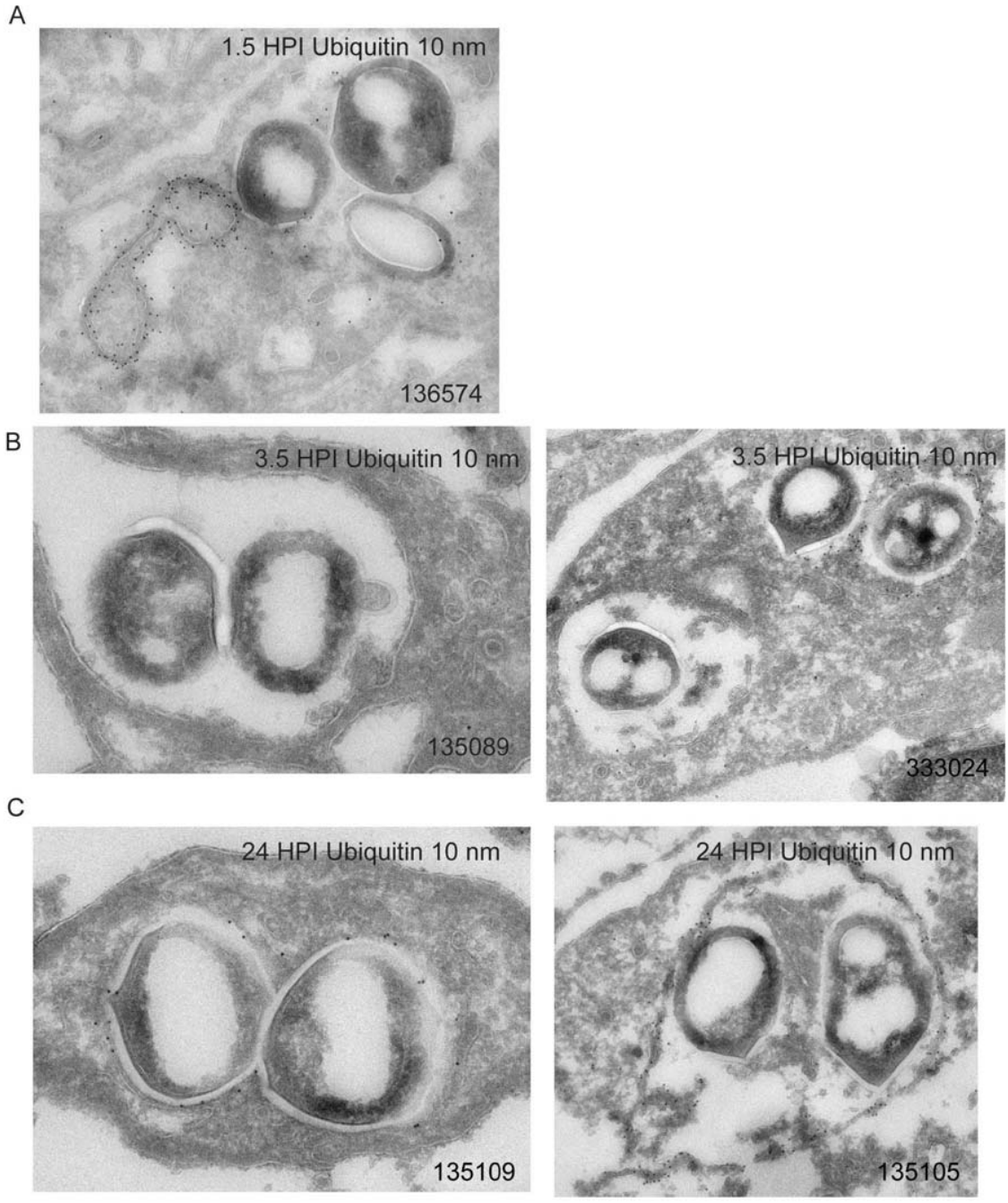

Figure 14: *Saponin permeabilization and anti-ubiquitin (FK2) labeling at 1.5, 3.5 and 24 HPI*

A) Mm in the cytoplasm and associated with ubiquitin at 1.5 HPI.

B) Left image shows interesting "bleb" structure attached to right Mm within a

phagosome at 3.5 HPI. Right image shows ubiquitin on membranes and associated with Mm at 3.5 HPI.

C) Mm associated with ubiquitin at 24 HPI. Left image shows ubiquitinated Mm in dense vacuole; right image shows most ubiquitin on membranes enclosing Mm.

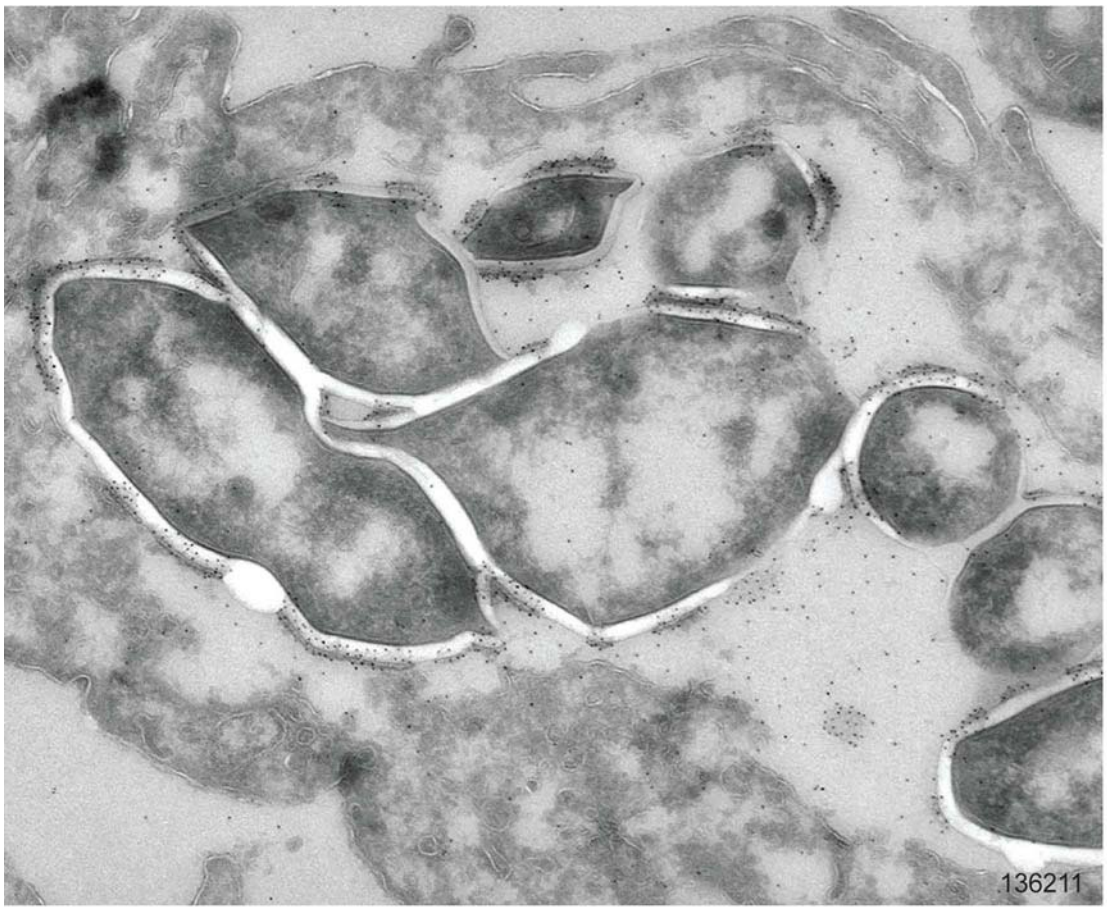

Figure 15*: Fluorescein labeled Mm at 3.5 HPI*

This image shows localization of fluorescein on mycobacterial cell wall. The majority of fluorescein does not appears to penetrate to the cytoplasmic membrane of the bacteria, with most label on the outer surface of the wall. Unlabeled areas may be where chunks of the wall have sloughed off, or where new wall is growing.

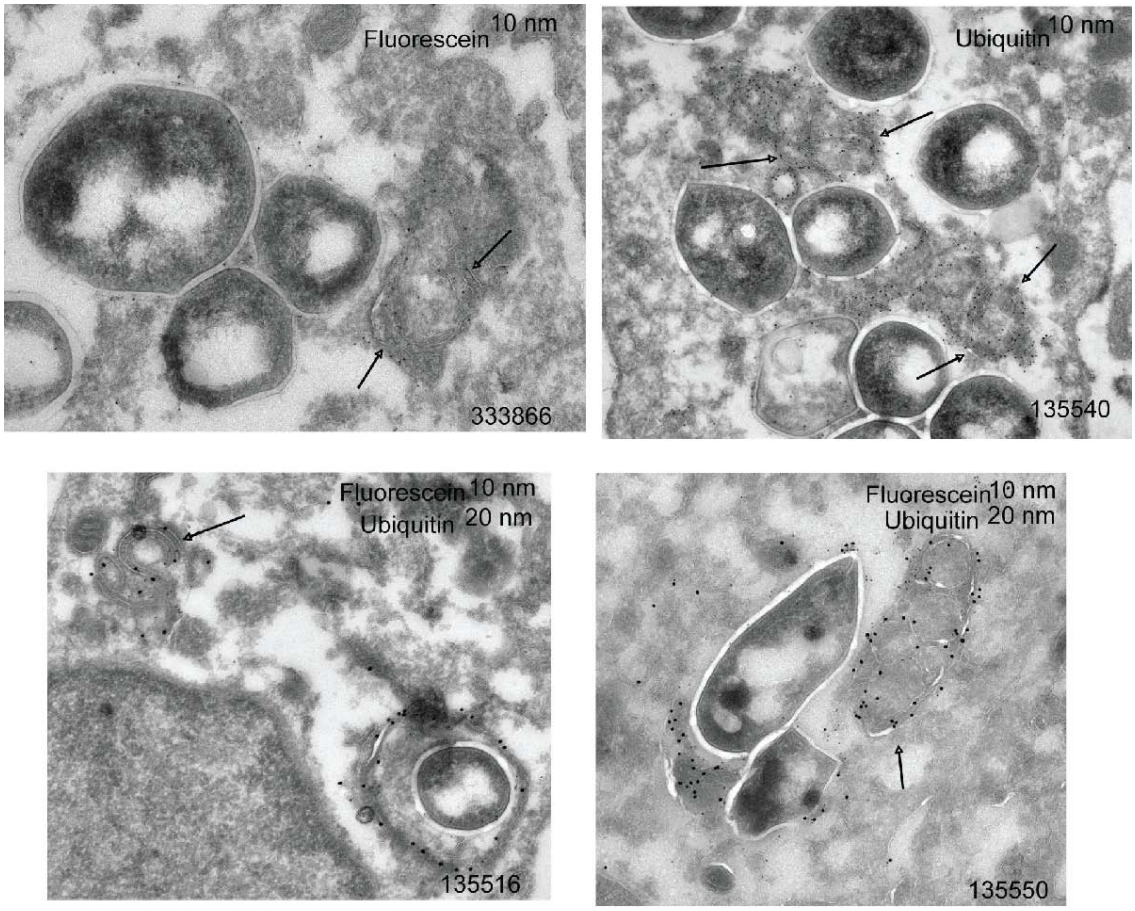

Figure 16: *Fluorescein labeled Mm and ubiqutiin at 3.5 HPI*

The two images show individual labeling of fluorescein (left) and ubiquitin (right) in dense membrane networks (arrows) near bacteria. The bottom two images show costaining in the dense membrane networks (arrows).

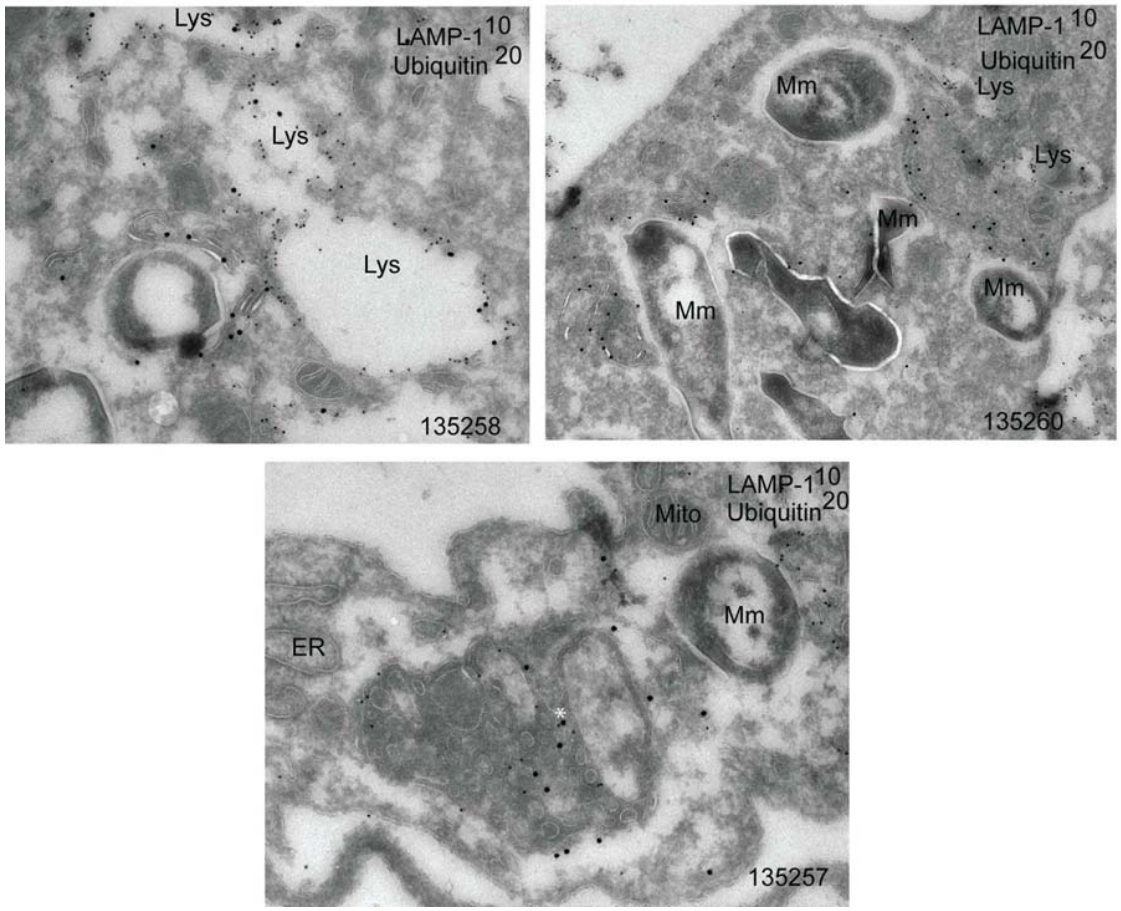

Figure 17: *LAMP-1 and ubiquitin staining at 3.5 HPI*

These images show close association of LAMP-1 positive lysosomes with ubiquitin associated bacteria. In the top left image, ubiquitin is on dense membrane networks and the bacteria, next to LAMP-1 positive lysosomes ("Lys"). In top right image in the upper right corner, a lysosome has both ubiquitin and LAMP-1 labeling. In bottom image, colocalization of LAMP-1 and ubiquitin occurs in the center of the image (asterisk).

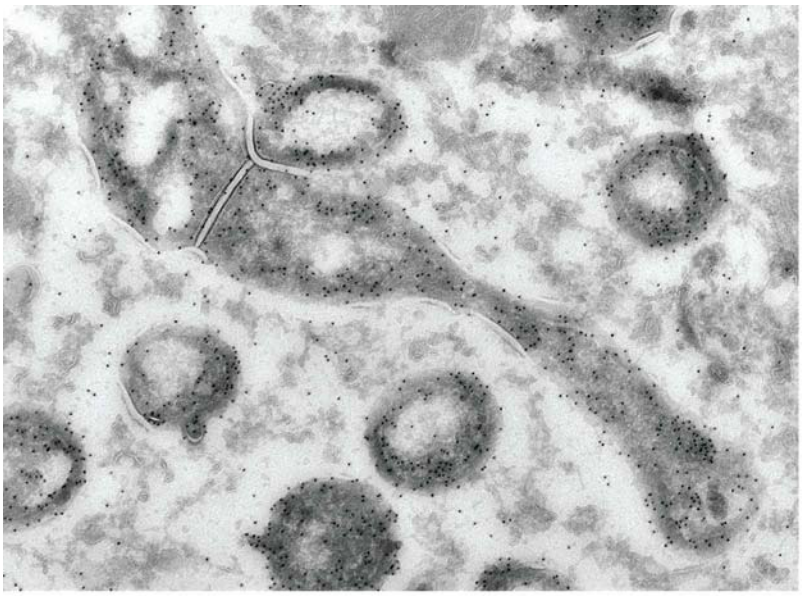

Figure 18: *Mm antibody at 24 hours*

This shows staining with the anti-Mm antibody to the ΔRD1 cell wall used in digitonin experiments for Figure 1 of Chapter 2. Mycobacterial material is widely dispersed throughout the macrophage.

Materials and Methods

(see Chapter 2 Materials and Methods for infections, fluorescein labeling, *in vitro* ubiquitination and electron microscopy methods)

Antibodies

The anti-His mouse monoclonal for FACS was from Santa Cruz Biotechnology (Santa Cruz, CA) . For quantification of fluorescein blebs, cells were stained with rabbit anti-fluorescein from Invitrogen (Carlsbad, CA). For electron microscopy of fluoresceinated Mm, the same anti-fluorescein from Zymed (South San Francisco, CA) was used as in Chapter 2.

Cells

Atg3-/-, Atg3+/+, Atg7-/- and Atg7+/+ MEFs were a gift Jayanta Debnath with permission from Masaaki Komatsu. IPAF, ASC and Nalp3/Cryopyrin deficient bone marrow derived macrophages were provided by Fredric Carlsson.

Lysotracker Red

129/SvJ bone marrow derived macrophages were infected for 3 or 23.5 hours, washed 1x with PBS and incubated with Lysotracker Red (Invitrogen, Carlsbad, CA) at a dilution of 1:5000 for 30 minutes at 32 degrees C. Cells were washed 1x with PBS and fixed with 4% PFA for 12 minutes, permeablized with 0.1% saponin for 6 minutes and stained with anti-ubiquitin (FK2) and goat anti-mouse IgG Alexa 350 $F(ab')_2$.

Chapter 4

Concluding Remarks

Role of Ubiquitin in Infection with Mycobacteria

This thesis has described the ubiquitination of Mm in bone marrow derived macrophages. Ubiquitination of Mm appears to lead to its targeting to LAMP-1 positive vacuoles, though this hypothesis remains unproven. Unexpectedly, these vacuoles do not appear to be acidic. Therefore it is unclear whether the ubiquitinated Mm are targeted for destruction or sequestered by membranes and continue to survive and/or grow. Further experiments will be crucial in determining the effects of ubiquitination on bacterial growth. In addition to effects on growth, ubiquitination and sequestration may be involved in antigen presentation, as ubiquitin and the proteasome affect both Class I and Class II restricted presentation.

Future Directions

Identification of the enzymes involved in ubiquitination

Ubiquitin is involved in many cellular processes and in order to understand its role in mycobacterial pathogenesis, specific disruption of mycobacterial ubiquitination is crucial. Determination of the E2 conjugating enzymes and E3 ligase involved in ubiquitinating Mm would allow for specific depletion or use of cells deficient in these enzymes. Discovery of the E2 and E3 enzymes could occur through use of a lentiviral shRNA library in bone marrow derived macrophages, or more easily through siRNA transfection of mouse embryonic fibroblasts, since we have demonstrated Mm ubiquitination in these cells. Once these enzymes are depleted, we could ask whether LAMP-1 targeting continues at the same rate and whether there is an effect on bacterial survival. It would also be interesting to ask whether these same enzymes affect

ubiquitination of other bacterial species, such as *Listeria monocytogenes* and *Salmonella typhimurium*.

Identification of targets of ubiquitination

Another important future direction will be to determine the molecules targeted by ubiquitination. As described in Chapter 1, several bacterial virulence factors are ubiquitinated. Perhaps discovery of the ubiquitinated molecules will uncover proteins not yet known to be important during infection, or highlight the significance of already discovered virulence factors. Alternatively, the ubiquitin machinery may recognize many proteins on the highly hydrophobic mycobacterial surface. How many foreign proteins are recognized by the host ubiquitination machinery would also be a very interesting mechanistic question. Identification of ubiquitinated proteins could be approached through *in vitro* ubiquitination, purification of mycobacterial ubiquitinated proteins and mass spectrometry. Any proteins identified could be validated by purifying ubiquitinated proteins from infected macrophages.

Investigating mechanism of targeting Mm to LAMP-1 positive vacuoles

Our data suggests the existence of an autophagy independent pathway to bacterial sequestration. Another way to assesss the significance of bacterial ubiquitination would be to identify and attempt to interfere the process of sequestration. One hypothesis is that the ESCRT pathway targeting ubiquitinated receptors to multivesicular bodies may be involved. This hypothesis could be studied through siRNA depletion or genetically deficient mouse macrophages or embryonic fibroblasts.

References

Chapter 1

1. Pickart CM (2001) Mechanisms underlying ubiquitination. Annu Rev Biochem 70: 503-533.

2. Liu Y-C (2004) Ubiquitin ligases and the immune response. Annu Rev Immunol 22: 81-127.

3. Welchman RL, Gordon C, Mayer RJ (2005) Ubiquitin and ubiquitin-like proteins as multifunctional signals. Nature Rev Mol Cell Biol 6:599-609.

4. Hicke L, Dunn R (2003) Regulation of membrane protein transport by ubiquitin and ubiquitin-binding proteins. Annu Rev Cell Dev Biol 19:141-172.

5. Clague MJ, Urbé S (2006) Endocytosis: the DUB version. Trends Cell Biol 16: 551-559.

6. Winborn BJ, Travis SM, Todi SV, Xu P, Peng J, *et al*. (2008) The deubiquitinating enzyme ataxin-3 edits K63-linkages in mixed linkage chains. FASEB J 22:607.3.

7. Ikeda F, Dikic I (2008) Atypical ubiquitin chains: new molecular signals. EMBO Reports 9: 536-542.

8. Newton K, Matsumoto ML, Wertz IE, Kirkpatrick DS, Lill JR (2008) Ubiquitin chain editing revealed by polyubiquitin linkage-specific antibodies. Cell 134: 668-678.

9. Groll M, Clausen T (2003) Molecular shredders: how proteasomes fulfill their role. Curr Opin Struct Biol 13: 665-673.

10. Seong KM, Baek J-H, Yu M-H, Kim J (2007) Rpn13p and Rpn14p are involved in the recognition of ubiquitinated Gcn4p by the 26s proteasome. FEBS Letters 13: 2567-

2573.

11. Yewdell JW (2005) Immunoproteasomes: regulating the regulator (2005) Proc Natl Acad Sci USA 102: 9089-9090.

12. Hicke L (2001) Protein regulation by monoubiquitin. Nat Rev Mol Cell Biol 2: 195-201.

13. Di Fiore PP, Polo S, Hofmann K (2003) When ubiquitin meets ubiquitin receptors: a signaling connection. Nature Rev Mol Cell Biol 4:491-497.

14. Chen ZJ (2005) Ubiquitin signaling in the NF-κB pathway. Nature Cell Biol 7: 758-765.

15. Lamothe B, Besse A, Campos AD, Webster WK, Wu H, *et al.* (2007) Site-specific Lys-K63-linked Tumor Necrosis Factor Receptor-associated Factor 6 auto-ubiquitination is a critical determinant of IKK activation. J Biol Chem 282: 4102-4112.

16. Abbot DW, Wilkins A, Asara JM, Cantley LC (2004) The Crohn's disease protein, NOD2, requires RIP2 in order to induce ubiquitinylation of a novel site on NEMO. Curr Biol 14: 2217-2227.

17. Loureiro J, Ploegh HL (2006) Antigen presentation and the ubiquitin-proteasome system in host-pathogen interactions. Adv Immun 92: 225-305.

18. Krüeger E, Kuckelhorn U, Sijts A, Kloetzel PM (2003) The components of the proteasome system and their role in MHC class I antigen processing. Rev Physiol Biochem Pharmacol 148: 81-104.

19. Michalek MT, Grant EP, Gramm C, Goldberg AL, Rock KL (1993) A role for the ubiquitin-dependent proteolytic pathway in MHC class I-restricted antigen presentation. Nature 363: 552-554.

20. Imai J, Hasegawa H, Maruya M, Koyasu S, Yahara I (2005) Exogenous antigens are processed through the endoplasmic reticulum-associated degradation (ERAD) in cross-presentation by dendritic cells. Int Immunol 17: 45-53.

21. Heath, WR, Carbone FR (2001) Cross-presentation in viral immunity and self-tolerance. Nat Rev Immunol 1: 126-134.

22. Boyer L, Lemichez E (2004) Targeting of host-cell ubiquitin and ubiquitin-like pathways by bacterial factors. Nat Rev Micro 2: 779-788.

23. Zhou H, Monack DM, Kayagki N, Wertz I, Yin J, *et al*. (2005) Yersinia virulence factor YopJ acts as a deubiquitinase to inhibit NF-κB. J Exp Med 202: 1327-1332.

24. Rytkönen A, Poh J, Garmendia J, Boyle C, Thompson A, *et al.* (2007) SseL, a *Salmonella* deubiquitinase required for macrophage killing and virulence. Proc Natl Acad Sci USA 104: 3502-3507.

25. Neish AS, Gewirtz AT, Zeng H, Young AN, Hobert ME, *et al.* (2000) Prokaryotic regulation of epithelial responses by inhibition of IκB-α ubiquitination. Science 289:1560-1563.

26. Zhang Y, Higashide W, Dai S, Sherman DM, Zhou D (2005) Recognition and ubiquitination of *Salmonella* Type III effector SopA by a ubiquitin E3 ligase, HsRMA1. J Biol Chem 280: 38682-38688.

27. Kubori T, Hyakutake A, Nagai H (2008) Legionella translocates an E3 ubiquitin ligase that has multiple U-boxes with distinct functions. Mol Microbiol 67: 1307-1319.

28. Rosebrock TR, Zeng L, Brady JJ, Abramovitch RB, Xiao F, *et al.* (2007) A bacterial E3 ubiquitin ligase targes a host protein kinase to disrupt plant immunity. Nature 448: 370-374.

29. Zhu Y, Li H, Hu L, Wang J, Zhou Y, *et al.* (2008) Structure of a *Shigella* effector reveals a new class of ubiquitin ligases. Nature Struct Mol Biol 15: 1302-1308.

30. Schnupf P, Portnoy DA, Decatur AL (2005) Phosphorylation, ubiquitination and degradation of listeriolysin O in mammalian cells: role of the PEST-like sequence. Cell Microbiol 8: 353-364.

31. Kubori T, Galán J (2004) Temporal regulation of *Salmonella* virulence effector function by proteasome-dependent protein degradation. Cell 115: 333-342.

32. Perrin AJ, Jiang X, Birmingham CL, So NSY, Brumell JH (2004) Recognition of bacteria in the cytosol of mammalian cells by the ubiquitin system. Curr Biol 14: 806-811.

33. Mizushima N (2005) The pleiotropic role of autophagy: from protein metabolism to bactericide. Cell Death Diff 12: 1535-1541.

34. Klionsky DJ (2005) The molecular machinery of autophagy: unanswered questions. J Cell Sci 118: 7-18.

35. Kirkegaard K, Taylor MP, Jackson WT (2004) Cellular autophagy: surrender, avoidance and subversion by microorganisms. Nature Rev Microbiol 2: 301-314.

36. Swanson MS (2006) Autophagy: eating for good health. J Immunol 177: 4945-4951.

37. Clemens DL, Lee B-Y, Horwitz MA (2002) The *Mycobacterium tuberculosis* phagosome in human macrophages is isolated from the host cell cytoplasm. Infect Immun 70: 5800-5807.

38. van der Wel N, Hava D, Houbeben D, Fluitsma D, van Zon M, *et al.* (2007) M. tuberculosis and M. leprae translocate from the phagolysosome to the cytosol in myeloid cells. Cell 129: 1287-1298.

39. Gutierrez MG, Master SS, Singh SB, Taylor GA, Colombo MI, *et al.* (2004) Autophagy is a defense mechanism inhibiting BCG and *Mycobacterium tuberculosis* survival in infected macrophages. Cell 119: 753-756.

40. Birmingham CL, Canadien V, Gouien E, Troy EB, Yoshimori T, *et al.* (2007) *Listeria monocytogenes* evades killing by autophagy during colonization of host cells. Autophagy 3: 442-451.

41. Ogawa M, Yoshimori T, Suzuki T, Sagara H, Mizushima N, *et al.* (2005) Escape of intracellular *Shigella* from autophagy. Science 307: 727-731.

42. Talloczy Z, Jiang W, Virgin HWT, Leib DA, Scheuner D, *et al*. (2002) Regulation of starvation- and virus-induced autophagy by the eIF2alpha kinase signaling pathway. Proc Natl Acad Sci USA 99: 190–195.

43. Singh SB, Davis AS, Taylor GA, Deretic V (2006) Human IRGM induces autophagy to eliminate intracellular mycobacteria. Science 313: 1438-1441.

44. Dengjel J, Schoor O, Fishcer R, Reich M, Kraus *et al*. (2005) Autophagy promotes MHC class II presentation of peptides from intracellular source proteins. Proc Natl Acad Sci USA 102: 7922-7927.

45. Münz C (2006) Autophagy and antigen presentation. Cell Microbiol 8: 891-898.

46. Fortun J, Dunn WA, Joy S, Li J, Notterpek L (2003) Emerging role for autophagy in removal of aggresomes. J Neuro 23: 10672-10680.

47. Kim PK, Hailey DW, Mullen RT, Lippincott-Schwartz J (2008) Ubiquitin signals autophagic degradation of cytosolic proteins and peroxisomes. Proc Natl Acad Sci USA 105: 20567-20574.

48. Bjørkøy G, Lamark T, Brech A, Ouzen H, Perander M, *et al.* (2005) p62/SQSTM1

forms protein aggregates degraded by autophagy and has a protective effect on huntingtin-induced cell death. J Cell Biol 171: 603-614.

49. Birmingham CL, Smith AC, Bakowski MA, Yoshimori T, Brumell JH (2006) Autophagy controls *Salmonella* infection in response to damage to the *Salmonella*-containing vacuole. J Biol Chem 281: 11374- 11383.

50. Flynn JL, Chan J (2001) Immunology of tuberculosis. Annu Rev Immunol 19: 93-129.

51. World Health Organization (2009) WHO Report 2009 Global Tuberculosis Control. Available: http://www.who.int/tb/publications/global_report/2009/en/.

52. Aderem A, Underhill DM (1999) Mechanisms of phagocytosis in macrophages. Annu Rev Immunol 17: 593-623.

53. Ulricks T, Kaufmann SHE (2005) New insights into the function of granulomas in human tuberculosis. J Path 208: 261-269.

54. Malik ZA, Thompson CR, Hashimi S, Porter B, Iyer SS, *et al.* (2003) *Mycobacterium tuberculosis* blocks Ca2+ signaling and phagosome maturation in human macrophaes via specific inhibition of sphingosine kinase. J Immunol 170: 2811-2815.

55. Vergne I, Chua J, Deretic V (2003) Tuberculosis toxin blocking phagosome maturation inhibits a novel Ca2+/ Calmodulin-PI3K hVPS34 cascade. J Exp Med 198: 653-659.

56. Sturgill-Koszycki S, Schlesinger PH, Chakraborty P, Haddix PL, Collins HL, *et al.* (1994) Lack of acidification in Mycobacterium phagosomes produced by exclusion of the vesicular proton-ATPase. Science 263: 678-681.

57. DiGiuseppe Champion PA, Cox JS (2007) Protein secretion systems in mycobacteria.

Cell Microbiol 9: 1376-1384.

58. Lewis KN, Liao R, Guinn KM, Hickely MJ, Smith S, *et al.* (2003) Deletion of RD1 from *Mycobacterium tuberculosis* mimics bacilli Calmette-Guerin attenuation. J Infect Dis 187: 117-123.

59. Simeone R, Bottai D, Brosch R (2009) ESX/type VII secretion systems and their role in host-pathogen interaction. Curr Opin Microbiol 12: 4-10.

60. Stanley SA, Raghavan S, Hwang WW, Cox JS (2003) Acute infection and macrophage subversion by *Mycobacterium tuberculosis* require a specialized secretion system. Proc Natl Acad Sci USA 100: 13001–13006.

61. Smith J, Manoranjan J, Pan M, Bohsali A, Xu J, *et al.* (2008) Evidence for pore formation in host cell membranes by ESX-1-secreted ESAT-6 and its role in *Mycobacterium marinum* escape from the vacuole. Infect Immun 76: 5478-5487.

62. Hsu T, Hingley-Wilson SM, Chen B, Chen M, Dai AZ, *et al.* (2003) The primary mechanism of attenuation of bacillus Calmette-Guerin is a loss of secreted lytic function required for invasion of lung interstitial tissue. Proc Natl Acad Sci USA 100: 12420–12425.

63. Clark HF, Shepard CC (1963) Effect of environmental temperatures on infection with *Mycobacterium marinum* (balnei) of mice and a number of poikilothermic species, J. Bacteriol 86: 1057–1069.

64. Stamm LM, Brown EJ (2004) *Mycobacterium marinum*: the generalization and specialization of a pathogenic mycobacterium. Microbes Infect 6: 1418-1428.

65. Barker LP, George KM, Falkow S, Small PL (1997) Differential trafficking of live and dead *Mycobacterium marinum* organisms in macrophages. Infect Immun 65: 1497-

1504.

66. Gao L-Y, Guo S, McLaughlin B, Morisaki JH, Engel JN, *et al.* (2004) A mycobacterial virulence gene cluster extending RD1 is required for cytolosis, bacterial spreading, and ESAT-6 secretion. Mol Microbiol 53: 1677-1693.

67. Stamm LM, Morisaki JHM, L-Y Gao, Jeng RL, McDonald KL, *et al.* (2003) *Mycobacterium marinum* escapes from phagosomes and is propelled by actin-based motility. J Exp Med 198: 1361-1368.

68. Stamm LM, Pak MA, Morisaki JH, Snapper SB, Rottner K, *et al.* (2005) Role of the WASP family for *Mycobacterium marinum* actin tail formation. Proc Natl Acad USA 102: 14837-14842.

69. Schroder K, Hertzog PJ, Ravasi T, Hume DA (2004) Interferon-gamma: an overview of signals, mechanisms and functions. J Leukoc Biol 75: 163-189.

70. Chan J, Xing Y, Magliozzo RS, Bloom BR (1992) Killing of virulent *Mycobacterium tuberculosis* by reactive nitrogen intermediates produced by activated murine macrophages. J Exp Med 175: 1111-1122.

71. Taylor GA, Feng CG, Sher A (2004) p47 GTPases: regulators of immunity to intracellular pathogens. Nat Rev Immunol 4: 100-109.

72. Singh SB, Davis AS, Taylor GA, Deretic V (2006) Human IRGM induces autophagy to eliminate intracellular mycobacteria. Science 313: 1438-1441.

73. MacMicking JD, Taylor GA, McKinney JD (2003) Immune control of tuberculosis by IFN-gamma-inducible LRG-47. Science 302: 654-659.

74. Alonso S, Pethe K, Russell DG, Purdy GE (2007) Lysosomal killing of Mycobacterium mediated by ubiquitin-derived peptides is enhanced by autophagy. Proc

Natl Acad Sci USA 104: 6031-6036.

75. Serbina NV, Flynn JL (2001) CD8+ T cells participate in the memory immune response to *Mycobacterium tuberculosis*. Infect Immun 69: 4320-4328.

Chapter 2

1. Stamm LM, Brown EJ (2004) *Mycobacterium marinum*: the generalization and specialization of a pathogenic mycobacterium. Microbes Infect 6: 1418-1428.

2. Tobin DM, Ramakrishnan L (2008) Comparative pathogenesis of *Mycobacterium marinum* and *Mycobacterium tuberculosis*. Cell Microbiol 10: 1027-1039.

3. Lewis KN, Liao R, Guinn KM, Hickey MJ, Smith S *et al*. (2003) Deletion of RD1 from *Mycobacterium tuberculosis* mimics bacille Calmette-Guérin attenuation. J Infect Dis 187: 117-123.

4. Pym AS, Brodin P, Brosch R, Huerre M, Cole ST (2002) Loss of RD1 contributed to the attenuation of live tuberculosis vaccines *Mycobacterium bovis* BCG and *Mycobacterium microti*. Mol Microbiol 46: 709-717.

5. Tan T, Lee WL, Alexander DC, Grinstein S, Liu J (2006) The ESAT-6/CFP-10 secretion system of *Mycobacterium marinum* modulates phagosome maturation. Cell Microbiol 8: 1417–1429.

6. Gao LY, Guo S, McLaughlin B, Morisaki H, Engel JN, Brown EJ (2004) A mycobacterial virulence gene cluster extending RD1 is required for cytolysis, bacterial spreading and ESAT-6 secretion. Mol Microbiol 53: 1677–1693.

7. Smith J, Manoranjan J, Pan M, Bohsali A, Xu J, *et al*. (2008) Evidence for pore

formation in host cell membranes by ESX-1 secreted ESAT-6 and its role in *Mycobacterium marinum* escape from vacuole. Infect Immun 76: 5478-5487.

8. Davis J, Ramakrishnan L (2009) The role of the granuloma in expansion and dissemination of early tuberculous infection. Cell 136: 37-49.

9. Clemens DL, Lee B-Y, Horwitz MA (2002) The *Mycobacterium tuberculosis* phagosome in human macrophages is isolated from the host cell cytoplasm. Infect Immun 70: 5800-5807.

10. Van der Wel N, Hava D, Houben D, Fluitsma D, van Zon M *et al*. (2007) M. tuberculosis and M. leprae translocate from the phagolysosome to the cytosol in myeloid cells. Cell 129: 1287-1298.

11. Hsu T, Hingley-Wilson SM, Chen B, Chen M, Dai AZ, *et al*. (2003) The primary mechanism of attenuation of bacillus Calmette-Guérin is a loss of secreted lytic function required for invasion of lung interstitial tissue. Proc Natl Acad Sci USA 100: 12420-12425.

12. Stamm LM, Morisaki JH, Gao L-Y, Jeng RL, McDonald KL, *et al*. (2003) *Mycobacterium marinum* escapes from phagosomes and is propelled by actin-based motility. J Exp Med 198: 1361-1368**.**

13. Perrin AJ, Jiang X, Birmingham CL, So NS, Brumell JH (2004). Recognition of bacteria in the cytosol of mammalian cells by the ubiquitin system. Curr Biol 14: 806-811.

14. Mizushima N (2007) Autophagy: process and function. Genes Dev 21:2861-2873.

15.Kim PK, Hailey DW, Mullen RT, Lippincott-Schwartz J (2008) Ubiquitin signals autophagic degradation of cytosolic proteins and peroxisomes. Proc Natl Acad Sci USA

105: 20567-20574.

16.Birmingham CL, Smith AC, Bakowski MA, Yoshimori T, Brumell JH (2006) Autophagy controls *Salmonella* infection in response to damage to the *Salmonella*-containing vacuole. J Biol Chem 281: 11374-11383.

17. Birmingham CL, Canadien V, Gouin E, Troy EB, Yoshimori T, *et al*. (2007) *Listeria monocytogenes* evades killing by autophagy during colonization of host cells. Autophagy 3: 442-451.

18. Nakagawa I, Amano A, Mizushima N, Yamamoto A, Kamimoto T, *et al*. (2004) Autophagy defends cells against invading group A Streptococcus. Science 306: 1037-1040.

19. Ogawa M, Yoshimori T, Suzuki T, Sagara H, Mizushima N, *et al.* (2005). Escape of intracellular *Shigella* from autophagy. Science 307: 727-731.

20. Gutierrez M, Master S, Singh S, Taylor G, Colombo M, *et al*. (2004) Autophagy is a defense mechanism inhibiting BCG and *Mycobacterium tuberculosis* survival in infected macrophages. Cell 119: 753-766.

21. Woodworth SJ, Fortune SM, Behar, SM (2008) Bacterial protein secretion is required for priming of CD8+ T cells specific for the *Mycobacterium tuberculosis* antigen CFP-10. Infect Immun 76: 4199-4205.

22. Stanley SA, Johndrow JE, Manzanillo P, Cox JS. (2007) The Type I IFN response to infection with *Mycobacterium tuberculosis* requires ESX-1-mediated secretion and contributes to pathogenesis. J Immunol 178: 3143-3152.

23. Koo IC , Wang C , Raghavan S , Morisaki JH , Cox JS , *et al*. (2008) ESX-1-dependent cytolysis in lysosome secretion and inflammasome activation during

mycobacterial infection. Cell Microbiol 10: 1866-1878.

24. Checroun C, Wherly TD, Fishcer ER, Hayes SF, Celli J (2006) Autophagy-mediated reentry of Francisella tularensis into the endocytic compartment after cytoplasmic replication. Proc Natl Acad Sci USA 39: 14578-14583.

25. Kerscher O, Felberbaum R, Hochstrasser M (2006) Modification of proteins by ubiquitin and ubiquitin-like proteins. Annu Rev Cell Dev Biol 22: 159-180.

26. Newton K, Matsumoto ML, Wertz IE, Kirkpatrick DS, Lill JR, *et al.* (2008) Ubiquitin chain editing revealed by polyubiquitin linkage-specific antibodies. Cell 134: 668-678.

27. Gao L-Y., Pak M, Kish R, Kajihara K, Brown EJ (2006) A mycobacterial operon essential for virulence in vivo and invasion and intracellular persistence in macrophages. Infect Immun 74: 1757-1767.

28. Mizushima N, Yamamoto A, Hatano M, Kobayashi Y, Kabeya Y, *et al.* (2001) Dissection of autophagosome formation using Apg5-deficient mouse embryonic stem cells. J Cell Biol 152: 657-668.

29. Stamm LM, Pak MA, Morisaki JH, Snapper SB, Rottner K, *et al*. (2005) Role of the WASP family proteins for *Mycobacterium marinum* actin tail formation. Proc Natl Acad Sci USA 102: 14837-14842.

30. Beatty WL, Russell DG (2000) Identification of mycobacterial surface proteins released into subcellular compartments of infected macrophages. Infect Immun 68: 6997–7002.

31. Dramsi S, Cossart P (1998) Intracellular pathogens and the actin cytoskeleton. Annu Rev of Cell and Dev Biol 14: 137-166.

32. Inohara N, Nuñez G (2003) NODs: intracellular proteins involved in inflammation and apoptosis. Nature Rev Immunol 3: 371-382.

33. Singh, SB, Davis AS, Taylor GA, Deretic V (2006) Human IRGM induces autophagy to eliminate intracellular mycobacteria. Science 313: 1438-1441.

34. Katzmann DJ, Babst M, Emr SD (2001) Ubiquitin-dependent sorting into the multivesicular body pathway requires the function of a conserved endosomal protein sorting complex, ESCRT-I. Cell 106: 145-155.

35. de Waal EJ, Vreeling-Sindelárová H, Sehellens JPM, Houtkooper JM, James J (1986) Quantitative changes in the lysosomal vacuolar system of rat hepatocytes during short-term starvation. Cell Tissue Res 243: 641-648.

36. Bjørkøy G , Lamark T , Brech A , Outzen H , Perander M , *et al.* (2005). p62/SQSTM1 forms protein aggregates degraded by autophagy. J Cell Biol 171: 603-614.

37. Behar SM, Dascher CC, Grusby MJ, Wang CR, Brenner MB (1999) Susceptibility of mice deficient in CD1d or TAP1 to infection with *Mycobacterium tuberculosis*. J Exp Med 189: 1973–1980.

38. Flynn JL, Goldstein MM, Triebold KJ, Koller B, Bloom BR (1992). Major histocompatibility complex class I-restricted T cells are required for resistance to *Mycobacterium tuberculosis* infection. Proc Natl Acad Sci USA 89: 12013-12017.

39. Angot A, Vergunst A, Genin S, Peeters N. (2007) Exploitation of eukaryotic ubiquitin signaling pathways by effectors translocated by bacterial Type III and Type IV secretion systems. PLoS Pathog 3: e3. doi:10.1371/journal.ppat.0030003

40. Rubin EJ, Hett EC (2008) Bacterial growth and Cell Division: a Mycobacterial

Perspective. Microbiol and Mol Biol Rev 72: 126-156.

41. Alonso S, Pethe K, Russell DG, Purdy GE (2007) Lysosomal killing of Mycobacterium mediated by ubiquitin-derived peptides is enhanced by autophagy. Proc Natl Acad Sci USA 104: 6031-6036.

42. Cole ST, Brosch R, Parkhill J, Garnier T, Churcher C, *et al.* (1998) Deciphering the biology of *Mycobacterium tuberculosis* from the complete genome sequence. Nature 393: 537-544.

43. Rechsteiner M, Rogers, SW (1996) PEST sequences and regulation by proteolysis. Trends Biochem Sci 21: 261-271.

44. Cosma CL, Humbert O, Ramakrishnan L (2004) Superinfecting mycobacteria home to established tuberculous granulomas. Nature Immun 5: 828-835.

45. Roach TI, Slater SE, White LS, Zhang X, Majerus PW, *et al.* (1998) The protein tyrosine phosphatase SHP-1 regulates integrin-mediated adhesion of macrophages. Curr Biol 8: 1035–1038.

46. Owen KA, Pixley FJ, Thomas KS, Vicente-Manzanares M, Ray BJ, *et al.* (2007) Regulation of lamellipodial persistence, adhesion turnover, and motility in macrophages by focal adhesion kinase. J Cell Biol 179: 1275-1287.

47. Slot JW, Geuze HJ (2007) Cryosectioning and immunolabeling. Nature Prot 2: 2480-2491.

48. Breitschopf K, Bengal E, Ziv T, Admon A, Ciechanover A (1998) A novel site for ubiquitination: the N-terminal residue, and not internal lysines of MyoD, is essential for conjugation and degradation of the protein. EMBO J 17: 5964-5973.

49. N'Diaye E-N, Kajihara KK, Hsieh I, Morisaki H, Debnath J *et al.* (2009) PLIC

proteins or ubiquilins regulate autophagy-dependent cell survival during nutrient starvation. EMBO J 10: 173-179.

Chapter 3

1. Mizushima N (2005) The pleiotropic role of autophagy: from protein metabolism to bactericide. Cell Death Diff 12: 1535-154.

2. Klionsky DJ (2005) The molecular machinery of autophagy: unanswered questions. J Cell Sci 118: 7-18.

3. Sou YS, Waguri S, Iwata J, Ueno T, Fujimara T, *et al.* (2008) The Atg8 conjugation system is indispensable for proper development of autophagic isolation membranes in mice. Mol Biol Cell 11:4762- 4775.

4. Komatsu M, Waguri S, Ueno T, Iwata J, Murata S, *et al.* (2005) Impairment of starvation-induced and constitutive autophagy in Atg7-deficient mice. J Cell Biol 169: 425-434.

5. Ichimura Y, Imamura Y, Emoto K, Umeda M, Noda T, *et al.* (2004) In vivo and *in vitro* reconstitution of Atg8 conjugation essential for autophagy. J Biol Chem 279:40584-40592.

6. Zhao Z, Fux B, Goodwin M, Dunay I, Strong D, *et al.* (2008) Autophagosome-independent essential function for the autophagy protein Atg5 in cellular immunity to intracellular pathogens. Cell Host Microbe 4: 458-469.

7. Luzio JP, Pryor PR, Bright NA (2007) Lysosomes: fusion and function. Nature Rev Mol Cell Biol 8: 622-632.

8. Alvarez HM, Steinbüchel (2002) Triacylglycerols in prokaryotic microorganisms. Appl Microbiol Biotechnol 60: 367-376.

9. Koo IC, Wang C, Raghavan S, Morisaki JH, Cox JS, *et al.* (2008) ESX-1-dependent cytolysis in lysosome secretion and inflammasome activation during mycobacterial infection. Cell Microbiol 10:1866-1878.

10. Mariathasan S, Monack DM (2007) Inflammasome adaptors and sensors: intracellular regulators of infection and inflammation. Nat Rev Immunol 7: 31-40.

11. McLaughlin B, Chon JS, MacGurn JA, Carlsson F, Cheng TL, *et al.* (2007) A mycobacterium ESX-1-secreted virulence factor with unique requirements for export. PLoS Pathog 3(8): e105. doi:10.1371/journal.ppat.0030105.

UCSF Library Release

Publishing Agreement

It is the policy of the University to encourage the distribution of all theses, dissertations, and manuscripts. Copies of all UCSF theses, dissertations and manuscripts will be routed to the library via the Graduate Division. The library will make all theses, dissertations, and manuscripts accessible to the public and will preserve these to the best of their abilities, in perpetuity.

Please sign the following statement:
I hereby grant permission to the Graduate Division of the University of California, San Francisco to release copies of my thesis, dissertation, or manuscript to the Campus Library to provide access and preservation, in whole or in part, in perpetuity.

Catherine A. Wolin 6/1/2009

Author Signature Date